Aus dem Fachbereich Medizin
der Johann Wolfgang Goethe-Universität
Frankfurt am Main

Institut für Biochemie I – Pathobiochemie
Direktor: Professor Dr. Bernhard Brüne

Macrophage polarization by apoptotic cancer cells – a RNAi high-throughput screen and validation of interleukin 10 regulation

Dissertation
zur Erlangung des Doktorgrades der theoretischen Medizin
des Fachbereichs Medizin
der Johann Wolfgang Goethe-Universität
Frankfurt am Main

vorgelegt von

Stephanie Ley
aus Stuttgart

Frankfurt am Main, 2012

Dekan:	Prof. Dr. Josef M. Pfeilschifter
Referent	Prof. Dr. Bernhard Brüne
Koreferent:	Prof. Dr. Heiko Mühl
2. Koreferent:	Prof. Dr. Alexander Steinle
Tag der mündlichen Prüfung:	18.10.2012

Do what you can,
with what you‘ve got,
where you are.

(Theodore Roosevelt)

List of figures

List of tables

Abbreviations

Ab	Antibody
ABC	ATP-binding cassette
AC	Adenylate cyclase
ACM	Apoptotic cancer cell supernatant
ACM-siSK2	ACM from MCF-7 cells carrying a knockdown of sphingosine kinase 2
ADORA2A	Adenosine receptor A2A
AIF	Apoptosis-inducing factor
AKT	Protein kinase B
ANOVA	Analysis of variance
AP-1	Activator protein-1
Apaf-1	Apoptotic protease activating factor
APC	Antigen-presenting cell
ATP	Adenosine triphosphate
Bax	Bcl-2 associated protein x
Bcl-2	B-cell lymphoma 2
Bcl-X_L	B-cell lymphoma extra long
BDNF	Brain-derived growth factor
Bid	BH3 interacting-domain death agonist
C/EBP	CCAAT/enhancer-binding protein
cAMP	Cyclic adenosine monophosphate
CBA	Cytometric bead array
CBR2	Cannabinoid receptor 2
CCL	Chemokine (C-C motif) ligand
Cer	Ceramide
CPE	Cytopathogenic effect
CpG	Cytosine guanin oligodesoxynucleotides
CREB	Camp response element binding
CTLA-4	Cytotoxic T-lymphocyte-associated antigen 4
d	Day(s)
Da	Dalton
DC	Dendritic cell
DISC	Death-inducing signaling complex
DMEM	Dulbecco's Modified Eagel Medium
ECM	Extracellular matrix
EGF	Epidermal growth factor

EGFR	Epidermal growth factor receptor
ELISA	Enzyme-linked immunosorbent assay
EMA	European Medicines Agency
ER	Endoplasmatic reticulum
ERK1/2	Extracellular signal-regulated kinase 1/2
FACS	Fluorescence activated cell sorting
FADD	Fas-associated death domain protein
FCS	Fetal calf serum
FcγR	Fragment crystallizable gamma receptor
FDA	United States Food and Drug Administration
FGF	Fibroblast growth factor
Gab1/2	Grb-2-associated binder-1/2
GFRA	Glycosylphosphatidylinositol (GPI)-anchored glia cell line neurotrophic factor (GDNF) family receptor alpha
GM-CSF	Granulocyte macrophage colony-stimulating factor
GPCR	G protein-coupled receptor
Grb-2	Growth factor receptor-bound protein-2
h	Hour(s)
HA	Hemagglutinin
HDAC	Histone deacetylase
HIF-1α	Hypoxia inducible factor-1 alpha
HMGB1	High-mobility group box 1
HMG-CoA	3-hydroxy-3-methylglutaryl coenzyme-A
HMGCR	3-hydroxy-3-methylglutaryl coenzyme-A (HMG-CoA) reductase
HTS	High-throughput screen
IAP	Inhibitor of apoptosis
IDO	Indolamine 2,3-dioxygenase
IF	Immunofluorescence
IFN-γ	Interferon gamma
IL	Interleukin
IL-1ra	Interleukin 1 receptor antagonist
IL-4Rα	Interleukin 4 receptor-alpha
IP	Immunoprecipitation
IQR	Interquartile range
IU	Infectious units
JAK	Janus kinase
JNK	Jun N-terminal kinase

LAP	Latency-associated dimeric propeptide
LPC	Lysophosphatidylcholine
LPS	Lipopolysaccharide
LTBP	Latent TGF-beta binding protein
M	Molar
m	Meter
MΦ	Macrophage(s)
MAPK	Mitogen-activated protein kinase
MCP-1	Monocyte chemotactic protein-1
M-CSF	Macrophage colony-stimulating factor
MEK1/2	Mitogen-activated protein kinase kinase 1/2
MHC	Major histocompatibility complex
min	Minute(s)
MMP	Matrix metalloproteinase
MSD	Mesoscale discovery
mTOR	Mammalian target of rapamycin
Nachr	Nicotinic acetylcholine receptor
NFκB	Nuclear factor-kappa B
NGF	Nerve growth factor
NK cell	Natural killer cell
NO	Nitric oxide
NT	Neurotrophin
OD	Optical density
P38	Mitogen-activated protein kinase p38
PGE2	Prostaglandin E2
PI3K	Phosphoinositide 3-kinase
PKC	Protein kinase C
PLC	Phospholipase C
PyMT	Polyoma middle T-antigen
Qrt-PCR	Quantitative real-time polymerase chain reaction
Rac, Rho	Family members of Rho gtpase
Raf	Murine leukemia viral oncogene homolog 1
Ras	Rat sarcoma
RET	Rearranged during transfection
ROS	Reactive oxygen species
RPMI	Roswell Park Memorial Institute medium
RT	Room temperature

RTK	Receptor tyrosine kinase
S1P	Sphingosine-1-phosphate
SDS	Sodium dodecyl sulfate
sec	Second(s)
SEM	Standard error of the mean
Shc	Src homologous
SK	Sphingosine kinase
SM	Sphingomyelin
Smac/DIABLO	Second mitochondria-derived activator of caspase/direct inhibitor of apoptosis-binding protein
Sos	Son of sevenless
SP1	Specificity protein 1
Sph	Sphingosine
Spns2	Spinster homolog 2
Src	Sarcoma tyrosine kinase
STAT	Signal transducer and activator of transcription
TAM	Tumor-associated macrophage(s)
Tbid	Truncated Bcl-2 interacting domain death agonist
TEMED	Tetramethylethylenediamine
TGFBR	TGF-beta receptor
TGF-β	Transforming growth factor beta
Th1/2	Type 1/2 T helper cell
TLR	Toll-like receptor
TNF-α	Tumor necrosis factor-alpha
TRAF2	TNF receptor associated factor 2
TRAIL	TNF-related apoptosis inducing ligand
TRAIL	TNF-related apoptosis-inducing ligand
Treg	Regulatory T cell
TRK A-C	Tyrosine kinase receptor A-C
TRKA	Neurotrophin tyrosine kinase receptor A
UPAR/PLAUR	Urokinase plasminogen activator receptor
V_	Version (shRNA target sequence)
VCM	Viable cancer cell supernatant
VEGF	Vascular endothelial growth factor
WB	Western blotting

1 Summary

Tumor-associated macrophages (TAM) are a major supportive component within neoplasms and by their plasticity promote all phases of tumor development. Mechanisms of macrophage (MΦ) attraction and differentiation to a tumor-promoting phenotype, defined among others by distinct cytokine patterns such as pronounced immunosuppressive interleukin 10 (IL-10) production, are largely unknown. However, a high apoptosis index within tumors and strong MΦ infiltration correlate with poor prognosis. Thus, I aimed at identifying signaling pathways contributing to generation of TAM-like MΦ by using supernatant of apoptotic cancer cells (ACM) as stimulus.

To distinguish novel factors involved in generating TAM-like MΦ, I used an adenoviral RNAi-based approach. The primary read-out was production of IL-10. However, mediators modulating IL-10 were re-validated for their impact on regulation of the cytokines IL-6, IL-8 and IL-12. Following assay development, optimization and down-scaling to a 384-well format, primary human MΦ were transduced with 8495 constructs of the adenoviral shRNA SilenceSelect® library of Galapagos BV, followed by activation to a TAM-like phenotype using ACM. I identified 96 genes involved in IL-10 production in response to ACM and observed a pronounced cluster of 22 targets regulating IL-10 and IL-6. Principal validation of five targets of the IL-10/IL-6 cluster was performed using siRNA or pharmacological inhibitors. Among those, IL-4 receptor-α and cannabinoid receptor 2 were confirmed as regulators of IL-10 and IL-6 secretion.

One protein identified in the screen, the nerve growth factor (NGF) receptor TRKA was chosen for in-depth validation, based on its involvement in IL-10, IL-6 and IL-12 secretion from ACM-stimulated human MΦ. TRKA possesses a cardinal role in neuronal development, but compelling evidence emerges suggesting participation of TRKA in cancer development. First experiments using pharmacological inhibitors principally confirmed the involvement of TRKA in IL-10 secretion by ACM-stimulated MΦ and revealed PI3K/AKT and to a lesser extend MAPK p38 as important signaling molecules downstream of TRKA activation. Signaling through TRKA required the presence of its ligand NGF, as indicated by NGF neutralization experiments. NGF was not induced by or present in ACM, but was constitutively secreted by MΦ. Interestingly, MΦ responded to authentic NGF with neither AKT and p38 phosphorylation nor IL-10 production. TRKA is well known to be transactivated by

other receptors and in neurons its cellular localization is decisive for its function. Inhibitors of common transactivation partners did not influence IL-10 production by human MΦ. Rather, ACM-treatment provoked pronounced translocation of TRKA to the plasma membrane within 10 minutes as observed by immunofluorescence staining. Consequently, I was intrigued to clarify mechanisms of TRKA trafficking in response to ACM.

The bioactive lipid sphingosine-1-phosphate (S1P) has been previously identified as important apoptotic cell-derived mediator involved in TAM-like MΦ polarization. Indeed, I observed S1P and src kinase involvement in ACM-mediated IL-10 induction. Furthermore, inhibition of S1P receptor (S1PR) signaling or src kinase activity prevented TRKA translocation, whereas a TRKA inhibitor or anti-NGF did not block TRKA trafficking to the plasma membrane in response to ACM. Thus, autocrine secreted NGF activated TRKA to promote IL-10 secretion, which required previous S1PR/src-dependent translocation of TRKA to the plasma membrane.

Following the detailed analysis of IL-10 regulation, I was interested whether other TAM phenotype markers were influenced by ACM and whether their expression was regulated through TRKA-dependent signaling. Five of six markers were up-regulated on mRNA level by ACM, and secretion of IL-6, IL-8 and TNF-α was triggered. S1PR-signaling was essential for induction of all but one marker, whereas TRKA signaling was only required for cytokine secretion. Interestingly, none of the investigated TAM markers was regulated identically to IL-10, emphasizing a tight and exclusive regulation machinery of this potent immunosuppressive cytokine.

Finally, I aimed to validate the *in vitro* findings in human ACM-stimulated MΦ. Therefore, I isolated murine TAM as well as other major mononuclear phagocyte populations from primary oncogene-induced breast cancer tissue. Indeed, TRKA-dependent signaling was required for spontaneous cytokine production selectively by primary murine TAM. Besides IL-10, the TRKA pathway was decisive for secretion of IL-6, TNF-α and monocyte chemotactic protein-1, indicating its relevance in cancer-associated inflammation.

In summary, my findings highlight a fine-tuned regulatory system of S1P-dependent TRKA trafficking and autocrine NGF signaling in TAM biology. Both factors, S1P as well as NGF, might be interesting targets for future cancer therapy.

2 Zusammenfassung

Tumor-assoziierte Makrophagen (TAM) begünstigen verschiedene Phasen der Tumorentwicklung. Bisher ist das Wissen über die Mechanismen der Rekrutierung und Differenzierung von Makrophagen (MΦ) zu TAM, die sich unter anderem durch eine ausgeprägte Produktion von immunsuppressivem Interleukin 10 (IL-10) auszeichnen, unvollkommen. Eine Korrelation zwischen dem Ausmaß der MΦ-Infiltration sowie der Zelltotrate innerhalb von Tumoren und einer schlechten Prognose für Krebspatienten wurde berichtet. Auf Grundlage dessen, untersuchte ich in der vorliegenden Arbeit Signalwege, die zur Entstehung von TAM-ähnlichen MΦ führen. Dazu stimulierte ich humane primäre MΦ mit Überständen von apoptotischen Tumorzellen (ACM).

Zuerst führte ich ein RNAi-basiertes adenovirales Hochdurchsatzverfahren (HTS) zur Identifizierung unbekannter Faktoren, die zur Entstehung von TAM-ähnlichen MΦ beitragen, durch. Als primären Endpunkt analysierte ich zunächst die Produktion von IL-10. Die identifizierten IL-10-regulierenden Faktoren wurden im nächsten Schritt auf ihre Beteiligung an der Synthese von weiteren tumorfördernden (IL-6, IL-8) und tumorinhibierenden (IL-12) Zytokinen getestet. MΦ wurden mit 8495 adenovirale *shRNAs* der SilenceSelect® Bibliothek der Firma Galapagos BV transduziert und mit ACM zu TAM-ähnlichen MΦ polarisiert. 96 Gene, die eine Rolle in der ACM-vermittelten IL-10 Produktion spielen, wurden identifiziert. Davon zeigten 22 Gene eine bisher nicht beobachtete Koregulation von IL-10 und IL-6 auf. Fünf Kandidaten aus dieser Gruppe wurden mit Hilfe von Inhibitoren oder *siRNA* validiert und eine Beteiligung des IL-4 Rezeptors α sowie des Cannabinoid Rezeptors 2 an der IL-10 und IL-6 Regulation konnte bestätigt werden. In darauffolgenden Versuchen verifizierte ich im Detail die Beteiligung des *nerve growth factor* (NGF) Rezeptors TRKA an der Ausbildung TAM-ähnlicher MΦ nach ACM-Behandlung. Die Ausschaltung des Gens im HTS hatte zu einer verminderten Sekretion von IL-10 und IL-6 sowie einer Zunahme von IL-12 geführt. TRKA ist essentiell an der Entwicklung des Nervensystems beteiligt und neuere Berichte weisen auf seine Beteiligung in der Tumorbiologie hin. Pharmakologische Inhibitoren bestätigten die Notwendigkeit von TRKA an der ACM-vermittelten IL-10 Produktion, sowie die TRKA-abhängige Aktivierung der Signalmoleküle PI3K/AKT und, wenn auch weniger ausgeprägt, MAPK p38. Die Neutralisation von NGF demonstrierte, dass von MΦ konstitutiv autokrin sezerniertes

NGF für die IL-10 Sekretion benötigt wurde. Synthetisches NGF zeigte jedoch keinen Effekt auf die AKT und p38 Phosphorylierung oder auf die Produktion von IL-10. Interessanterweise legten Immunfluoreszenzaufnahmen von ACM-stimulierten MΦ eine deutliche Zunahme von TRKA an der Plasmamembran nach 10-minütiger Simulation offen, die durch Inhibition von TRKA oder Neutralisation von NGF nicht beeinflusst wurde. Dieses Phänomen war Anlass für weiterführende Studien.

Sphingosine-1-Phosphat (S1P) wurde im Vorfeld als wichtiger Mediator in der ACM-vermittelten MΦ Polarisierung identifiziert und ich konnte eine Abhängigkeit der IL-10 Produktion von S1P und Src Kinasen zeigen. Des Weiteren wurde die Anreicherung von TRKA an der Plasmamembran durch Inhibitoren von Src sowie S1P Rezeptoren verhindert. Diese Daten indizieren eine komplexe Regulation der ACM-vermittelten IL-10 Produktion in primären MΦ. S1P, generiert von apoptotischen Krebszellen, vermittelt S1P Rezeptor- und Src Kinasen-abhängig die Translokalisation von TRKA an die Zelloberfläche von MΦ. Der Rezeptor wird daraufhin von autokrin sezerniertem NGF aktiviert und initiiert darauffolgend die Produktion von IL-10.

In einem weiteren Schritt untersuchte ich zusätzliche biologische Marker, die eine Rolle bei der Funktion von TAM spielen. ACM bewirkte eine starke Sekretion von IL-6, IL-8 und TNF-α, sowie eine Hochregulation weiterer Marker auf *mRNA*-Ebene. Die S1P Rezeptoraktivität war für nahezu alle Marker essentiell. Die Zytokinsekretion war ebenfalls abhängig von TRKA, jedoch wurde keiner der untersuchten Faktoren analog zu IL-10 reguliert. Diese Befunde unterstreichen die fein abgestimmte und exklusive Regulation dieses hochpotenten immunsuppressiven Zytokins.

Um meine *in vitro* Daten zu bestärken, isolierte ich TAM und weitere mononukleare Phagozytenpopulationen aus primärem Onkogen-induzierten Brustkrebsgewebe der Maus und untersuchte die spontane Zytokinproduktion dieser Zellen. Auch in diesem Modell zeigte sich eine, auf TAM beschränkte, TRKA-abhängige Produktion von IL-10, IL-6, TNF-α und *monocyte chemotactic protein-1*, und die Rolle von TRKA im Tumor-assoziierten Entzündungsgeschehen wurde bekräftigt.

Zusammenfassend konnte ich Mechanismen der S1P- und NGF-abhängigen TRKA Signaltransduktion und deren Funktion im Bezug auf Makrophagen im Tumorgeschehen identifizieren. Sowohl S1P als auch NGF stellen somit interessante Zielmoleküle in der künftigen Krebstherapie dar.

3 Introduction

3.1 Cell death

Cell death research is almost as old as the cell theory. The cell as the basic unit of life, was proposed by Schleiden and Schwann in the mid nineteenth century. Virchow extended this model by stating, a cell cannot be created de novo, but has to derive from an existing one '*omnis cellula e cellula'*, resulting in the modern cell theory. Soon after declaration of the cell theory, Vogt described the physiological appearance of cell death (1-3). The foundation of cellular research on life and death was laid.

Different modes of cell death are described. Apoptosis and necrosis, by far, are the best studied mechanisms of cell death mechanisms and the nomenclature is based on morphological features observed during the processes. Necrotic cell death leads to inflammatory responses due to 'uncontrolled' leakage of cell content. Harsh conditions such as heat or strong detergents lead to a poorly defined necrotic death characterized by cytoplasmic swelling, rupture of plasma membranes, loss of intracellular content and only moderate chromatin condensation. However, evidence is accumulating that necrotic cell death is finely regulated under physiological conditions and fulfils important roles in physiology and pathology (4-6). Contrarily, the fine-tuned apoptotic cell death is better understood and consequences for the organism are better defined.

3.1.1 Apoptosis

First described in 1972 by Kerr and colleagues (7), apoptosis is essential for embryonic development and maintenance of cellular homeostasis in adult organisms. Highly controlled apoptotic death is associated with cell rounding, shrinkage, plasma membrane bebbing, cellular fragmentation into apoptotic bodies, nuclear shrinkage and fragmentation, chromatin condensation and finally engulfment of the dying cell by resident phagocytes. The controlled destruction is mediated by a family of proteases – the caspases, which are activated by either the extrinsic or intrinsic apoptosis pathway (8).

The extrinsic pathway is triggered by ligand-receptor binding on the cell surface. Upon ligand-binding (e.g. Fas-Ligand (FasL), TRAIL) the so-called death receptors (e.g. TNF-related apoptosis-inducing ligand (TRAIL) –R1 and –R2) trimerize and recruit adaptor proteins and procaspase-8 to form the death inducing signaling complex

(DISC). Procaspase-8 is cleaved to the active form caspase-8 and triggers the apoptotic effector caspase cascade ((8-10) and Figure 1).

Stress, such as growth factor deprivation, heat, irradiation or DNA-damage by chemotherapeutic agents induces the intrinsic pathway and leads to cytochrome c release from mitochondria into the cytosol. Subsequently, caspase adaptor molecule Apaf-1 (apoptotic protease-activating factor 1) and procaspase-9 are recruited and activated. Subsequently, interaction with cytochrome c leads to the formation of the holoenzyme complex called the apoptosome. Consequently, the proteolytic activity of caspase-9 cleaves and activates effector caspases 3, 6 or 7 leading to apoptosis by proteolysis of cellular substrates ((8, 10) and Figure 1). Cytochrome c is not the only pro-apoptotic factor released by mitochondria during stress. Apoptosis-inducing factor (AIF) and IAP-binding-motive (IBM)-domain proteins, like Smac/DIABLO, are released to fuel the apoptotic process. Smac/DIABLO inhibits IAPs (inhibitor of apoptosis), which are commonly overexpressed in tumors. The oncogenic IAPs are pro-survival proteins inhibiting caspase activation and promoting their degradation (11). Another mechanism to fine-tune the balance between cell survival and death provide the members of the B-cell lymphoma (Bcl) -2 family. Anti-apoptotic family members, such as Bcl-2 and Bcl-X_L, are membrane proteins especially found in the mitochondria, endoplasmatic reticulum (ER) and nuclear membranes. Pro-apoptotic members (e.g. Bax, Bad, Bim, Bid) are mainly localized in the cytosol and upon death signals translocate to the mitochondria membranes. By forming heterodimers of anti- and pro-apoptotic family members, the pro-apoptotic capacity is inhibited and thereby cytochrome c release prevented. Thus, the relative amount of the opposing family members influences the susceptibility of cells to death signals (12).

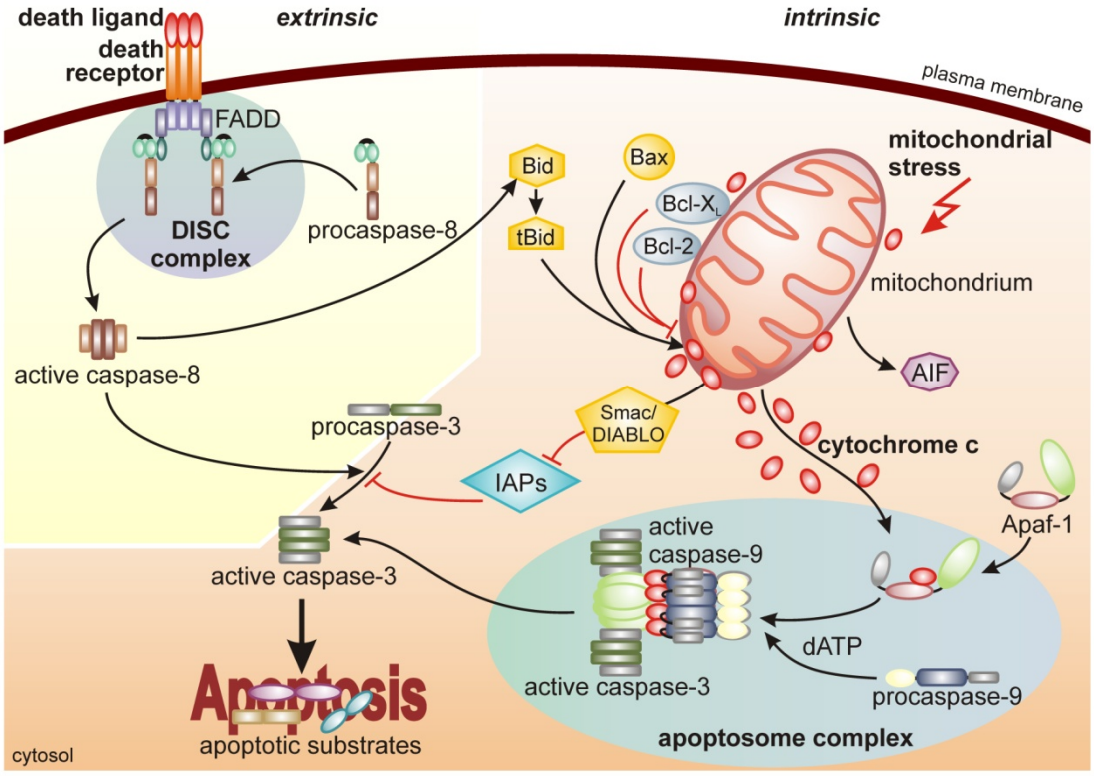

Figure 1: Apoptosis: the extrinsic and intrinsic pathway to caspase activation
The extrinsic pathway is triggered by members of the death receptor family. After binding of ligands, FADD and procaspase-8 are recruited and form the active DISC complex with functional caspase-8. Caspase-8 induces activation of pro-apoptotic Bid and of the effector caspases (e.g. caspase-3). The intrinsic pathway is used in response to DNA damage and extracellular stress. It results in perturbation of mitrochondria leading to release of potent pro-apoptotic proteins, such as cytochrome c, AIF and Smac/DIABLO. Smac/DIABLO inhibits the pro-survival properties of IAPs. Bcl-2 family members take part in regulating the release of cytochrome c. Cytosolic pro-apoptotic (e.g. tBid, Bax) or membrane bound anti-apoptotic (e.g. Bcl-2, Bcl-X_L) family members compete in tuning cytochrome c release. Once released into the cytosol, cytochrome c binds to Apaf-1 and together with procaspase-9 forms the apoptosome complex, resulting in effector caspase activation. Subsequent cleavage of cellular substrates finally results in apoptotic cell death. Abbreviations: AIF, apoptosis inducing factor; Apaf-1, apoptotic protease activating factor 1; Bax, Bcl-2 associated protein x; Bcl-2, B-cell lymphoma 2; Bcl-X_L, B-cell lymphoma extra long; IAP, inhibitor of apoptosis; DISC, death-inducing signaling complex; FADD, Fas-associated death domain protein; tBid, truncated Bcl-2 interacting domain death agonist; Smac/DIABLO, second mitochondria-derived activator of caspase/direct inhibitor of apoptosis-binding protein.

3.1.2 Cell death in health and disease

Disturbance within the apoptotic machinery results in pathological conditions. Insufficient apoptosis is observed in cancer and autoimmune diseases, whereas accelerated cell death is pronounced in degenerative diseases, immunodeficiency and infertility. Low affinity or autoreactive T and B cells are eliminated through apoptosis

to preserve a functional immune system. Defects in this mechanism result in B cell lymphomas and autoimmune diseases such as multiple sclerosis, rheumatoid arthritis, lupus erythematosus or diabetes (10, 13). Next to dysregulated apoptosis, insufficient clearance of apoptotic debris is a major factor in a variety of pathologies. Persistence of apoptotic debris is observed in atherosclerotic plaques and results in pro-inflammatory events fueling the disease (14). In regard to tumor biology, resistance to apoptosis is one of the hallmarks of cancer (Figure 41). Nevertheless, through rapid proliferation and lack of nutrients, solid tumors show marked apoptosis, and a correlation between high apoptosis indices in tumors and poor prognosis for patients has been observed (15, 16).

3.1.2.1 Soluble factors released by apoptotic cells and their implication in disease

Dying cells expose various molecules on their surface and release a variety of soluble factors. The context, in which cell death occurs, thereby determines the immune response. Apoptotic cells secrete 'find-me' signals, e.g. lysophosphatidylcholine (LPC), sphingosine-1-phosphate (S1P), adenosine triphosphate (ATP) and uridine triphosphate, to attract the major professional phagocytes – the macrophages (MΦ) (16). On the other hand, so called 'keep-out' signals, such as lactoferrin, are described to suppress the recruitment of neutrophiles and other granulocytes, which would foster inflammatory responses (17). Once phagocytes have found the apopotic cell, distinct 'eat-me' signals are presented to enable effective recognition, phagocytosis and immunologically silent removal of the cell to restore tissue homeostasis (18-20). Noteworthy, silencing of an inflammatory immune response to apoptotic cells does not necessarily require phagocytosis of the apoptotic cells. Recognition of phosphatidylserine or of apoptotic cell mediators was shown to be sufficient for phagocytes to produce anti-inflammatory factors, such as transforming growth factor-β (TGF-β), interleukin 10 (IL-10) or prostaglandin E2 (PGE2). Of note, not only the interaction of apoptotic cells with phagocytes establishes an immunosuppressive milieu, apoptotic cells themselves were shown to produce considerable amounts of the anti-inflammatory mediators mentioned above (16). Interestingly, many of the signaling molecules exert more than one function in the course of apoptotic cell clearance. Their pluripotency is necessary to guarantee appropriate responses and re-establishment of tissue function. Two of these versatile mediators are the 'find-me'

signals lactoferrin and the sphingolipid S1P, which have been described to inhibit pro-inflammatory mediators, promote expression of anti-inflammatory factors and function as growth and differentiation factors (16, 21).

3.2 Sphingosine-1-phosphate (S1P)

Sphingolipids are a class of cell membrane lipids, important for membrane integity. Some derivatives evolve as important lipid mediators in a growing body of cellular functions. One important member is the phosphosphingolipid S1P, a potent intracellular second messenger and extracellular receptor agonist, which has been identified more than 20 years ago (22). S1P derives from sphingosine (Sph), named in 1884 after the Greek mythological creature, the Sphinx, because of its enigmatic dual nature in structure as well as biological function. High S1P levels are found in the blood where it is mainly produced by erythrocytes and is bound primarily to chaperones such as HDL or albumin (23, 24). In other tissues its levels are generally very low, but can increase during injury and inflammation (25).

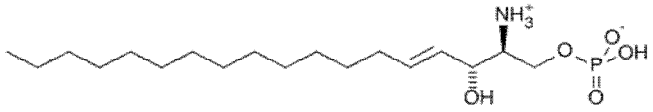

Figure 2: Sphingosine-1-phosphate (S1P)

3.2.1 S1P synthesis and secretion

De novo synthesis of sphingolipids originates at the cytoplasmic side of the endoplasmatic reticulum. Several paths lead to ceramide formation and subsequent conversion to sphingosine (Sph). Two sphingosine kinase isoforms SK1 and SK2 finally phosphorylate Sph to S1P. To tightly regulate S1P levels, the phosphosphingolipid can be either irreversibly degraded by S1P lyase to hexadecenal and phosphoethanolamine or reversibly dephosphorylated by S1P phosphatase back to Sph (24, 26, 27).

Certain growth factors, hormones and cytokines such as vascular endothelial growth factor (VEGF) , nerve growth factor (NGF), estradiol, tumor necrosis factor α (TNF-α) or transforming growth factor β (TGF-β) and others are known to stimulate SK1 activity (28). Activation and translocation of SK1 to the plasma membrane leads to S1P production and subsequent secretion of S1P was found to be facilitated by several transporters such as ATP-binding cassette (ABC)-transporters (29-31) and spinster homolog 2 (Spns2) (32). Furthermore, SK1-dependent S1P production and release by

apoptotic cells was described as “come-and-get-me” signal for phagocytes to remove dying cells (33). Work from our group demonstrated the necessity of SK2 for the production of S1P by apoptotic cells (34), thereby release of a truncated form of SK2 during apoptosis was crucial for S1P production (35). In line, catalytically active SK1 was found in plasma from mice (36) and degradation of sphingomyelin to sphingosine at the outer leaflet of the plasma membrane is known ((37) and Figure 3).

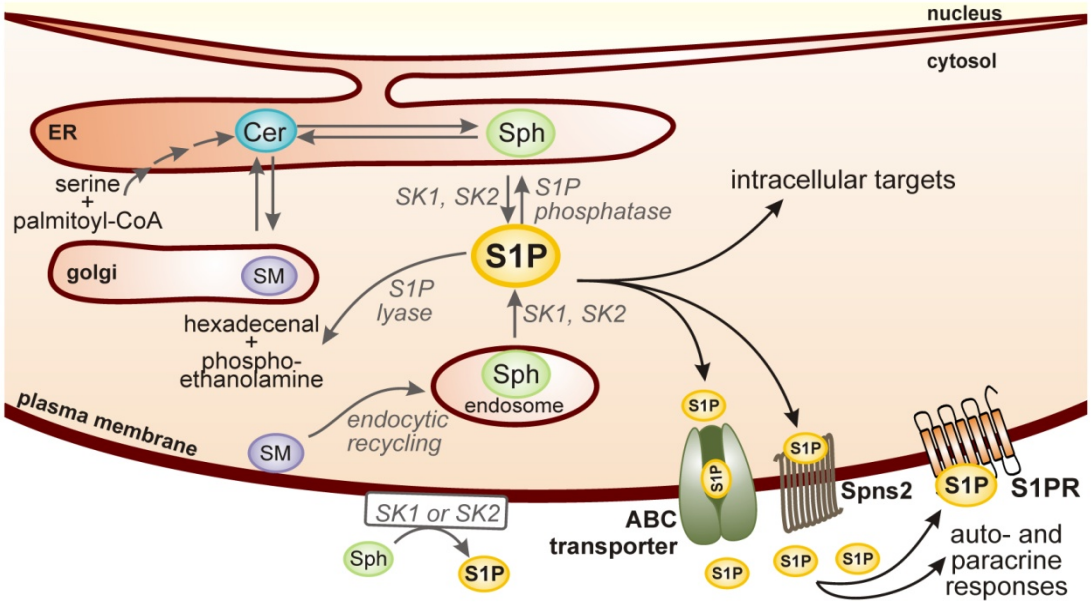

Figure 3: Sphingosine-1-phosphate synthesis and export
De novo synthesis of sphingolipids is initiated at the endoplasmatic reticulum (ER) through multiple enzymatic steps forming ceramide (Cer). Sphingosine (Sph) can also arise from endocyclic recycling of the plasma membrane component sphingomyelin (SM). Both paths join in the conversion of Sph by sphingosine kinases 1 or 2 (SK1/2) to S1P, which can be either converted back to Sph or irreversibly degradated by S1P lyase. S1P exerts intracellular functions or is transported out of the cell by ATP-binding cassette (ABC) transporters or Spinster homolog 2 (Spns2). Additionally, S1P can be synthesized at the outer leaflet of the plasma membrane. Extracellularly, it binds to ligand specific G protein-coupled S1P receptors (S1PR) to induce downstream signaling events and cellular responses. Adopted from (25, 26, 35).

3.2.2 S1P function

S1P regulates diverse physiological and immunological processes by signaling through at least 5 G protein-coupled receptors (S1PR1-5) or by acting as second messenger on intracellular targets. In a physiological context, S1P is vital in embryonic development of the central nervous and cardiovascular system by orchestrating several complex biological circuits such as survival, proliferation and migration (38).

3.2.2.1 Intracellular functions of S1P

One early discovered role of S1P was its negative regulation of cell death compared to the pro-apoptotic ceramide, termed the 'sphingolipid rheostat', determining the cell's fate (39). The two S1P-producing isoforms SK1 and SK2 differ in their kinetic properties, subcellular localization and tissue distribution. They show some redundancy as single knockout mice are viable and reproduce whereas simultaneous knockout of both isoforms is lethal (40). Differential intracellular effects are reported for S1P derived from the two isoforms, but substantiated studies in physiological contexts are lacking. Recently, detailed intracellular actions of SK1, SK2 and S1P were unravelled by Sarah Spiegel and coworkers. They indicated S1P as a co-factor for TNF-α receptor-associated factor 2 (TRAF2), leading to activation of nuclear factor 'kappa-light-chain-enhancer' of activated B cells (NFκB) (41). Another study elucidated SK2 and S1P assembly with histone deacetylase 1 and 2 (HDAC1-2) resulting in up-regulation of p21 and c-fos (42). However, intracellular targets of S1P remain largely elusive.

3.2.2.2 Extracellular receptor mediated functions of S1P

After release, S1P selectively binds with affinities ranging from 2 nM to 63 nM to its receptors (S1PR1-5) for autocrine or paracrine signaling (43). S1PR1, 2 and 3 are nearly ubiquitously expressed, whereas S1PR4 and 5 show tissue-specific distribution. This correlates with the observation that in mice only knockout of S1PR1 or double knockout of S1PR2 and 3 are embryonically lethal (44). S1PR1 and 2 show similar expression patterns, S1PR3 is highest in the cardiovascular system (45), S1PR4 is predominantly found on lymphoid cells (46) and S1PR5 seems to be restricted to NK cells (47), dendritic cell subsets (48) and the central nervous system (49). Downstream of the G protein-coupled S1P receptors activation of Gi for S1R1, Gi, Gq, G12/13 for S1PR2 and 3 and Gi, G12/13 for S1PR4 and 5 is reported. This results in multiple and complex downstream signaling cascades, including small GTPase modulation (Rac and Rho), adenylate cyclase (AC) activation or inhibition, phospholipase C (PLC) activation and intracellular calcium mobilization, together with AKT and extracellular signal-activated-kinase (ERK) phosphorylation events, as shown in Figure 4. Corresponding to differences in activated G proteins, stimulation of S1P receptors especially S1PR1 and S1PR2 sometimes triggers adverse effects. E.g. S1PR1 signaling stimulates migration

through Rac activation, whereas S1P can inhibit cancer cell motility through S1PR2-dependent regulation of Rho (50). Nevertheless, S1PR2-mediated cell invasiveness has also been reported (51). In addition to these various signals, transactivation of or by other signaling systems, or generation and secretion of additional factors are known, adding complexity to the S1P/S1PR system (25, 52).

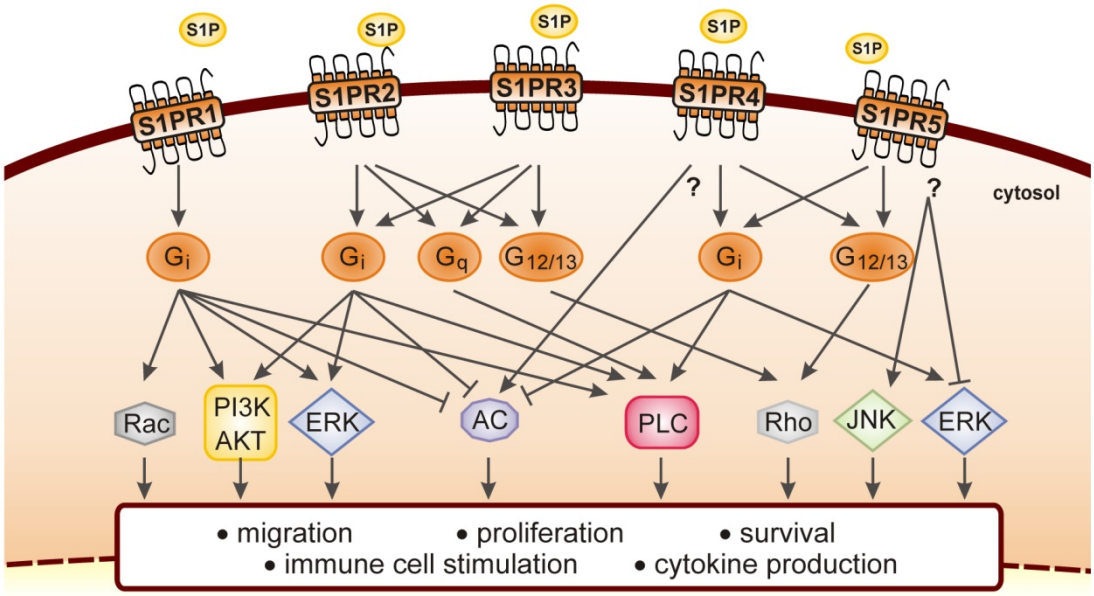

Figure 4: S1P/S1P receptor signaling
Extracellular S1P selectively binds to 5 S1P specific receptors S1PR1-5. Downstream of the receptors multiple signaling pathways are activated or inhibited, either directly or through G proteins (Gi, Gq or G12/13), resulting in a variety of cellular responses. Abbreviations: AC, adenylate cyclase; AKT, protein kinase B; ERK, extracellular signal-regulated kinases; JNK, jun N-terminal kinase; PI3K, phosphatidylinositol-3 kinase; PLC, phospholipase C; Rac, Rho, family members of Rho GTPase; S1P, sphingosine-1-phosphate. Adopted from (25, 50, 53).

3.2.2.3 Physiological function of S1P receptor signaling

S1P is a key player in neurogenesis, cardiac function, maturation of the vascular system, blood vessel permeability and pathophysiological angiogenesis.

Angiogenesis is strongly dependent on S1P, as knockout of S1PR1 is embryonic lethal due to migration failure of vascular smooth muscle cells (54). Immune cell migration is another critical attribute of this sphingolipid. Lymphoid organs show low S1P levels compared to high concentrations in the circulation. This gradient and the expression of S1PR1 on lymphocytes are requisites for lymphocyte egress (55). In contrast, S1PR4 activity was not connected to migration, but affected cytokine secretion of S1P-stimulated T cells. S1P coupling to S1PR4 enhanced IL-10, which replaced inflammatory and proliferative cytokines (IFNγ, IL-2, IL-4) to create an

immunosuppressive milieu (56). A newly FDA approved therapy for multiple sclerosis takes advantage of this S1P/S1PR1-mediated T cell migration. The sphingosine analogue FTY720 (fingolimod, Gilenya™) is intracellularly phosphorylated by SK2 and released as FTY720-phosphate (FTY-P). The active derivative is then able to bind all S1P receptors except for S1PR2. It induces lymphopenia by receptor internalization and degradation, thereby inhibiting egress from lymph nodes. Consequently, an attack of autoreactive lymphocytes on the central nervous system is prevented. Additionally, FTY-P reduces inflammatory cytokine release by astrocytes and might have pro-survival functions on oligodendrocytes and neurons (27, 57). Other immunological functions of S1P include enhancing dendritic cell (DC) localization at the site of antigen uptake (58) and anti-inflammatory properties of NK cells by inhibiting NK cell-mediated cell lysis and release of inflammatory cytokines (59). The detailed effects of S1P on MΦ are summarized in *3.3.3* and in the presented experimental work herein.

3.2.2.4 S1P and cancer

In most cancer cells SK1 is upregulated by diverse mechanisms such as activation through growths factor signaling, lack of nutrients, or hypoxia. S1P exerts powerful pro-tumor function e.g. protection from apoptosis, facilitation of cell transformation, induction of proliferation, migration and promotion of angiogenesis ((60) and Figure 5). These effects are mediated either by intracellular actions of S1P, or by extracellular receptor-mediated processes. Several mechanisms of transactivation, functional complex formation, SK induction, or autocrine loops of growth factors interacting with S1P and the corresponding receptors are described (50). As one example, epidermal growth factor (EGF) was shown to stimulate the expression of SK1 and/or SK2 to induce cell migration (61, 62). S1P in turn was reported to augment EGF receptor (EGFR) expression and to facilitate EGF release from cells for activation of EGFR (63, 64).

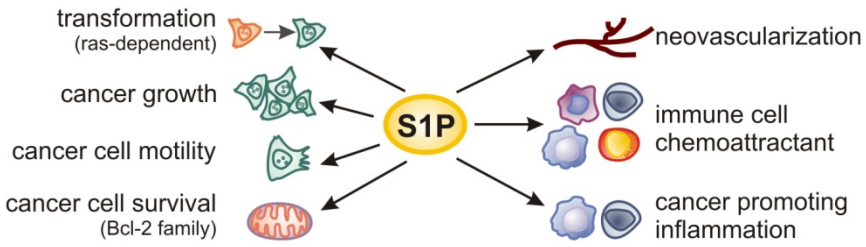

Figure 5: S1P action in cancer
Multiple processes in the course of cancer are influenced by S1P, including cell transformation, cancer cell growth, survival and motility. Neovascularization, immune cell attraction and cancer promoting inflammation are further attributed to S1P. Abbreviations: Bcl-2, B-cell lymphoma 2; ras, rat sarcoma; S1P, sphingosine-1-phosphate. Adopted from (50).

To target S1P signaling for cancer therapy, a S1P-neutralizing antibody (sphingomab) was used in murine xenograft models. Diminished tumor volume and reduced pathology-associated parameters were achieved (65). The humanized highly specific anti-S1P antibody (sonepcizumab, ASONEP™) was recently investigated as a single agent in a Phase I trial in refractory advanced solid tumor patients. Sonepcizumab is also tested in clinical trials for age-related macular degeneration, caused by new leaky blood vessel growth, and shows superior effects to standard anti-VEGF treatment (60). Additionally, phosphorylated FTY720 has been shown to have anti-cancer properties (66, 67), to provoke cancer cell-selective apoptosis (68) and to reduce tumor vascularization (69, 70). Interestingly, also the prodrug FTY720 was shown *in vitro* to have anti-proliferative effects on cancer cells, arguing for an S1PR-independent effect (71). Unfortunately, referring to www.clinicaltrials.gov, no clinical trials in regard to FTY720 and cancer are performed or planned in the near future.

To add an additional layer of complexity, S1P not only contributes to tumor growth by influencing tumor and stromal cells, but also by its impact on immune cells present in the tumor microenvironment (Figure 5). One major immune cell type in this context is the macrophage.

3.3 Macrophages

Inflammation is an immune response to exogenous or endogenous noxious stimuli, such as microbial products, allergens, or signals released from stressed or dead cells (72). The immune response is divided into adaptive and innate immunity. Tissue-resident macrophages (MΦ) are the first innate immune cells encountering noxious stimuli. Through their large repertoire of receptors, MΦ recognize pathogens, cellular

danger signals or adaptive immunity-derived immunomodulators. Consequently, MΦ produce of a wide array of inflammatory mediators such as chemokines and cytokines to evoke immune responses. Thus, additional innate immune cells, mainly neutrophils and monocytes, are recruited from the blood stream for further release of cytotoxic factors, phagocytosis and clearance of the inflammatory stimulus. Through phagocytosis, digestion and subsequent antigen presentation, MΦ are an important link between the immediate unspecific innate immune response and the delayed, highly antigen-specific adaptive immunity mediated by T and B cells. Finally, when the noxious stimulus is eradicated, MΦ adapt their machinery to repair tissue damage and to restore homeostasis by secreting proteases and growth factors (72-74).

MΦ originate from myeloid progenitor cells in the bone marrow. In the presence of myeloid cytokines as granulocyte macrophage colony-stimulating factor (GM-CSF) or macrophage colony-stimulating factor (M-CSF), the progenitor cells differentiate into monocytes. These migrate into the blood, from where they can be rapidly recruited to peripheral tissues where they finally differentiate into mature MΦ with distinct features and functions depending on the microenvironment of their destination. Some tissues show 10-20% resident MΦ, such as microglial cells in the brain or Kupffer cells in the liver. As summarized in Table 1, MΦ exert vital function in almost every organ.

Table 1: Diversity of tissue macrophages

Tissue	Tissue-specific designation	Function	Ref.
Bone	Bone marrow macrophage	Erythropoiesis	(75)
	Osteoclast	Bone remodelling	(76)
Brain	Microglial cell	Neuronal development, survival and repair	(77)
Epidermis	Langerhans cell (more dendritic cell phenotype)	Immune surveillance	(78)
Eye		Vascular modelling/ remodelling	(79)
Gut		Immune-tolerance	(80)
Kidney		Organ development, injury, repair	(81)
Liver	Kupffer cell	Clearance of debris from blood and liver tissue, liver regeneration, pathogen killing	(82)
Mammary gland		Branching and ductal development, postpartum mammary involution	(83, 84)
Ovary		Steroid hormone production and ovulation	(76, 85)
Pancreas		Islet development	(86)
Uterine desidua		Maternal immune tolerance to fetus	(87)
Uterus		Cervical ripening, remodeling	(88)

3.3.1 Macrophage phenotypes

The remarkable degree of heterogeneity in MΦ and their specialized functions are due to the impact of microenvironmental factors they encounter at the site of residence (89). Two rather opposing microenvironments are the pathogen-rich gut and the blood brain barrier-protected brain. In the pathogen-rich milieu of the gut, the immune response of the resident MΦ is blunted, shown by defects in toll-like receptor (TLR) responses, while preserving their bactericidal capacity to establish tolerance (80). On the other hand, MΦ in tissues with low pathogen exposure, such as microglia in the nervous system, are highly sensitive to environmental alterations. They respond to changes by chemokine release to orchestrate the infiltration of peripheral immune cells, phagocytic activity or cytokine or neurotrophin release for neuroprotection (77). These MΦ rather function as sentinels as compared to the barrier-building intestinal or alveolar macrophages.

Although MΦ are well adapted to the needs of distinct environments, they are still highly plastic. At sites of tissue injury, where the local microenvironment is disturbed, MΦ are activated by recognition of danger signals and acquire a phenotype denoted as 'classically activated MΦ', which was first described by Mackaness (90). Danger signals relevant in this process are microbial products, such as the TLR4 agonist lipopolysaccharide (LPS), adaptive immunity-derived cytokines such as interferone γ (IFN-γ), or mediators leaking from damaged cells, such as ATP (91) or high-mobility group box (HMGB)1 protein (92). *In vitro*, these MΦ can be generated by stimulation with the microbial cell wall component LPS or tumor necrosis factor (TNF)-α in combination with interferon (IFN)-γ. This results, amongst others, in the production of nitric oxide (NO) and superoxide, which are necessary for pathogen killing, as well as the release of proinflammatory cytokines such as TNF-α, IL-1β and IL-12 to activate bystander immune cells (74).

Identification of a distinct MΦ subpopulation, which was generated by IL-4 receptor activation led to coining the term 'alternatively activated' MΦ, based on a different surface marker and secretome profile compared to classically activated MΦ (93). This discovery of MΦ heterogenicity resulted in extended mostly *in vitro* research on different MΦ populations depending on stimulation with various immunomodulatory agents. To avoid the arising confusion regarding the different use of terminology to describe these MΦ subpopulations, several attempts to develop a common classification were undertaken during the last ten years. Gordon and coworkers proposed five subclasses of MΦ (74). Beside classically (LPS and IFN-γ) and alternatively activated (IL-4/IL-13) MΦ, innate activation due to microbial stimuli without IFN-γ, humoral activation by Fc or complement receptor agonists and deactivation by immunosuppressive cytokines such as IL-10 and transforming growth factor (TGF)-β or apoptotic cells were proposed.

Alternatively, Mantovani grouped MΦ phenotypes in analogy to the T helper cell nomenclature along a linear scale into M1 macrophages (classically activated) or M2 (alternatively activated) MΦ (94). M1 MΦ are generated (as classically activated MΦ from Gordon) by stimulation with IFN-γ and LPS or TNF-α and are characterized by an IL-12^{high}/IL-10^{low} profile, together with production of NO, reactive oxygen species (ROS), IL-1, TNF-α, IL-6 and expression of major histocompatibility complex class (MHC)

II important for pathogen killing and tumor resistance. M2 MΦ, which all share the IL-10^{high}/IL-12^{low} profile and show immunoregulatory and tumor promoting functions, were further divided into M2a, M2b and M2c subclasses. M2a MΦ match Gordon's alternatively activated macrophages with expression of MHC II, mannose receptor, scavenger receptor, production of polyamines and IL-1 receptor antagonist (IL-1ra). These M2a MΦ are especially involved in Th2 response inflammation, allergy and helminth infection. M2b MΦ are comparable to humorally activated cells (stimulated with immune complexes and TLR or IL-1 receptor ligands) and show enhanced secretion of inflammatory cytokines TNF-α, IL-1 and IL-6 with concomitant high IL-10 and low IL-12 expression. This MΦ subset was shown to protect mice against LPS toxicity and promoted Th2 differentiation and antibody production. As the last M2-family subgroup, M2c MΦ were proposed to arise from stimulation with IL-10 (corresponding to deactivated macrophages). By secretion of IL-10, transforming TGF-β and matrix components these MΦ are thought to be especially involved in immunoregulatory processes and tissue remodelling (94).

The above described models, especially the rough M1/M2 classification, might be useful to avoid confusion. However, the focus of these classifications is on the mediators shaping distinct MΦ phenotypes rather than on the physiological outcome, which might be similar for different 'phenotyping' stimuli. On this account, Mosser and Edwards recently classified MΦ along three functional states in analogy to the three primary colors in a color wheel. They discriminated classically activated (analogous to M1) from wound healing (analogous to alternatively activated or M2a) and regulatory or anti-inflammatory macrophages. This model allows the occurrence of 'hybrid-type' macrophages corresponding to secondary colors in the color spectrum (95). Thereby, it depicts very nicely the infinite number of possible MΦ subtypes, mirroring the *in vivo* situation where an array of factors influences MΦ activation. Figure 6 tries to summarize the functional activation states of MΦ. Noteworthy, a recent report on tumor-associated MΦ in a murine carcinoma model substantiates the proposal of Mosser and Edwards, as these MΦ showed simultaneous expression of 'typical' M1 and M2 characteristics (96).

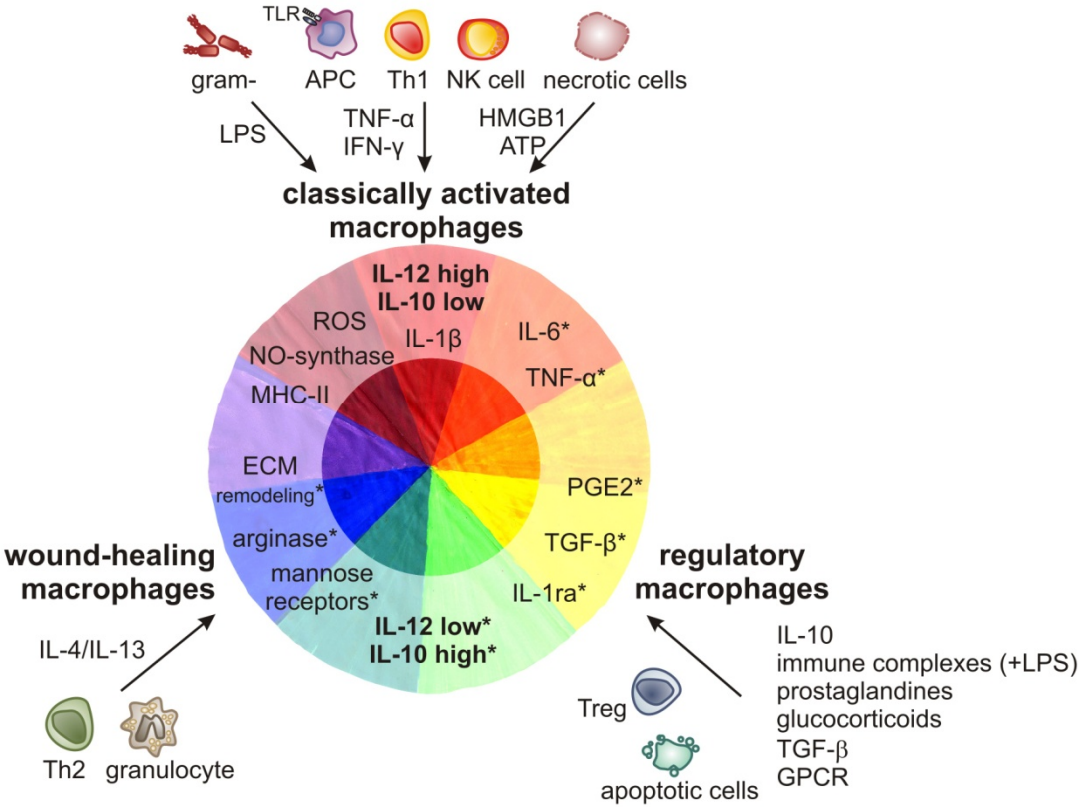

Figure 6: Macrophage phenotypes

Microenvironmental factors shape the functional phenotype resulting in a dynamic repertoire of MΦ represented by all secondary color variations, with rough distinctions between classically activated MΦ (primary color red) expressing inflammatory mediators, wound-healing MΦ (primary color blue) and regulatory, anti-inflammatory MΦ (primary color yellow). Factors and cells mediating one of the basic MΦ phenotypes are depicted, as well as typical factors/receptors/enzymes expressed by these MΦ. Characteristics marked with * are common for tumor-associated MΦ. Abbreviations: APC, antigen-presenting cell; ATP, adenosine triphosphate; ECM, extracellular matrix; GPCR, G protein-coupled receptor; HMGB1, high-mobility group box 1; IFN-γ, interferon gamma; IL, interleukin; IL-1ra, IL-1 receptor antagonist; LPS, lipopolysaccharide; MΦ, macrophage; NK cell, natural killer cell; NO, nitric oxide; ROS, reactive oxygen species; PGE2, prostaglandin E2; TGF-β, transforming growth factor beta; Th1/2, type 1/2 T helper cell; TLR, toll-like receptor; TNF-α, tumor necrosis factor alpha; Treg, regulatory T cell. Adopted from (95, 97, 98).

3.3.2 Cancer-immunoediting and tumor-associated macrophages

3.3.2.1 Cancer-immunoediting

In 1909 Paul Ehrlich introduced a connection between immunology and cancer by stating that the immune system scans the body for transformed cells to eliminate them (99). Unfortunately, this proposal of protective immunosurveillance was proven not to be true. By the 1990s, sophisticated mouse models permitted to reassess the role of immunity in cancer, which led to the term ‘immunoediting’ to describe the

sequential phases of cancer elimination, equilibrium and escape (100). In the elimination phase, characterized by cancer immunosurveillance, innate and adaptive immune cells detect and destroy transformed cells before the tumor becomes clinically apparent. Expression of tumor antigens, release of IFN-γ, or HMGB1 activate innate immune cells to release pro-inflammatory cytokines and to develop a tumor-specific adaptive immune response (101). In this early stage of carcinogenesis, MΦ show an inflammatory anti-tumoral M1 phenotype with pronounced IL-12, TNF-α and ROS production (102, 103). If some tumor cells persist and escape the initial elimination phase, they may enter the so-called equilibrium phase where tumor growth and adaptive anti-tumor responses are in balance resulting in cancer dormancy. This phase is thought to be the longest in the cancer immunoediting process and may, in many cases, extend throughout life of an individual and may explain years of latency between first cancer prognosis, therapy and final metastatic outgrowth (104). Nevertheless, some poorly immunogenic and highly proliferative tumor cells may escape the equilibrium phase. Constant selection of transformed cells leads to reduced immune recognition and increased resistance to cytotoxic immune-derived factors. These tumor cells arise as aggressively growing tumors, often characterized by expression of pro-oncogenic transcription factors, such as signal transducer and activatior of transcription (STAT) 3 or anti-apoptotic proteins of the Bcl-2 family (101). The pro-tumoral microenviroment in the escape phase is predominated by tumor-associated-macrophages (TAM) fostering a tumor-supportive milieu ((98) and Figure 7).

3.3.2.2 Tumor-associated macrophages

In many human tumors, especially breast cancer, MΦ can make up to 50% of the tumor mass and a high density of tumor-associated macrophages (TAM) often correlates with poor prognosis (105). A variety of signals were shown to be implicated in the recruitment and differentiation of these tumor-promoting MΦ, among them are factors released by tumor cells such as IL-10, M-CSF or TGF-β (103). Additionally, overexpression of the primary monocyte/MΦ proliferation and differentiation factors M-CSF and monocyte chemoattractant protein-1 (MCP-1, CCL2) have been linked to disease progression and poor prognosis (106-109). Furthermore, $CD4^+$ T cells were shown to release IL-4 to promote TAM generation in pulmonary metastases of

mammary carcinomas (110). IL-10 and TGF-β derived from regulatory T cells further fuel the immunosuppressive tumor microenvironment and TAM generation (111). Hypoxia within tumors is another important feature. Many tumor-promoting and immunomodulatory genes are regulated through hypoxia-inducible factors (HIFs) thereby facilitating further tumor growth (112). Manifold factors in the tumor-environment lead to TAM generation and TAM exert manifold functions in promoting the malignancy, e.g. immunosuppression, angiogenesis, tumor cell survival, proliferation and invasion (98). To simplify, I will only concentrate on the best described and most pronounced functions and factors released by TAM.

In general, TAM have a phenotype similar to alternative M2 MΦ with a typical IL-10^{high}/IL-12^{low} expression pattern, which is mainly responsible for establishing and maintaining the immunosuppressive environment (Figure 6). Additionally, immuno-suppression is achieved by induction of indoleamin 2,3-dioxygenase (IDO) in tumor cells, DCs and TAM (113). IDO converts tryptophan into metabolites known as kynurenines and thereby tryptophan in the vicinity is depleted. IDO activity has fundamental consequences for T cell populations. Clonal expansion of $CD8^+$ and $CD4^+$ T cells as well as the generation and activation of cytotoxic T cells and Th1 cells is blocked, due to the lack of tryptophan. Conversely, *de novo* Treg differentiation is promoted, shifting T cell populations to tumor-promoting subsets (114). Furthermore, enhanced secretion of TGF-β and prostaglandin E2 (PGE2) add to suppression of the adaptive immune response (115). To nourish solid tumor growth, established immunosuppression cooperates with further pro-tumoral functions of TAM. Among others, angiogenesis is a decisive step in the progression of cancer, as the highly proliferative cancer cells need abundant oxygen and nutrients. TAM produce and release high amounts of angiogenic factors, such as VEGF, EGF and IL-8. Moreover, many TAM-derived factors directly promote cancer cell survival and proliferation, the best described are EGF, IL-6, IL-8 and other growth factors. To substantiate disease progression, TAM engage in the remodelling of the extracellular matrix (ECM) and the breakdown of the basement membrane surrounding pre-metastatic tumors, thus, facilitating local growth, invasion and distant metastases. (97, 98, 116-119). In conclusion TAM express a multitude of factors promoting all aspects of tumor progression, as summarized in Figure 6 and Figure 7.

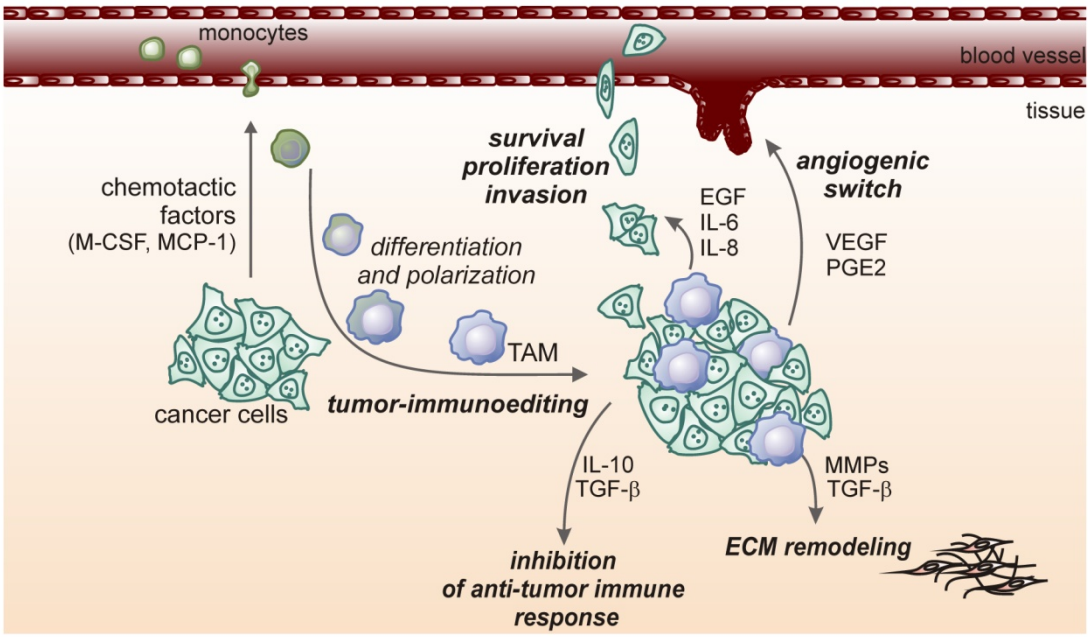

Figure 7: Macrophages in the tumor environment

By secretion of various chemotactic factors, cancer cells recruit monocytes from the blood stream to the tumor site. In the course of tumor-immunoediting tumor cells succeed to evade the cytotoxic immune response, and a tumor-promoting immune environment is established. Differentiated macrophages acquire an anti-inflammatory, immunosuppressive, tumor-promoting phenotype. These so called TAM foster cancer cell survival, proliferation, invasion, metastasis, angiogenesis, facilitate ECM remodeling and inhibit the anti-tumor immune response by the release of various factors. Abbreviations: ECM, extracellular matrix; EGF, epidermal growth factor; IL, interleukin; MCP-1, monocyte chemotactic protein-1; M-CSF, macrophage colony-stimulating factor; MMP, matrix metalloproteinase; PGE2, prostaglandin E2; TAM, tumor-associated macrophages; TGF-β, transforming growth factor beta; VEGF, vascular endothelial growth factor.

3.3.3 Function of S1P on macrophages

Inflammatory as well as regulatory MΦ were shown to express high levels of SK1 mRNA (120, 121). However, functional significance is on modulation of SK activity. Inflammatory mediators, such as TNF-α or LPS, activate SK1 in MΦ as a component of inflammatory responses (122-124) by TRAF2-dependent NF-κB activation (41, 125). The relevance and mechanistics of SK1 in inflammatory diseases requires extensive research. Divergent effects in different disease models might be explained by its localization, interaction with other factors, transcription factors and finally the localization and effect of S1P, either acting as intracellular signaling molecule, intracellular receptor ligand or by exhibiting extracellular functions (21, 126).

MΦ express S1P receptors to different extents depending on the species and maturation state. Murine MΦ express S1PR1, S1PR2 (127) and S1PR3 (128), whereas S1PR1-4 are expressed in the human counterparts (129). In this context, MΦ attraction, protection from apoptosis and MΦ phenotyping has been assigned to the potent phospholipid S1P (21, 38). In contrast to the primarily inflammatory intracellular properties of S1P, binding of extracellular S1P to S1PR1 blocked LPS-mediated NF-κB activation and the concomitant production of TNF-α and IL-12 in murine and human MΦ. In addition, induction of anti-inflammatory IL-10 as well as TGF-β was observed through S1PR signaling (127, 130). For long, STAT3 has been recognized for its central role in oncogenic signaling pathways, being constitutively active in tumor cells as well as immune cells of the tumor environment. By a 'vicious circle' IL-10, as well as IL-6, activate STAT3 signaling. STAT3, in turn, promotes the production of immunosuppressive factors and restrains inflammatory responses leading to a tumor-promoting environment (131). Recently, STAT3 activation in tumors was shown to enhance S1PR1 expression and in turn S1P/S1PR1 led to persistent STAT3 activation in both tumor cells and tumor-associated myeloid cells, promoting tumor growth and metastasis (132). In human MΦ STAT3 activation was achieved by apoptotic cell (AC)-derived S1P binding to S1PR1, leading to induction of heme oxygenase-1 and adenosine receptor A2A (ADORA2A) (133). In the same model of MΦ stimulated with apoptotic cell supernatant (ACM), S1P together with TGF-β induced HIF-1α mRNA under normoxia, concomitant with augmented VEGF mRNA and differentiation of embryonic stem cells to $CD31^+$ cells (134). Other studies showed S1P-mediated increase in arginase 1 and 2 via cyclic AMP (cAMP) /cAMP responsive element binding (CREB) signaling as characteristics of alternative MΦ activation (127, 135). Elevation of cAMP and subsequent decrease in inflammatory responses of different MΦ cell lines have also been reported for catecholamines, dopamine and other neuromediators, signaling through G_s-coupled receptors (136). These reports collaborate with the notion of cAMP being a major determinant of anti-inflammatory MΦ activation in mice (137). On the other hand, studies demonstrated that S1PR2-deficient MΦ from apoE knockout mice showed reduced NF-κB activity and reduced inflammatory cytokine production (138, 139).

In summary, S1P exerts a powerful impact on MΦ activation, either by intracellular inflammatory actions or by binding to its receptors provoking pro- or anti-inflammatory responses. Whether S1P drives MΦ to an inflammatory or anti-inflammatory phenotype depends on the expression pattern of S1P receptors on MΦ and other factors influencing MΦ activation, which are present in the microenvironment of the chosen disease model or in the *in vitro* used combination of stimuli e.g. ACM.

The work on apoptotic cell-derived S1P and reports from others with the same notion of S1P screwing MΦ population towards an anti-inflammatory or alternatively activated phenotype, highlights the potential impact of S1P on MΦ function in tumors.

3.4 Interleukin 10

Cytokines are a heterogeneous group of secreted, soluble polypeptides and glycoproteins. They are pleiotropic mediators promoting growth, differentiation, activation and migration. Immune cells are the major source. Nontheless, other cells have the capability to produce cytokines as means of communication. Depending on the source and the microenvironment, the secreted factors have either pro- or anti-inflammatory/immunosuppressive effects. Thus, cytokines are engaged in all inflammation-associated diseases, such as rheumatoid arthritis, multiple sclerosis, inflammatory bowel disease, diabetes and cancer (140).

Interleukins (IL) belong to the superfamily of cytokines (141). IL-10 was originally discovered by Mosmann and colleagues as product of Th2 cells inhibiting cytokine synthesis of Th1 cells and was named cytokine synthesis inhibitory factor (CSIF) (142). IL-10 is expressed by a wide range of cells of the adaptive and innate immune system and even non-immune cells including epithelial and tumor cells (143). The IL-10 gene encodes a polypeptide of 178 amino acids and functional IL-10 protein is a noncovalent homodimer of two 18 kDa subunits (144, 145). The functional receptor complex consists of two subunits of IL-10 receptor 1 (IL-10R1) and IL-10R2 and is expressed by most cells of hematopoetic and non-hematopoetic origin. IL-10 binds to two IL-10R1 and through recruitment of IL-10R2 the functional complex is formed and signal transduction, mainly via the janus kinase JAK/STAT3 pathway, can occur (146).

3.4.1 Function of IL-10

IL-10 influences expression of cytokines, growth factors and cell surface molecules and has strong anti-inflammatory, immunosuppressive properties. The relevance of IL-10 is drastically shown in IL-10 deficient mice, which spontaneously develop chronic enterocolitis (147) and IL-10 receptor mutations were found in colitis patients (148). Along this line, IL-10 null mice were shown to succumb to CNS inflammation (149). During infection with viruses, bacteria, fungi, protozoa or helminths IL-10 serves as key immunoregulator. Excessive T cell responses are suppressed by IL-10 through inhibition of IL-2 production, important for T cell development and activation, and through suppression of pro-inflammatory cytokines. On the other hand, IL-10 strongly induces regulatory T cell differentiation and function. Furthermore, IL-10 acts as a potent B cell stimulator, enhancing activation, proliferation and differentiation of B cells. Looking at the various effects of IL-10 on immune cells, over- or mistimed IL-10 production might lead to immune evasion of pathogens, resulting in fast disease progression with either fatal outcome or chronic manifestation (150).

One major attribute of IL-10 is the ability to diminish antigen presentation by monocytes, MΦ and DCs and subsequent T cell activation. Cell surface expression of major histocompatibility complex class 2 (MHC-II) and costimulatory CD80 and CD86 molecules, among others, are reduced (151). Interestingly, the phagocytic capacity of monocytes and MΦ is enhanced by IL-10, although the ability to kill the ingested pathogen is hampered, due to decreased production of ROS and NO. The reduced antigen presentation and killing capacity creates a niche for specialized intracellular pathogens, such as the cytomegalovirus and mycobacterium tuberculosis (152). In regard to soluble factors, such as cytokines and chemokines, IL-10 potently inhibits the production of pro-inflammatory cytokines and enhances the production of IL-1ra as well as soluble TNF receptors by MΦ. Together with the suppressed production of a wide array of chemokines implicated in recruitment of inflammatory immune cells, IL-10 establishes an anti-inflammatory, immunosuppressive environment (151) important in gut homeostasis, chronic infection and cancer promotion.

3.4.2 Regulation of IL-10 expression

IL-10 employs a multitude of mechanisms to control inflammatory responses and is expressed by various cells. Due to this, its expression needs to be tightly regulated and

kept at a beneficial level for the organism. In MΦ, its production is triggered by diverse stimuli, through signal transduction downstream of TLR (153), Fc receptor ligation (121), activation of receptor tyrosine kinases (154, 155), G protein-coupled receptors such as adenosine receptors (156), various neuromediator receptors (136), as well as interaction with apoptotic cells (AC) (157, 158) or apoptotic cell derived factors e.g. S1P (130). Consequently, a multitude of signaling pathways and post-transcriptional regulations are described to influence IL-10 expression (143, 159, 160). Transcription factors such as STAT3 (161, 162), specificity protein (SP)1 and SP3 (163, 164), activator protein (AP)-1 (165), CCAAT/enhancer-binding proteins (C/EBP) (166, 167) and CREB (168) are reported for IL-10 promoter activation. Furthermore, immune complex-binding to Fcγ receptors led to ERK-dependent modification of histone H3 within the IL-10 promoter rendering the promoter more accessible for SP1 and STAT3, which resulted in very rapid IL-10 production (169). Feed-forward loops, such as the autocrine induction of IL-10 by itself (162) or regulatory circuits involving inflammatory cytokines like TNF-α (170) add additional levels to the regulation of IL-10. The most established regulators are summarized in Figure 8.

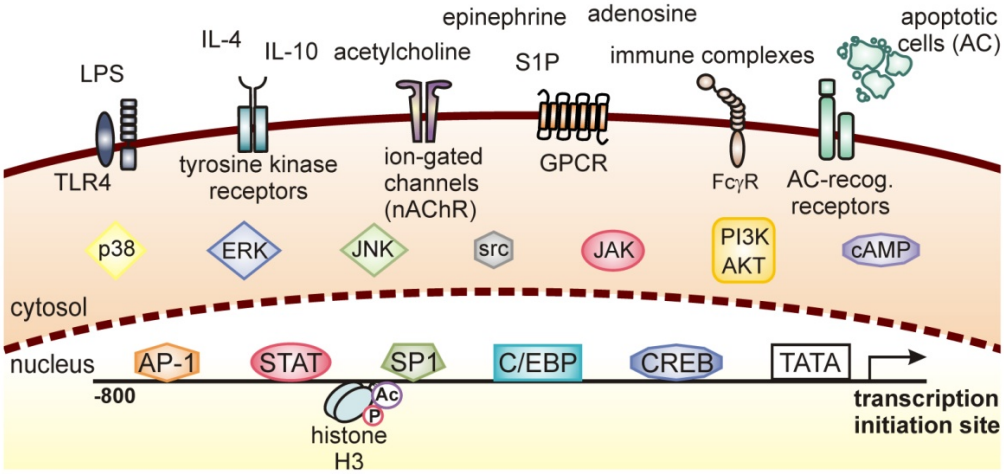

Figure 8: IL-10 regulation in macrophages

Summary of well known ligands, receptors, signaling molecules and TFs in IL-10 transcriptional regulation. Abbreviations: AKT, protein kinase B; AP-1, activator protein-1; cAMP, cyclic adenosine monophosphate; C/EBP, CCAAT/enhancer-binding protein; CREB, cAMP response element binding; ERK, extracellular signal-regulated kinases; FcγR, fragment crystallizable gamma receptor; GPCR, G protein-coupled receptor; JAK, janus kinase; LPS, lipopolysaccharide; IL, interleukin; nAChR, nicotinic acetylcholine receptor; p38, mitogen-activated protein kinase p38; PI3K, phosphoinositide 3-kinase; S1P, sphingosine-1-phosphate; SP1, specificity protein 1; src, sarcoma tyrosine kinase; STAT, signal transducer and activator of transcription 3; TF, transcription factor TLR4, toll like receptor 4.

3.4.3 Therapeutic interventions in regard to IL-10

Given the importance of IL-10 in immune regulation, many studies have been performed, especially in the 1990s, administering IL-10 or using neutralizing antibodies in animal studies. Beneficial effects of IL-10 application in various inflammatory animal models raised the hope for a therapeutic option in human diseases, such as colitis, arthritis or pancreatitis. Administering IL-10 in clinical phase 1 trials in healthy volunteers was well tolerated and showed IL-10 specific effects, such as reduction of T cells and induction of monocytes with decreased expression of MHC II in the white blood cell count. Unfortunately, large multicenter trials on IL-10 therapy of Crohn's Disease, a form of chronic colitis, were unsatisfying. Similar discouraging results were obtained for psoriasis and rheumatoid arthritis treatment (171).

In the context of cancer, production of IL-10 by TAM in non-small cell lung cancer correlated with poor anti-tumor response and poor prognosis for patients (172). Current tumor therapy strives for new adjuvants in combination with classical immunotherapy. One evolving approach is the activation of potent anti-tumor T cell responses by DC-based vaccines or antigen presenting cell-activators (e.g. TLR-9 agonist CpG). Anti-IL-10 in combination with these new strategies might enhance and prolong the tumoricidal immune response (173). This theory was strengthened by elegant murine tumor models showing drastic effects of combinatorial treatment with chemokine (C-C motif) ligand (CCL) 16, CpG and anti-IL10. CCL16 promoted accumulation of MΦ and DC at the site of established tumors. Intratumoral injection of CpG, together with systemically administered anti-IL-10 led to activation of DC with pronounced IL-12 and TNF-α production, migration to lymph nodes and adaptive immunity responses. TAM were shown to be redirected from a tumor-promoting to an inflammatory tumor-rejecting phenotype with pronounced production of IL-12, TNF-α and NO and were likely the major cell type responsible for dramatic tumor lysis within 16 h (174). Whether these promising results hold true in humans remains to be investigated.

3.5 Neurotrophin tyrosine kinase receptor 1 (TRKA, NTRK1)

In 1986 the Nobel prize in physiology or medicine was awarded for the discovery of growth factors, namely EGF and nerve growth factor (NGF) to Stanley Cohen and Rita Levi-Montalcini. NGF belongs to the neurotrophin protein family, which consists of

four members: NGF, brain-derived neurotrophic factor (BDNF) and neurotrophin (NT)3 and 4/5. Neurotrophins signal through neurotrophic tyrosine kinase receptors (TRK A-C or NTRK1-3), TRKA is the preferred receptor for NGF, TRKB has high affinity for BDNF and NT-4/5, while NT-3 mainly signals through TRKC. They are essential for neuronal survival, growth and differentiation (175) and recent work emphasizes their role in neuronal and non-neuronal cancer (176, 177), immunity (178, 179) and psychopathology (180).

Mature NGF is a glycoprotein of 118 amino acids. NGF protein is translated from two major transcripts, resulting in inactive pre-pro-NGF with molecular weights of 34 and 27 kDa. Within the ER, the pre-pro from is cleaved to pro-NGF (32 and 25 kDa) (181). Pro-NGF itself has been recognized as a pro-apoptotic effector by binding to $P75^{NTR}$, a member of the TNF receptor family, but is unable to activate TRKA signaling (182). To form mature NGF (13 kDa), pro-NGF is cleaved intracellularly by furin or pro-convertases and extracellularly by matrix metalloproteinases. Active NGF is comprised of two β-subunits, forming a stable non-covalently bound homodimer, which preferentially binds TRKA. The TRK receptors are composed of an extracellular domain containing leucine-rich motifs with cysteine clusters and two immunoglobulin-like C2 type domains, which are important for ligand binding. Additionally, the C2 domains are thought to stabilize the monomeric receptors to prevent auto-activation through spontaneous dimerization. Upon ligand binding, the receptors dimerize and autophosphorylate specific tyrosine residues. For TRKA the phosphorylation sites Y490 and Y785 serve as major docking sites for different adaptors and enzymes. Y490 primarily recruits Shc followed by activation of the PI3K/AKT and MAPK pathways, whereas Y785 recruits PLCγ leading to calcium release ((183, 184) and Figure 9).

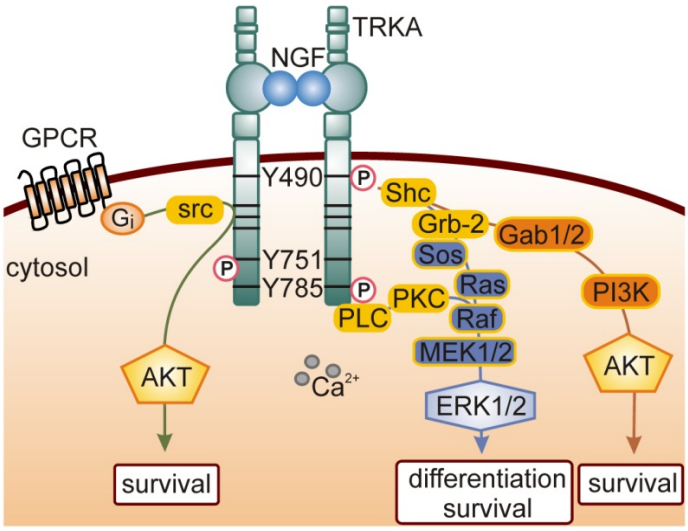

Figure 9: TRKA signaling

Ligand-binding of NGF to TRKA or transactivation by GPCR induces phosphorylation of different tyrosine kinase residues within the intracellular region of TRKA. Signaling through multiple adaptor proteins leads to differentiation and survival signaling through ERK1/2 and PI3K/AKT and calcium release. NGF-dependent or independent transactivation of TRKA is mediated through GPCRs and src, leading to AKT activation. Abbreviations: AKT, protein kinase B; ERK1/2, extracellular signal-regulated kinase 1/2; gab1/2, grb-2-associated binder-1/2; GPCR, G protein-coupled receptor; grb-2, growth factor receptor-bound protein-2; MEK1/2, mitogen-activated protein kinase kinase 1/2; NGF, nerve growth factor; PI3K, phosphatidylinositol 3-kinase; PKC, protein kinase C; PLC, phospholipase C; raf, murine leukemia viral oncogene homolog 1; ras, rat sarcoma; shc, src homologous; sos, son of sevenless; src, sarcoma tyrosine kinase ; TRKA, neurotrophin tyrosine kinase receptor A.

Neuronal survival largely depends on TRKA signaling through activation of PI3K/AKT and MAPK pathways, resulting in the induction of anti-apoptotic Bcl-2 family proteins. Furthermore, Raf and PLCγ/PKCδ/ERK cascades were described to be important for neurite outgrowth and differentiation (175). As tyrosine kinase receptors, TRKs are usually activated by ligand binding, but can be transactivated, often src-dependent, by G protein-coupled receptors like ADORA2A (185) and α2-adrenoceptor (186). In addition to neuronal functions, TRKA and its ligand have previously been associated with supporting or suppressing tumor growth (187). It was shown that especially breast cancer cells can benefit from NGF signaling (188, 189). A multitude of trials employing interference with neurotrophins are currently under way. Anti-NGF antibodies are tested in e.g. breast cancer, as NGF contributes to mammary tumor cell growth, angiogenesis and metastasis (177). However, producers and targets of neurotrophins in cancer are ill defined, and neurotrophin effects vary

between tumors, as in neuroblastoma high TrkA expression was favourable for patient survival (190, 191). On the other hand, high BDNF/TRKB indicated aggressiveness in neuroblastoma (192).

Furthermore, cells of the immune system broadly expressed neurotrophins and their receptors. Especially NGF affects differentiation, survival and chemotaxis of most immune cells, stimulates antibody synthesis in B cells and enhances phagocytosis (193, 194). Despite these observations, the role of neurotrophins in MΦ biology remains elusive with only a very limited number of studies performed in this context.

3.6 Aims of the study

Due to rapid proliferation, scarcity of oxygen, nutrients and/or therapeutic interventions solid tumors show a high rate of apoptosis. Macrophages as professional phagocytes clear the apoptotic debris and respond to apoptotic cells by phenotypical changes. Over the last years tumor-associated macrophages and their pronounced secretion of IL-10 have been recognized as key components in establishing a tumor-promoting milieu, but molecular mechanisms remain ill-defined. Detailed elucidation of immune cell function and regulation within tumors is critical to understand disease initiation and progression and will be of value for future cancer therapy.

Thus, the aim of this study was to elucidate the influence of apoptotic cancer cell supernatants on primary human macrophages in regard to TAM-related phenotypical changes, with special focus on IL-10 regulation.

In the first part of my studies I performed an adenoviral shRNA high-throughput screen to find novel regulators of IL-10 production. Additionally, regulation of three other cytokines related to cancer was investigated.

The aim of the second part of my thesis was the in-depth validation of one selected target identified in the screen. Thus, I performed experiments to clarify the underlying mechanistic principles of IL-10 induction after ACM treatment in regard to the chosen target. To analyse, if the identified regulatory pathway was unique for IL-10 regulation or a conjoint event for macrophage polarization by apoptotic cancer cell supernatant, an array of markers was investigated. Furthermore, tumor-associated macrophages of murine breast cancer tissue were examined for inter-species homology of cytokine regulation.

4 Material and Methods

4.1 Material

4.1.1 Cells

MCF-7 breast carcinoma cells

MCF-7 human breast adenocarcinoma cells were established from the pleural effusion of a 69-year-old Caucasian woman with metastatic mammary carcinoma after radio- and hormone therapy in 1970 (195).

A549 lung carcinoma cells

A549 human alveolar adenocarcinoma cells were developed from cancerous lung tissue of a 58-year-old Caucasian male in 1972 (196).

DU145 prostate cancer cells

DU145 human prostate adenocarcinoma cells were derived from brain-metastatic cells of a 69-year-old Caucasian male in 1978 (197).

HEK293 embryonic kidney cells

HEK293 cells were generated by transformation of human embryonic kidney cell cultures with sheared adenovirus 5 DNA and were first described in 1977 (198).

PC-12 rat pheochromocytoma cells

PC-12 rat pheochromocytoma cells were obtained from New England Deaconess Hospital strain white rats bearing a subcutaneously rat adrenal pheochromocytoma solid tumor and were established as cell line in 1976 (199).

PER.C6®E2A cells

PER.C6® cells were derived from a human embryonic retinoblast in 1998 and function as helper and packaging cell line for generation of replication-incompetent adenoviruses (200).

Primary human monocytes

Primary human monocytes were isolated from buffy coats obtained from DRK-Blutspendedienst Baden-Württemberg-Hessen, Institut für Transfusionsmedizin und Immunhämatologie, Frankfurt am Main or from Sanquin Bloedbank Region South West, Rotterdam, The Netherlands.

Primary murine leukocytes

Primary murine leukocytes were isolated from PyMT mammary tumor tissue of C57BL/6J mice carrying the PyMT oncogene under the control of the MMTV LTR promoter (FVB/N-TgN(MMTV-PyVT)634Mul/J) (201). All procedures performed on these mice followed the guidelines of the Hessian animal care and use committee.

4.1.2 Bacteria

Competent bacteria strains were provided by Stratagene GmbH (Amsterdam, The Netherlands). XL1-Blue® supercompetent cells were used for amplification, showing the genotype recA1 endA1 gyrA96 thi-1 hsdR17 supE44 relA1 lac [F´ proAB lacIqZ.M15 Tn10(Tetr)].

4.1.3 Stimulants and inhibitors

Table 2: Stimulants and inhibitors

Stimulants and inhibitors	Target	Provider
AG1478	EGFR inhibitor	Avanti Polar Lipids (Alabaster, USA)
AM630	CBR2 antagonist	Cayman Chemical (Ann Arbor, USA)
Atorvastatin	HMGCR inhibitor	Tocris Bioscience (Ellisville, MO)
BDNF (human)	TRKB ligand	ImmunoTools GmbH (Friesoythe)
Cerivastatin	HMGCR inhibitor	Sigma-Aldrich GmbH (Steinheim)
CSC (8-(3-Chlorostyryl)caffeine)	A2A adenosine receptor antagonist	Sigma-Aldrich GmbH (Steinheim)
Etoposide	Topoisomerase 2 inhibitor	Sigma-Aldrich GmbH (Steinheim)
GW441756	TRKA inhibitor	Sigma-Aldrich GmbH (Steinheim)
Janus kinase (JAK) inhibitor 1	JAK1 inhibitor	Merck KGaA (Darmstadt)
JTE-013	S1PR2 and 4 antagonist	Santa Cruz Biotechnology (Santa Cruz, USA)
K252a	TRK inhibitor	Sigma-Aldrich GmbH (Steinheim)
LFM-A13	BTK inhibitor	R&D Systems GmbH (Wiesbaden)

NT3 (human)	TRKC ligand	ImmunoTools GmbH (Friesoythe)
NT4 (human)	TRKB ligand	ImmunoTools GmbH (Friesoythe)
PP2	Src inhibitor	Enzo Life Sciences GmbH (Lörrach)
Propranolol hydrochloride	β-adrenoceptor antagonist	Sigma-Aldrich GmbH (Steinheim)
Rapamycin	mTOR inhibitor	Sigma-Aldrich GmbH (Steinheim)
SB203580	P38 inhibitor	Sigma-Aldrich GmbH (Steinheim)
SP600125	JNK inhibitor	Sigma-Aldrich GmbH (Steinheim)
S1P	S1PR ligand	Biomol GmbH (Hamburg)
STA-21	STAT3 inhibitor	Enzo Life Sciences GmbH (Lörrach)
Staurosporine (Sts)	Protein kinase inhibitor	Sigma-Aldrich GmbH (Steinheim)
UO126	ERK1/2/5 inhibitor	Enzo Life Sciences GmbH (Lörrach)
VPC23019	S1P1 antagonist	Avanti Polar Lipids (Alabaster, USA)
Wortmannin	PI3K inhibitor	Sigma-Aldrich GmbH (Steinheim)
Yohimbine hydrochloride	α-adrenoceptor antagonist	Sigma-Aldrich GmbH (Steinheim)
β-NGF (human)	TRKA ligand	ImmunoTools GmbH (Friesoythe)

4.1.4 Chemicals and kits

All chemicals were of the highest grade of purity, commercially available and usually purchased from Sigma-Aldrich GmbH (Steinheim, Germany), Roth GmbH (Karlsruhe, Germany) or Merck (Darmstadt, Germany). Cell culture media and supplements were from PAA (Cölbe, Germany). Special reagents and kits are listed in *Table 3*.

Table 3: Special reagents and kits

Chemical/Kit	Provider
Absolute™ qPCR SYBR® Green Fluorescein Mix	Fisher Scientific GmbH (Schwerte)
Accutase	PAA Laboratories GmbH (Cölbe)
Agarose	peqLab Biotechnologie GmbH (Erlangen)
Annexin-V-FITC	ImmunoTools GmbH (Friesoythe)
Brome phenol blue	Fluka GmbH (Buchs)
CD11b Microbeads (mouse)	Miltenyi Biotec GmbH (Bergisch-Gladbach)
CD14 Microbeads (human)	Miltenyi Biotec GmbH (Bergisch-Gladbach)
Collagen R	Serva GmbH (Heidelberg)
Collagenase 1A	Sigma-Aldrich GmbH (Steinheim)
DC Protein Assay Kit	BioRad GmbH (Munich)
DNAse 1	Promega GmbH (Mannheim)
Dynabeads Protein G	Life Technologies GmbH (Darmstadt)

HiPerFect	Qiagen GmbH (Hilden)
Human Inflammation Kit (CBA)	BD Biosciences GmbH (Heidelberg)
Human serum (AB positive), inactivated	DRK-Blutspendedienst Baden-Württemberg-Hessen (Frankfurt)
Human Soluble Protein Master Buffer Kit	BD Biosciences GmbH (Heidelberg)
Human Th1/Th2 Cytokine Kit II (CBA)	BD Biosciences GmbH (Heidelberg)
IL-10 (human)	BD Biosciences GmbH (Heidelberg)
IL-10 Flex Set (human)	BD Biosciences GmbH (Heidelberg)
IL-6 (human)	ImmunoTools GmbH (Friesoythe)
JetPEI™ transfection reagent	Biomol GmbH (Hamburg)
Lymphocyte separation medium (Ficoll)	PAA Laboratories GmbH (Cölbe)
MA6000 Human IL-10 384 Tissue Culture Kit	Meso Scale Discovery (Gaithersburg, USA)
Maxima® First Strand cDNA Synthesis Kit	Fermentas GmbH (St. Leon-Rot)
M-CSF	ImmunoTools GmbH (Friesoythe)
Mouse Inflammation Kit (CBA)	BD Biosciences GmbH (Heidelberg)
MA6000 Human IL-10 384 Tissue Culture Kit	Meso Scale Discovery (Gaithersburg, USA)
MS6000 384 4 Spot HB, Cytokine Plate-Human TC 4-Plex	Meso Scale Discovery (Gaithersburg, USA)
Neomycin (G 418)	PAA Laboratories GmbH (Cölbe)
Nonidet P-40	ICN Biomedicals Gmb (Eschwege)
NucleoBond Xtra Midi/Maxi Kit	Machery-Nagel GmbH (Düren)
ON-TARGETplus SMARTpool siRNA (human HMGCR, IL4R, THBS3)	Fisher Scientific GmbH (Schwerte)
Paraformaldehyde (PFA)	Sigma-Aldrich GmbH (Steinheim)
PBS (Instamed 9.55 g/ml)	Biochrom AG (Berlin)
peqGOLD RNAPure™	PeqLab Biotechnologie GmbH (Erlangen)
PhosSTOP	Roche GmbH (Grenzach)
Propidium iodide	Sigma-Aldrich GmbH (Steinheim)
Protease inhibitor mix (PIM)	Roche GmbH (Grenzach)
Proteinase K	New England Biolabs (Frankfurt)
Triton X100	Serva GmbH (Heidelberg)
Vectashield H-1400 mounting medium	Vector Labs (Burlingame, USA)

4.1.5 Antibodies

All antibodies were directed against human proteins (if not stated otherwise) and were used for neutralization (NEUTR), Western blotting (WB), immunoprecipitation (IP), immunofluorescence (IF), ELISA or FACS-based cell sorting as listed below in *Table 4*.

Table 4: Antibodies

Antibody	Provider	Application	Dilution
Anti-AKT	Cell Signaling Tech. Inc. (Danvers, USA)	WB	1:2000
Anti-CD11b-FITC clone M1/70.15.11.5 (mouse)	Miltenyi Biotec GmbH (Bergisch-Gladbach)	Cell Sorting	1µl/200µl/ 10^6cells
Anti-CD36 FITC	ImmunoTools GmbH (Friesoythe)	IF	1:100
Anti-CD45-Vioblue clone 30-F11.1 (mouse)	Miltenyi Biotec GmbH (Bergisch-Gladbach)	Cell Sorting	4µl/200µl/ 10^6cells
Anti-F4/80-PE-Cy7 clone BM8 (mouse)	eBioscience (Frankfurt)	Cell Sorting	2µl/200µl/ 10^6cells
Anti-HA.11	Covance Laboratories GmbH (Münster)	WB	1:1000
Anti-HLR-DR-APC clone M5/114.15.2 (mouse)	Miltenyi Biotec GmbH (Bergisch-Gladbach)	Cell Sorting	4µl/200µl/ 10^6cells
Anti-Ly6C-PerCP-Cy5.5 clone AL-21 (mouse)	BD Biosciences GmbH (Heidelberg)	Cell Sorting	1µl/200µl/ 10^6cells
Anti-Ly6G-PE clone 1A8 (mouse)	BD Biosciences GmbH (Heidelberg)	Cell Sorting	4µl/200µl/ 10^6cells
Anti-mouse Alexa Fluor 488	Life Technologies GmbH (Darmstadt)	IF	1:200
Anti-mouse IRDye680-labelled	Li-COR Biosciences GmbH (Bad Homburg)	WB	1:5000
Anti-mouse IRDye800-labelled	Li-COR Biosciences GmbH (Bad Homburg)	WB	1:5000
Anti-NGF (H-20)	Santa Cruz Biotechnology (Heidelberg)	WB	1:250
Anti-p38 MAP Kinase	Cell Signaling Tech. Inc. (Danvers, USA)	WB	1:2000
Anti-phospho-AKT (Ser473) (D9E) XP	Cell Signaling Tech. Inc. (Danvers, USA)	WB	1:2000
Anti-phospho-p38 MAP (Thr 180/Tyr 182)	Cell Signaling Tech. Inc. (Danvers, USA)	WB	1:2000
Anti-phospho-TRKA (Tyr 490)	Cell Signaling Tech. Inc. (Danvers, USA)	WB	1:1000
Anti-rabbit DyLight 594	Jackson ImmunoResearch Laboratories (Suffolk, UK)	IF	1:200
Anti-rabbit IRDye680-labelled	Li-COR Biosciences GmbH (Bad Homburg)	WB	1:5000
Anti-rabbit IRDye800-labelled	Li-COR Biosciences GmbH (Bad Homburg)	WB	1:5000
Anti-TRKA	Cell Signaling Tech. Inc. (Danvers, USA)	WB	1:1000

Anti-TRKA	Santa Cruz Biotechnology (Heidelberg)	IF, IP	IP: 4µg/1000µg protein IF: 1:100
Anti-tubulin	Sigma-Aldrich GmbH (Steinheim)	IF	1:250
Anti-β-NGF	R&D Systems GmbH (Wiesbaden)	NEUTR	5µg/ml
CD16/32 blocking ab, clone 93 (mouse)	BD Biosciences GmbH (Heidelberg)	Blocking for cell sorting	4µl/200µl/ 10^6cells
IgG1 Isotype Control	R&D Systems GmbH (Wiesbaden)	NEUTR	5µg/ml
IL-10 matched paired	ImmunoTools GmbH (Friesoythe)	ELISA	1:750
IL-6 matched paired	ImmunoTools GmbH (Friesoythe)	ELISA	1:1000

4.1.6 Plasmids

For overexpression of hemagglutinin (HA)-tagged TRKA, the CMV-HA-TRKA plasmid with ampicillin, neomycin resistance was kindly provided by Prof. Y-A Barde (202)

4.1.7 Oligonucleotides

Oligonucleotides were purchased from Biomers GmbH (Ulm) and described in *Table 5*. QuantiTect primers from Qiagen GmbH (Hilden) were used for human ADORA2A, IDO1, IL-6, IL-8, IL4RA, HMGCR, THBS3.

Table 5: Oligonucleotides

Primer	Forward	Reverse	annealing temperatur
18S rRNA (human)	5'-GTAACCCGTTGAACCCCATT-3'	5'-CCATCCAATCGGTAGTAGCG-3'	55°C
HIF-1α (human)	5'-CTCAAAGTCGGACAGCCTCA-3'	5'- CCCTGCAGTAGGTTTCTGCT-3'	60°C
IL-10 (human)	5'-AAGCCTGACCACGCTTTCTA-3'	5'-TAGCAGTTAGGAAGCCCCAA-3'	55°C
IL-1ra (human)	5'-ACCAATATGCCTGACGAAGG-3'	5'-CCTGTGACCAGGTTGTTGTG-3'	60°C
MRC-1 (human)	5'-GGCGGTGACCTCACAAGTAT-3'	5'-ACGAAGCCATTTGGTAAACG-3'	60°C
NGF (human)	5'-CATCATCCCATCCCATCTTC-3'	5'-CTCTCCCAACACCATCACCT-3'	60°C
TRKA (human)	5'-CAGCCGGCACCGTCTCT-3'	5'-TCCAGGAACTCAGTGAAGATG AAG-3'	60°C
VEGF (human)	5'-TACCTCCACCATGCCAAGTG-3'	5'-AAGATGTCCACCAGGGTCTC-3'	60°C

4.1.8 Consumables

Table 6: Consumables

Material	Provider
BZO Seal Film	Biozym Scientific GmbH (Hessisch Oldendorf)
Cover slips	Menzel GmbH (Braunschweig)
ELISA microplates, high binding	Greiner bio-one GmbH (Frickenhausen)
Hard-Shell® Full-Height 96-Well Semi-Skirted PCR Plates	Bio-Rad Laboratories GmbH (Munich)
Eppendorf Cups (0.5 ml; 1.5 ml; 2 ml)	Eppendorf GmbH (Hamburg)
FACS tubes	Sarstedt AG & Co. (Nürnbrecht)
Filcon (70 µm)	BD Biosciences GmbH (Heidelberg)
Filter paper	Whatman GmbH (Dassel)
Medicons	BD Biosciences GmbH (Heidelberg)
Microscope slides	Süsse Labortechnik (Gudensberg)
Pipet tips (10 µl; 100 µl; 1000 µl; 5000 µl)	Eppendorf GmbH (Hamburg)
Leucosep tubes	Greiner bio-one GmbH (Frickenhausen)
Plastic material (cell culture)	Greiner Bio-One GmbH (Frickenhausen)
Steril filters (0,22 µm)	Millipore GmbH (Schwalbach)
Tissue culture dishes	Sarstedt AG & Co. (Nürnbrecht)
Vivaspin 4 PES membrane falcons	Satorius AG (Goettingen)
Whatman PROTRAN® nitrocellulose membrane	Whatman GmbH (Dassel)

4.1.9 Instruments and software

Used instruments and software are listed in *Table 7* and *Table 8*.

Table 7: Instruments

Instruments	Provider
12-channel Eppendorf Research (200 µl)	Eppendorf GmbH (Hamburg)
16-channel Finnpipette (50µl]	Fisher Scientific GmbH (Schwerte)
AIDA Image Analyzer	Raytest GmbH (Straubenhardt)
Apochromat 64x/1.40 oil lense	Carl Zeiss MicroImaging GmbH (Jena)
Apollo-1 LB 911 photometer	Berthold Technologies GmbH & Co. KG (Bad Wildbad)
Autoclave HV 85	BPW GmbH (Süssen)
AutoMACS™ Separator	Miltenyi Biotec GmbH (Bergisch-Gladbach)
AxioCam MRm	Carl Zeiss MicroImaging GmbH (Jena)

AxioVert 200M fluorescence microscope equipped with the ApoTome	Carl Zeiss MicroImaging GmbH (Jena)
B250 Sonifier	Branson Ultrasonics (Danbury, USA)
Bacteria clean bench Hera guard	Heraeus GmbH (Hanau)
Bacteria incubator B5042	Heraeus GmbH (Hanau)
Bacteria incubator Innova®44	New Brunswick Scientific GmbH (Nürtingen)
CASY®	Schärfe System GmbH (Reutlingen)
Centrifuge 5415 R and 5810 R	Eppendorf GmbH (Hamburg)
DynaMag Magnet for 1.5-2 ml tubes	Life Technologies GmbH (Darmstadt)
FACSAria	BD Biosciences GmbH (Heidelberg)
Galaxy Mini	VWR International GmbH (Darmstadt)
Hera cell 150 (Lamina)	Fisher Scientific GmbH (Schwerte)
LabLine Orbit Shaker	Uniequip GmbH (Martinsried)
LSRIIFortessa	BD Biosciences GmbH (Heidelberg)
Magnetic stirrer Combimag RCH	IKA Labortechnik GmbH & Co. KG (Staufen)
Mastercycler®	Eppendorf GmbH (Hamburg)
Medimachine	Keul GmbH (Steinfurt)
Mini-PROTEAN 3 System	Bio-Rad Laboratories GmbH (Munich)
Multidrop 384	Thermo Fisher Scientific GmbH (Dreieich)
MyiQ iCycler system	Bio-Rad Laboratories GmbH (Munich)
NanoDrop ND-1000	Peqlab Biotechnologie GmbH (Erlangen)
Neubauer improved counting chamber	Labor Optik GmbH (Friedrichsdorf)
Odyssey infrared imaging system	Li-COR Biosciences GmbH (Bad Homburg)
Pipetboy	Hirschmann Laborgeräte GmbH & Co.KG (Eberstadt)
Pipettes (10 µl, 100 µl, 1.000 µl)	Eppendorf GmbH (Hamburg)
Power washer 384	Tecan Deutschland GmbH (Crailsheim)
Pure water system Purelab Plus	ELGA LabWater GmbH (Siershahn)
Reax Top	Heidolph Instruments GmbH & Co. KG (Schwabach)
Roller Mixer SRT1	Bibby Scientific Ltd. (Staffordshire, UK)
SECTOR Imager 6000	Meso Scale Discovery (Gaithersburg)
TeMO 384 Genesis robotic system	Tecan Deutschland GmbH (Crailsheim)
Thermomixer compact	Eppendorf GmbH (Hamburg)
Trans-Blot SD blotting machine	Bio-Rad Laboratories GmbH (Munich)

Table 8: Software

Software	Provider
AxioVision Release 4.7	Carl Zeiss MicroImaging GmbH (Jena)
BD Biosciences' FCAP software	BD Biosciences GmbH (Heidelberg)
CorelDRAW Graphics Suite X4	Corel Cooperation (Ottawa, Canada)

EndNote X2	Thomson Reuters Endnote (Carlsbad, USA)
FlowJo V7.6.1.	FlowJo (Ashland, USA)
Gemini™	Tecan Deutschland GmbH (Crailsheim)
Microsoft Office 2007	Mikrosoft Deutschland GmbH (Unterschleißheim)
MSD DISCOVERY WORKBENCH software	Meso Scale Discovery (Gaithersburg, USA)
MyiQ Optical Systems, Software 1.0	Bio-Rad Laboratories GmbH (Munich)
ND-1000 V3.2.1	Peqlab Biotechnologie GmbH (Erlangen)
Odyssey 2.1	Li-COR Biosciences GmbH (Bad Homburg)
Photo Read V1.2.0.0	Berthold Technologies GmbH & Co. KG (Bad Wildbad)
Prism 4	GraphPad Software (La Jolla, USA)

4.2 Methods

For all experiments except for the HTS, cells were starved over night in culture medium without FCS or human serum. Control cells, which were not stimulated with ACM, were treated with control medium containing equal amounts of FCS compared to ACM. Buffers and Solutions used for experimental procedures are listed and described in the Appendix.

4.2.1 Cell culture

MCF-7 breast carcinoma cells were cultured in RPMI 1640 medium supplemented with 1 x non-essential aminoacids, 10% heat-inactivated fetal calf serum (FCS) and 10 µg/ml bovine insulin. A549 lung carcinoma cells were cultured in high-glucose DMEM, 10% heat-inactivated FCS. DU145 prostate cancer cells were grown in MEM with 1 x nonessential amino acids, 10% FCS. HEK293 embryonic kidney cells were grown in RPMI 1640 supplemented with 10% heat-inactivated FCS. PC-12 rat pheochromocytoma cells were cultured on collagen R in DMEM high glucose supplemented with 5% heat-inactivated FCS, and 5% horse serum. PER.C6®E2A cells were cultured in DMEM supplemented with 10% FCS and 5 mM $MgCl_2$. All media were supplemented with 5 mM glutamine, 100 U/ml penicillin and 100 µg/ml streptomycin. Cells were kept in a humidified atmosphere of 5% CO_2 in air at 37°C and were transferred twice a week. Cell numbers were determined using the cell counter system Casy® or Neubauer improved counting chamber.

4.2.2 Isolation and culture of human monocytes

Human monocytes were isolated from buffy coats using Ficoll-Hypaque gradients as described previously (203). In brief, two 50 ml Leukosep® tubes per buffy were layered with 15 ml lymphocyte separation media, blood cells were added followed by density gradient centrifugation (440 x g, 35 min, break off, RT). PBMCs were collected, washed twice with leukocyte washing buffer, seeded in RPMI and were allowed to adhere to tissue culture dishes for 2 h at 37°C. Non-adherent cells were removed. Monocytes were then differentiated into MΦ with RPMI 1640 containing 5% heat-inactivated AB^+ human serum, 5 mM glutamine, 100 U/ml penicillin, and 100 µg/ml streptomycin for 7 days, medium was changed every second day. Cells were then used up to 3 weeks after isolation at cell densities between 60 – 90% confluency.

4.2.3 Monocyte isolation and MΦ culture for screening procedure

Peripheral blood mononuclear cells were isolated as described in *4.2.2*, and $CD14^+$ cells were extracted using MACS CD14 microbeads and the AutoMACS Separator (*4.2.5*.). Cells were resuspended in RPMI 1640 supplemented with 10% heat-inactivated FCS, 5 mM glutamine, 100 U/ml penicillin, 100 µg/ml streptomycin and 100 ng/ml M-CSF and were differentiated for 4 days in 384-well plates at a density of 1×10^4/well before adenoviral transduction (*4.2.8.2*) was performed.

4.2.4 Isolation of murine lymphocytes of PyMT breast cancer tissue

Mice carrying the Polyoma middle T-antigen (PyMT) oncogene under the control of the mouse mammary tumor virus (MMTV) long terminal repeat (LTR) promoter (FVB/N-TgN(MMTV-PyVT)634Mul/J) were a kind gift of Thomas Reinheckel (University of Freiburg, Germany). Mice were backcrossed for at least six generations into the C57BL/6J background. 20 week-old tumor-bearing mice were sacrificed and the tumors extracted by Benjamin Weichand. 1 g of tumor tissue was minced with a scalpel followed by lysis in 2 ml tumor lysis buffer for 30 min at 37°C. Lysis was stopped with 6 ml DMEM + 10% FCS and the lysate was further processed using Medicons and the Medimachine. After centrifugation, erythrocyte lysis in 6 ml erythrocyte lysis buffer was performed for 4 min at 4°C. Cells were resuspended in 10 ml leukocyte running buffer, brought to a single cell suspension using a Filcon (70 µm), counted and CD11b-expressing cells were isolated via magnetic cell sorting (*4.2.5*) or single cell suspensions

were stained and sorted for distinct immune cell populations (*4.2.6*). Immediately after isolation 400,000 $CD11b^+$ cells per well were seeded in 24-well plates. For distinct populations 6,000 cells or 20,000 cells per well were seeded in 96-well plates. Cells were cultured in RPMI 1640 supplemented with 1% heat-inactivated FCS, 5 mM glutamine, 100 U/ml penicillin and 100 µg/ml streptomycin.

4.2.5 Magnetic cell sorting

Human $CD14^+$ cells and murine $CD11b^+$ were sorted using the AutoMACS Separator. According to the manufacturer's protocol, cells were washed and resuspended in leukocyte running buffer (80 µl/1 x 10^7 cells). For magnetic labelling, 10 µl beads /1 x 10^7 cells of CD14 or CD11b microbeads were added and incubated at 4°C for 15 min. Cells were washed with 25 ml leukocyte running buffer, centrifuge at 300 x g for 10 min, 4°C and re-suspended in 2ml leukocyte running buffer. Cells were sorted using the AutoMACS program <posselD> for positive selection. The eluted positive fraction was washed with 20 ml leukocyte running buffer and centrifuged at 300 x g for 10 min. Supernatant was discarded and cells were resuspended in appropriate culture medium. The cell concentration was determined with help of the Neubauer counting chamber, and cells were seeded at appropriate cell densities in either 24, 96 or 384-well plates.

4.2.6 Multi-color FACS cell sorting

Single cell suspensions of murine PyMT tumors (*4.2.4*) were divided into 6 tubes à 10^6 cells in 200 µl. To minimize unspecific binding, Fc-receptors were blocked for 15 min, 4°C with CD16/CD32 blocking antibody, followed by staining with CD45-Vioblue, CD11b-FITC, HLR-DR-APC, F4/80-PE-Cy7, Ly6G-PE, Ly6C-PerCP-Cy5.5 antibodies for 30 min on ice. Cells were pooled, singled out using a Filcon and $CD45^+CD11b^+Ly6G^+$ granulocytes, $CD45^+CD11b^+F4/80^-HLR\text{-}DR^-Ly6C^+$ monocytes, $CD45^+CD11b^+F4/80^-HLR\text{-}DR^-Ly6C^-$ monocytes and $CD45^+CD11b^+F4/80^+HLR\text{-}DR^+$ macrophages were sorted using a BD FACSAria. Cells were seeded and stimulated after 15 min with inhibitors.

4.2.7 Generation of apoptotic cancer cell supernatant (ACM)

To generate apoptotic cancer cell supernatant from MCF-7 cells (ACM) cells were cultured in FCS-free medium and stimulated with 0.5 µg/ml staurosporine for 2 h provoking apoptotic cell death as described previously (34). Afterwards cells were

washed twice with medium to remove staurosporine and were incubated over night with fresh medium containing 10% heat-inactivated FCS, glutamine, penicillin and streptomycin. For A549-ACM and DU145-ACM, etoposide (250 µM, 3 h) was applied to induce apoptosis. Apoptotic cell death (%) was comparable to staurosporine. The volume of medium was adjusted to cell number to obtain ACM with a concentration of approximately 2.5 x 10^6 cells/ml. The generated ACM was centrifuged (1000 g, 10 min, 4°C) and filtered through a 0.22 µm filter to remove cell debris and apoptotic bodies. For generation of viable cell supernatant (VCM), the same procedure was followed, without induction of apoptosis. A 5:1 ratio of apoptotic/viable cells to MΦ was used when stimulating MΦ with ACM.

4.2.7.1 Verification of cell death in cells used for ACM generation

For determination of cell death, cells were detached from culture dishes using accutase and stained with propidium iodide and annexin-V-FITC in Annexin-V binding buffer for 20 min. Samples were acquired on a BD LSRIIFortessa flow cytometer, and analyzed using FlowJo V7.6.1.. Cells used for ACM showed at least 35% apoptosis (Annexin V^+/PI^-) compared to a basal level of not more than 13% of apoptosis in viable cells used for VCM.

4.2.7.2 Generation of deproteinated ACM

ACM was treated for 1 h with 50 µg/ml proteinase K at 37 °C followed by 1 h incubation at 100°C. The obtained deproteinated ACM (Deprot-ACM) was then filtered through a 0.22 µm filter and used for stimulation.

4.2.8 Transduction and transfection procedures

4.2.8.1 Repropagation of adenoviruses and IU determination

Replication defective adenoviruses, lacking the E1 and E2A region in their genome, were repropagated in the packaging cell line Per.C6/E2A (200, 204), containing the two required regions for virus replication. In brief, PER.C6/E2A cells were seeded in a 96-well format and at 80% confluency were transduced with virus and cultured for 7 – 10 days at 34°C and 10% CO_2. The cytopathogenic effect (CPE), cell lysis due to production of adenoviral particles, was determined by eye. When cells reached full CPE, cells were frozen (-20°C) to completely permeabilize, than thawn and spun down to remove cell debris. The supernatants containing infectious virus particle were aliquoted for storage

(-80°C), sequencing and infectious unit (IU) concentration titration. For IU determination PER.C6/E2A were transduced with serial dilutions of viruses and 48 h later stained for virus specific hexon protein to determine the transduction efficiency (performed by BioFocus). The average IU per ml of the used library was 7 x 10^7, for the rescreen 4.5 x 10^7.

4.2.8.2 Adenoviral transduction

$CD14^+$ MΦ (*4.2.3*) were transduced for 24h at day 4 after monocyte isolation. Transduction of controls using Ad5C01-shRNA constructs and empty vector from BioFocus/Galapagos BV (Leiden, The Netherlands) was performed at an IU of 85. Library viruses were used at an optimized volume (*5.2.1*). Medium was replaced and after additional 5 days transduced MΦ were treated with ACM for 24 h. Supernatants were harvested and stored at -80°C until cytokine measurement (*4.2.11.1*).

4.2.8.3 Transient transfection

For overexpression experiments in HEK293 cells, cells were seeded on cover slips in 6-well plates at a density of 5 x 10^4 cells per well. 24 h later, cells were transfected with 3 µg HA-tagged TRKA expression plasmid using JetPEI transfection reagent, following the manufacture's transfection protocol. After 24 h, cells were starved over night and stimulated with ACM or control medium for 30 min. Thereafter, immunoflourescence staining (*4.2.12*) was performed. For knockdown studies in primary human MΦ, monocytes were isolated as described in *4.2.2* and seeded in 6-well plates at 80-90% confluency. For transfection with siRNA, ON-TARGETplus SMARTpool siRNA and transfection reagent HiPerFect were used. In detail, cells were treated for 6 h with 16.8 µl HiPerFect and 150 µM siRNA in 500 µl RPMI 1640, thereafter 1 ml RPMI 1640 was added and incubation continued over night. The next day, MΦ were treated with ACM or control medium for 24 h. Knockdown efficiency was controlled by qRT-PCR (*4.2.9.3*) in control medium-treated cells.

4.2.9 mRNA expression analysis

4.2.9.1 RNA isolation

Total RNA was isolated using peqGold RNAPure™ Kit as described by the manufacturer. 1 ml peqGold RNAPure™ was added to cells (6-well or 6-cm dish), cells were lysed for

5 min and transferred to a 1.5 ml tube. After addition of 200 µl chloroform, samples were vortexed thoroughly and incubated at RT for 5 min. Subsequently, samples were centrifuged at 12,000 x g for 10 min to separate the RNA containing water phase from the phenol- and inter-phase. To precipitate RNA, 0.5 ml 2-propanol was added to the collected water phase, incubated for 20 min at RT or over night at -20°C and centrifuged (12,000 x g, 15 min, 4°C). Precipitated RNA was washed twice with 75% ethanol in DEPC-H_2O, dried (5 min, 70°C) and finally dissolved in 20-50 µl DEPC-H_2O for 45 min at 60°C. RNA concentration was determined using the NanoDrop ND-1000 and optical density (OD) at 260 nm. An OD_{260} of 1 is equivalent to 40 ng/µl RNA.

4.2.9.2 Reverse transcription

To determine the amount of specific RNA transcripts, reverse transcription was performed according to the provided manual using Maxima® cDNA Synthesis Kit. In brief, 1 µg of isolated mRNA was mixed with 4 µl 5 x reaction mix, 2 µl Maxima® reverse transcriptase and nuclease-free H_2O was added to 20 µl. The reaction mix was incubated for 10 min at 25°C, 15 min at 50°C and finally 5 min at 85°C for inactivation of the enzyme. The resulting cDNA was diluted to 1 µg/800µl.

4.2.9.3 Quantitative real-time polymerase chain reaction (qRT-PCR)

For qRT-PCR, 8 µl of cDNA (*4.2.9.2*) was used and mixed with either 2 µl QuantiTect Primer Assay or 0.5 µl forward and reverse primer (5 µM) each and 10 µl Absolute™ qPCR SYBR ® Green Fluorescein Mix. The volume was adjusted to 20 µl with distilled H_2O. The mixtures were transferred to a qRT-PCR compatible plate. The plate was briefly centrifuged and sealed with BZO Seal Film, an optical adhesive seal. QRT-PCR was performed using the MyiQ Single-Color Real-time PCR Detection System and the following thermal cycling program.

Enzyme activation:	95°C, 15 min	
Denaturation:	95°C, 15 s	} 35 – 45 cycles
Annealing:	55-60°C, 30 s	
Extension:	72°C, 30 s	

To confirm specificity of the multiplication, a melting curve was created using the following program:

Denaturation:	95°C, 30 s
Starting temperature:	60°C, 30 s
Melting step:	60°C, 10 s, + 0.5°C per cycle, 80 cycles

4.2.10 Protein analysis by Western blotting and Immunoprecipitation

4.2.10.1 Protein determination (Lowry)

The protein content of cell lysates was determined using the DC Protein Assay Kit, based on the Lowry method (205). Briefly, a standard dilution series of bovine serum albumin (BSA) in urea lysis buffer was prepared (0.625 to 10 mg/ml). 2 µl of each sample as well as of the standard dilutions were pipetted in duplicates into a clear flat-bottom 96-well plate, 20 µl solution A were added, and the colorimetric reaction was started by adding 160 µl of solution B. After incubation for 15 min (shaking; RT), extinction was measured at 750 nm using the Apollo-8 LB 912 photometer.

4.2.10.2 SDS-PAGE/Western analysis

For Western analysis 60-90% confluent MΦ or PC12 cells on 6- or 10-cm dishes were stimulated, washed with ice-cold PBS and scraped off in 200 - 400 µl urea lysis buffer at 4°C and sonicated for 15 x 1 s on ice. After centrifugation (16,000 x g, 10 min, 4°C), protein concentration was determined (*4.2.10.1*). 100 µg protein was mixed with 4 x SDS (sodium dodecyl sulfate) sample buffer and denatured at 95°C for 10 min. Proteins were separated on 6 or 10% SDS-polyacrylamide gels – depending on the size of the protein to detect. 1 x SDS-running buffer and the Mini-PROTEAN 3 system were used. Seperated proteins were transferred onto a nitrocellulose membrane by semi-dry blotting. To minimize unspecific binding, membranes were blocked with 5% BSA/TBS or 5% milk/TBS, depending on the thereafter used antibody, for 1 h at RT. Membranes were incubated with primary antibodies in 5% BSA/TBS at 4°C over night at indicated concentrations (*4.1.5*). For protein detection, membranes were washed 3 times with TBS or TTBS for 7 min and incubated with IRDye secondary antibodies in 5% BSA/TBS for 1 h at RT. The membrane was washed again 3 times for 7 min (2 x TBS, 1 x TTBS) and proteins were detected and densitometrically analysed using the Odyssey infrared imaging system.

4.2.10.3 Immunoprecipitation (IP)

Primary human MΦ of two 10-cm dishes per sample were stimulated for 30 min, washed with ice-cold PBS, scraped off in 600 µl NP40 Cell Lysis Buffer and lysed in 1.5 ml tubes for 30 min at 4°C while shaking. Lysates were centrifuged at 10,000 g, 10 min, 4°C to remove remaining cell debris and protein amount was determined (*4.2.10.1*) and conventional Western blotting samples were taken (*4.2.10.2*) and stored at -20°C. For IP, the DYNAL IP Kit - Dynabeads® Protein G protocol was followed. Briefly, 50 µl beads per sample were incubated with 4 µg polyclonal rabbit anti-TRKA (763) ab per sample in IP buffer for 90 min, RT, rotating. After formation of the Dynabead-ab complex, the liquid phase was removed with the help of the DynaMag magnet. The complex was washed with 200 µl IP buffer and 1 mg protein lysate in 500 µl NP40 buffer was added to the complex and incubated rotating at 4°C over night. The following day, the Dynabeads-ab-TRKA complex was washed three times with 200 µl PBS, with help of the DynaMag magnet. The complex was then transferred in 100 µl PBS into a fresh tube. Using the DynaMag, the complex was separated from PBS and TRKA protein was eluted by using 30 µl 2 x SDS sample buffer at 70°C. The liquid phase, containing TRKA was collected and the elution repeated twice (1 x 70°C, 1 x 95°C). After combining the three elutions, 1/3 of the IP samples and crude cell lysates were loaded onto 6% SDS-polyacrylamide gels and proceeded as in *4.2.10.2.* Membranes were stained with polyclonal rabbit anti-phospho-TRKA (Y490) ab as well as polyclonal rabbit anti-TrkA (763) ab.

4.2.11 Analysis of secreted proteins

4.2.11.1 Cytometric Bead Array (CBA) and Meso Scale Discovery (MSD)

Cytokine measurement in the supernatant of primary human MΦ was performed by FACS analysis using the CBA Flex Set for IL-10, CBA Human Th1/Th2 Cytokine Kit II and CBA Human Inflammation Kit for multi-cytokine measurements, following the manufacturer's instructions. For PyMT tumor leukocytes, cytokines were measured with the CBA Mouse Inflammation Kit. In brief, 50 µl supernatant and standards were incubated with beads, coated with specific antibodies and a PE-labeled detection reagent for 3 h. Samples were acquired with the LSR Fortessa flow cytometer and analyzed with BD Biosciences' FCAP software.

Cytokine measurement during the HTS at BioFocus/Galapagos, was performed using the MSD System, an immunoassay using electro-chemiluminescence. 384-well plates were purchased pre-coated with anti-IL-10 ab (MA6000 Human IL-10 384 Tissue Culture Kit), or anti-IL-6, IL-8, IL-12p70, IL-13 antibodies in 4-spot wells (MS6000 384 4 Spot HB, Cytokine Plate-Human TC 4-Plex). The provided MSD protocol was followed. In brief, 10 µl of MΦ supernatant or standards was transferred to MSD plates, either by hand or using the TeMO 384 robot. Plates were incubated for 2 h, RT, shaking. 10 µl detection antibody (1 µg/ml) was added to each well, using a 16-channel pipette. After incubation (2 h, RT, shaking), plates were washed three times with 50 µl washing buffer using the Tecan Power Washer 384. Wells were emptied and 35 µl Read Buffer T was added with the Multidrop 384. Plates were measured with the SECTOR Imager 6000 following the manufactures protocol and analyzed with MSD DISCOVERY WORKBENCH software.

4.2.11.2 Enzyme-linked immunosorbent assay (ELISA)

For validation experiments of the screening data, IL-10 and IL-6 protein measurement in supernatant of primary human MΦ was performed by ELISA, using IL-10 and IL-6 matched antibody pairs and standards from ImmunoTools. The assays were performed following the ImmunoTools' protocol on 96-well ELISA microplates. In brief, microplates were coated with coating antibodies diluted 1:1000 in ELISA coating buffer over night at 4°C. Following five washing steps with PBS, unspecific binding of samples was diminished by 1 h incubation with ELISA blocking buffer at RT, shaking. Plates were washed five times with ELISA washing buffer and incubated with 100 µl sample or standard for 1 h, RT, shaking. Washing as before was repeated and biotinylated detection antibody in ELISA dilution buffer was added for 1 h. Plates were washed and incubated for 30 min with streptavidin-HRP (1:200) in ELISA dilution buffer. After thorough washing, color substrate (Substrate Reagent Pack containing Tetramethylbenzidine and H_2O_2) was added for 5 to 30 min. Reaction was stopped by an equal volume of 1 M H_2SO_4. Absorbance was measured on the Apollo-1 LB 911 photometer within 15 min, measuring at 450 nm and subtracting background absorbance at 560 nm. Samples for the IL-6 ELISA had to be diluted 1:5 to be within the standard range (0 – 100 ng/ml), for IL-10 samples were within the standard range (0 – 1000 pg/ml).

4.2.11.3 Western blotting of secreted NGF

For detection of NGF, primary human MΦ were starved over night and then incubated for 20 min with ACM or with control medium C with equal amounts of FCS. After stimulation, supernatants were harvested, filtered through 0.22 µm pores and concentrated to 50 µl using Vivaspin 4 PES membrane falcons with an molecular weight cut off of 10,000 Da. Concentrates were mixed with equal volume of 4 x SDS sample buffer and heated for 10 min at 95°C. Samples were then subjected to 15% SDS-polyacrylamide gels (see *4.2.10.2*). Before blotting, gels were cut above the 40 kDa marker to remove albumin overload, which interfered with blotting and detection.

4.2.12 Immunofluorescence (IF) staining

Primary human MΦ were trypsinized 7d after isolation, reseeded at a density of 1 x 10^5 cells on a sterile cover slip in 6-well plates and cultured for additional 3 days. After over-night starvation, cells were stimulated, washed with PBS and fixed in 4% PFA for 2 h at RT. Mouse anti-human-CD36 FITC (1:100) in PBS was added for 2 h, followed by 3 washing steps with IF washing buffer and incubation for 30 min with IF permeabilization buffer. Cover slips were blocked for 1 h with IF blocking buffer, followed by over-night incubation with polyclonal rabbit anti-TrkA (763) ab, mouse anti-tubulin or, regarding HEK293 cells, mouse anti-human HA.11 ab in IF binding buffer at 4°C. After 3 x washing, cells were incubated for 2.5 h with anti-mouse DyLight 594 ab and anti-rabbit Alexa Fluor 488 ab in IF binding buffer. Finally, cover slips were washed 5 times and mounted on microscope slides using Vectashield H-1400 mounting medium. For image acquisition, AxioVert 200M fluorescence microscope equipped with an ApoTome, a Plan Apochromat 63x/1.40 Oil lens and a charge-coupled device camera was used at RT together with AxioVision 4.7 software.

4.2.13 Microbiology

4.2.13.1 Transformation of bacteria by heat-shock

Bacteria were transformed with plasmid DNA by heat-shock. 50 µl of bacteria glycerol stocks were thawn on ice, plasmid DNA was added and incubated for 30 min on ice. After a heat-shock for 30 s at 42°C, bacteria were incubated for 5 min on ice. For initial growth, 450 µl of SOC medium was added followed by 1 h incubation at 37°C, shaking

at 250 rpm. 200 µl were inoculated on a LB agar plate containing 100 µg/ml ampicillin and incubated over night at 37°C to select positive, plasmid carrying bacteria clones.

4.2.13.2 Bacterial culture and plasmid preparation

For preparation of plasmids a single clone was picked from the LB agar plate, transferred into 2 ml LB medium with 100 µg/ml ampicillin and cultured over night at 37°C with shaking (250 rpm). The next day, the culture was transferred into 150 ml LB medium containing 100 µg/ml ampicillin and again incubated over night at 37°C. Isolation of plasmids was performed according to the manufacturer's protocol using the NucleoBond Xtra Midi/Maxi Kit. DNA content was measured with the NanoDrop ND-1000.

4.2.14 Data analysis of screening procedure

4.2.14.1 Quality criteria

Donor and experimental performance

Control plates with controls evenly distributed over the plates were taken along during the screen at the start and end of a batch. Donor performance and consistency throughout the assay procedure were controlled. No differences in cytokine secretion between start and end control plates were observed, although processing of a complete batch needed up to 4 hours. In the rescreen cells of one donor did not respond to ACM and cells were dismissed from analysis.

Conformity between wells and plates

Heat maps of MSD IL-10 signal intensity throughout the library plates were created, to visualize edge effects (performed by BioFocus/Galapagos). Edge effects were observed for plates of one batch. For this batch, hit calling was performed separately between inner and outer wells. Consequently, the two outer rows of wells were left empty during the rescreen to avoid edge effects. Consistency between duplicate plates was monitored using kappa statistics (206). The kappa values were calculated as: 2x [(duplicate hits x non hits) - (single hits plate 1 x single hits plates 2)] / [((single hits plate 2 + duplicate hits) x (single hits plate 2 + non hits)) + ((single hits plate 1 + duplicate hits) x (single hits plate 1 + non hits))]. A kappa value of 1 shows perfect agreement between duplicate plates and values close to 0 indicate no better

agreement than by chance. Duplicate plates had to pass a kappa value greater than 0.3 (quality standard at BioFocus/Galapagos). During the screen, two duplicate plates failed this quality criteria, they were dismissed and rescreened.

4.2.14.2 Hit calling and statistical analysis

For hit calling in the primary screen the IQR method was used, as signals showed a non-Gaussian distribution. The top 5% of shRNAs which showed reduction (or induction for final target verification) of IL-10 signal intensity on both replicate plates were selected as hits. This percentage was reached on all plates at a cut off below < -1.6 IQR. In the rescreen, controls were included on the screening plates, and for hit calling the cut-off was based on negative controls, with a cut-off at ≤ -2 standard deviation from the mean of the negative controls. For screening of the three additional cytokines, shRNAs passed as hits at a cutoff ≤ -1.5 IQR for reduction and $\geq +1.5$ IQR for induction of the cytokine. Target sequences and gene names were mapped to Ensembl 61 (performed by J. K. Hériché, EMBL, Heidelberg). Target sequences, which did not exactly target one Ensembl 61 protein-coding gene, were dismissed from final analysis.

4.2.15 Non-screening statistical analysis

All experiments were performed at least three times using different donors unless stated otherwise. Data in bar graphs are presented as mean values $\pm$ standard error of the mean (SEM). Statistical analysis was performed using one-way analysis of variance (ANOVA) followed by Bonferroni's post test, or paired or unpaired two-tailed student's t-test as specified in figure legends. Differences were considered significant at $*^{/\#}$, $p \leq 0.05$; $**^{/\#\#}$, $p \leq 0.01$; $***^{/\#\#\#}$, $p \leq 0.001$.

5 Results

At sites of inflammation or in tumors, MΦ encounter dying cells. Cell-cell contact beween MΦ and dying cells or soluble factors of apoptotic cells induce a phenotype shift in MΦ characterized by enhanced IL-10 secretion (130, 157). IL-10 might be a major immunosuppressant in tumors. Thus, by limiting anti-tumor immunity, it might present an obstacle for successful cancer therapy. Therefore, in-depth analysis of IL-10 regulation is mandatory to understand its full importance and to evolve possible new cancer treatment strategies.

Throughout the experimental work, I used two distinct MΦ maturation protocols. Initial experiments to establish an adenoviral shRNA screening procedure for novel regulators of IL-10 and the post-screen target validation experiments were performed using MΦ differentiated from adhesion-selected human monocytes with AB^+ human serum. This set-up generates macrophage populations with a rather high functional and genetic variability, dependent on the donor cell as well as the donor serum. I deemed this set-up more suitable to identify meaningful targets that have a chance to affect cytokine production on a whole population scale. Nonetheless, for the shRNA screen I differentiated magnetic bead-selected $CD14^+$ monocytes to MΦ using M-CSF to generate a more homogenous setting that allowed for higher reproducibility in the screening procedure.

5.1 The nature of IL-10 induction by ACM-stimulated macrophages

5.1.1 S1P as modulator of IL-10 production

Supernatants of apoptotic MCF-7 breast cancer cells (ACM), as compared to viable cell supernatant (VCM), were sufficient to induce IL-10 mRNA and protein secretion in human (Figure 10) and murine (135) MΦ. Importantly, ACM from other solid tumor cell lines, driven into apoptosis alternatively with etoposide instead of staurosporine, induced IL-10 expression to a comparable level as ACM from MCF-7 cells. For the work presented here, I chose MCF-7 breast cancer cells, as strong MΦ infiltration and correlation with poor prognosis has been extensively described for breast cancer (105).

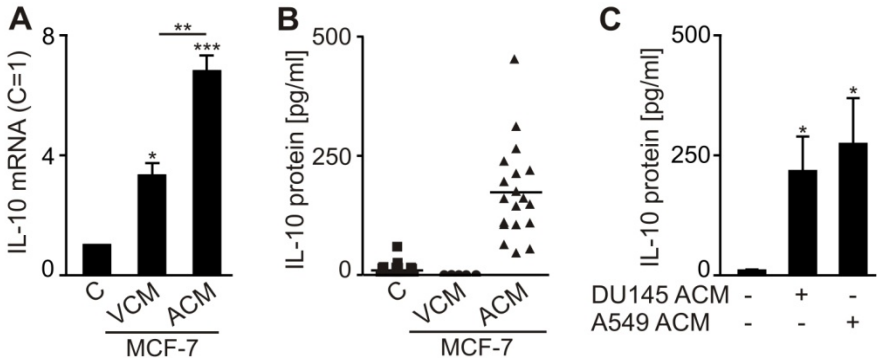

Figure 10: Apoptotic cell supernatant induces IL-10 in primary human macrophages
(A) MΦ were incubated for 3 h with supernatants of viable (VCM) or apoptotic (ACM) MCF-7 cells. IL-10 mRNA and ribosomal 18S RNA were quantified by qRT-PCR. The ratio of IL-10 mRNA versus ribosomal 18S RNA in untreated control cells C was set to 1, n = 4. **(B)** MΦ were stimulated for 24 h as in **(A)** and secreted IL-10 protein was measured by CBA and C was set to 1, n = 5 - 14. Statistics were performed using one-way ANOVA and Bonferroni's post test. **(C)** MΦ were incubated with ACM from etoposide-treated DU145 and A549 cells and secreted IL-10 was measured, n = 6. Statistics were performed using paired two-tailed student's t-test. All data are means ± SEM; *, $p \leq 0.05$; **, $p \leq 0.01$; ***, $p \leq 0.001$.

Prior work, which lead to my studies, identified the sphingolipid S1P to be released from dying tumor cells to promote MΦ survival (34). Additionally, it was observed that S1P release from dying tumor cells established an alternative, TAM-like MΦ phenotype with pronounced IL-10 and IL-8 and reduced TNF-α and IL-12 production (130). Corroborating these observations, ACM from MCF-7 cells carrying a knockdown of sphingosine kinase 2 (SK2) (ACM-siSK2) generated less S1P after induction of cell death (207) and dampened IL-10 mRNA induction in MΦ compared to ACM from control MCF-7 cells (Figure 11 A). The diminished potency of ACM-siSK2 compared to ACM on IL-10 mRNA was reproducible on IL-10 protein level after 24 h ACM/ACM-siSK2 treatment, but to a lesser extend. In another approach, I compared ACM to VCM supplemented with or without S1P or S1P alone. S1P alone or in combination with VCM did not show synergistic effects on IL-10 mRNA or protein level (Figure 11 B and C). This implies that, besides S1P, other apoptotic cell-derived factors are involved in IL-10 production by MΦ.

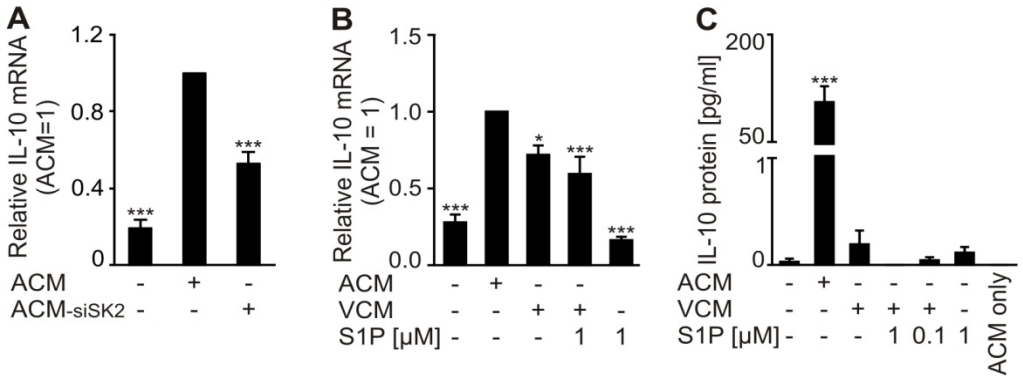

Figure 11: S1P is involved in IL-10 induction by ACM

(A) MΦ were treated for 3 h with ACM or ACM of MCF-7 cells with a knockdown for SK2 (ACM-siSK2). IL-10 mRNA and ribosomal 18S RNA were quantified by qRT-PCR. The ratio of IL-10 versus ribosomal 18S in ACM treated cells was set to 1, n = 8. **(B)** MΦ were stimulated for 3 h with ACM, VCM with or without S1P or S1P alone. IL-10 mRNA and ribosomal 18S RNA were quantified by qRT-PCR. The ratio of IL-10 versus ribosomal 18S in ACM-treated cells was set to 1, n = 7. **(C)** MΦ were incubated for 24 h as described in **(B)** and secreted IL-10 was measured in the supernatant by CBA, n = 4 – 5. Statistics were performed using one-way ANOVA and Bonferroni's post test. Data are means ± SEM. *, $p \leq 0.05$; **, $p \leq 0.01$; ***, $p \leq 0.001$.

5.1.2 Src, MAPK p38 and PI3K/AKT/mTOR are involved in IL-10 regulation

Numerous signaling pathways are acknowledged to contribute to IL-10 production by immune cells (159). As S1P seemed to be only one of the required mediators released from apoptotic cells, I investigated common signaling pathways and their involvement in ACM-induced IL-10 production in primary human MΦ. Well-described pharmacological inhibitors of major signal transducers were evaluated for their potency to repress ACM-dependent IL-10 mRNA induction. Expression of IL-10 often requires activation of STAT3 (162), a pathway activated downstream of S1P1 in MΦ in the tumor context *in vitro* (133) and *in vivo* (132). However, a non-selective janus kinase (JAK) inhibitor (JAK inhibitor I) as well as the STAT3 inhibitor STA-21 did not repress ACM-induced IL-10 mRNA (Figure 12 A). For the MAPK family, only the p38 inhibitor SB203580 significantly attenuated IL-10 mRNA levels, whereas ERK1/2 (UO126) and JNK (SP600125) inhibition did not alter IL-10 expression induced by ACM (Figure 12 B). Further experiments revealed that IL-10 production was also dependent on signaling through the PI3K/AKT/mammalian target of rapamycin (mTOR) pathway. This was demonstrated by use of the PI3K inhibitor wortmannin as well as the mTOR inhibitor rapamycin, which markedly decreased ACM-triggered IL-10 induction (Figure

12 C). Nonetheless, the most striking effect was observed when applying PP2, an inhibitor of src family tyrosine kinases (Figure 12 C).

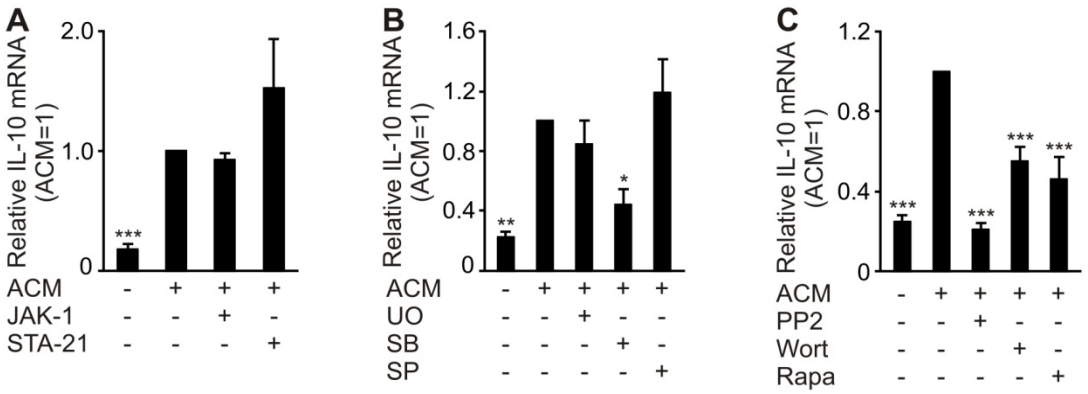

Figure 12: IL-10 induction requires PI3K/AKT and p38 MAPK signaling
(A-C) IL-10 mRNA and ribosomal 18S RNA were quantified by qRT-PCR after 3 h of incubation with ACM and inhibitors JAK-Inhibitor 1 (1 µM), STA-21 (10 µM), UO126 (10 µM), SB203580 (5 µM), SP600125 (10 µM), PP2 (10 µM), Wortmannin (100 nM), Rapamycin (50 nM). The ratio of IL-10 mRNA versus ribosomal 18S RNA in ACM-treated cells was set to 1, $n \geq 3$. All data are means ± SEM. *, $p \leq 0.05$; **, $p \leq 0.01$; **, $p \leq 0.001$. Statistics were performed using one-way ANOVA and Bonferroni's post test.

Next, I was interested if the missing factor might be a protein. I therefore degraded proteins in the apoptotic cell supernatant (Deprot-ACM) by incubation of ACM with proteinase K for 1 h at 37°C followed by 1 h at 100°C. IL-10 levels only reached 50% when cells were stimulated with Deprot-ACM compared to ACM. Interestingly, the MAPK p38 inhibitor SB203580 together with ACM showed the same effect as Deprot-ACM alone, whereas there was no further significant attenuation when using Deprot-ACM with SB203580 (Figure 13). This strengthened the assumption, that an ACM-derived protein factor was required for signaling through MAPK p38.

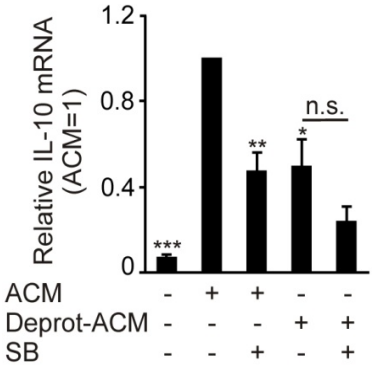

Figure 13: Deproteinated ACM shows reduced activity compared to ACM
MΦ were incubated for 3 h with ACM or deproteinated ACM, with or without SB203580 (5 µM). IL-10 mRNA and ribosomal 18S RNA were quantified by qRT-PCR. The ratio of IL-10 versus 18S RNA in ACM-treated cells was set to 1, n = 4. Statistics were performed using one-way ANOVA and Bonferroni's post test. Data are means ± SEM. *, $p \leq 0.05$; **, $p \leq 0.01$; ***, $p \leq 0.001$.

5.2 Adenoviral shRNA high-throughput screen

5.2.1 Establishing a high-throughput shRNA screen in primary human MΦ

In order to distinguish and investigate the contribution of other factors in the polarization of MΦ, I collaborated with the company BioFocus/Galapagos in Leiden, The Netherlands. The collaboration was supported by the European Commission within the Proligen project. The company has in depth expertise in high-content screening. One division is specialized in adenoviral copy (c)DNA and short-hairpin (sh)RNA libraries focusing on the druggable human genome (208). For identification of novel factors involved in MΦ polarization through ACM, I performed a shRNA adenoviral high-throughput screen (HTS). The employed recombinant adenoviral library is based on the adenovirus serotype 5 genome (Ad5C01Att01/A150100), from which the E1 and E2A regions have been deleted, to render them replication-incompetent in hosts (204). By using adenoviruses, gene knockdown in difficult-to-transfect cells such as MΦ can be efficiently achieved. Thus, adenoviral transduction enabled me to knockdown individual genes of interest and exploit their function in MΦ biology. I performed an adenoviral shRNA screen using a selected library of druggable targets including GPCRs, RTKs, secreted factors, ion channels, transporters, kinases and others.

First, I established the experimental set-up for screening in a 96-well format. The optimized protocol is indicated in Figure 14.

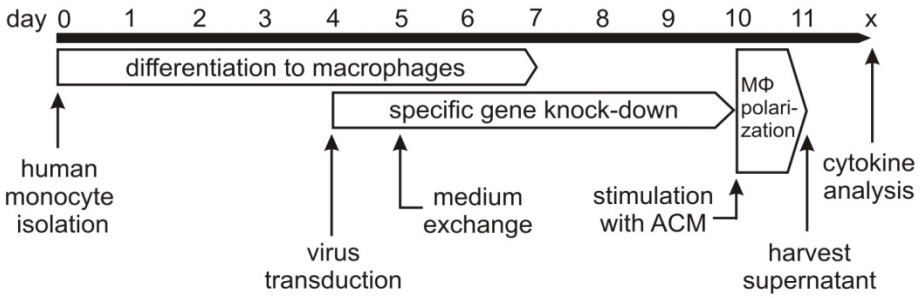

Figure 14: Time sequence of experimental steps during the screening procedure
$CD14^+$ cells were isolated from buffy coats at day 0 and differentiated to MΦ in M-CSF containing growth medium. 24 h transduction with shRNA viruses took place at day 4. At day 10 MΦ were stimulated with ACM for 24 h before supernatants were harvested and analyzed for secreted cytokines.

I determined optimal virus concentrations (infectious units (IU)/MΦ) and evaluated the respective robustness of the assay (Figure 15). CD14-expressing PBMC were isolated, 4.5 x 10^5 cells were seeded in individual wells of 96-well plates and differentiated to MΦ with 100 ng/ml M-CSF. At day 4 after isolation, cells were first transduced with virus containing a luciferase insert (luc_v13) as a negative control or containing shRNA against IL-10 (shIL10_v2) as the positive control at different IU per MΦ for 24 h (Figure 15 A). Following medium exchange, cells were maintained for another six days to reach optimal knockdown efficiency (208). Thereafter, MΦ were stimulated with ACM for 24 h, followed by collection of supernatants, which were stored at -80°C. IL-10 protein in the supernatant of MΦ was determined using CBA flex sets.

At an IU of 200 the luciferase construct showed non-specific reduction of IL-10, indicating unspecific virus effects. However, transduction with virus containing shIL10_v2 at an IU of 100 significantly and robustly reduced IL-10 levels to 20%. Importantly, the luciferase construct was inert regarding ACM-induced IL-10 production at this IU (Figure 15 A), providing a suitable window between the negative and positive control at an IU of 100.

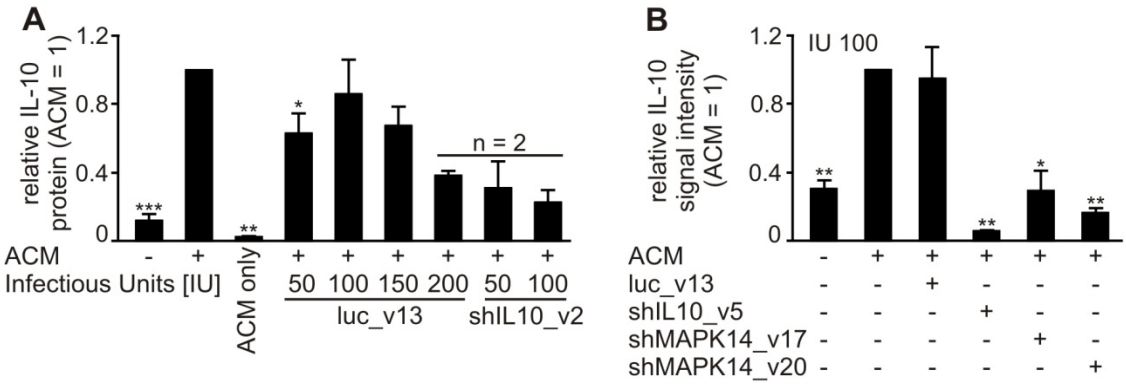

Figure 15: Implementation of screen controls

(A) Virus titration for optimal infectious units (IU) amount. MΦ were treated as shown in Figure 14 on a 96-well plate format, n = 2 – 4. **(B)** Further control viruses were assessed at an optimized IU of 100. Negative control: luc_v13, positive controls: shIL10_v5, shMAPK14_v17 and _v20, n = 3. IL-10 protein was measured by CBA. All data are means ± SEM. P-values were calculated using two-tailed student's t-test. *, $p \leq 0.05$; **, $p \leq 0.01$; ***, $p \leq 0.001$.

As observed in previous experiments, MAPK p38 seems to be involved in ACM-depended IL-10 production and to function downstream of an unknown protein factor within the ACM (Figure 12 and Figure 13). Having this in mind, I included two virus constructs targeting MAPK14/p38 as second positive controls. Both constructs reduced IL-10 secretion to a level comparable to the unstimulated control. In addition, a shRNA targeting a different sequence (version v_5) within the IL-10 mRNA was used to ensure specificity (Figure 15 B).

Since I observed high reproducibility in the 96-well format, I transfered the assay to BioFocus. Employing robotic systems, I down-scaled the assay to a 384-well format (10^4 cells per well), thereby drastically reducing the screening time, the number of donors needed for the primary screen and thereby limiting inter-donor variations. To substantiate the robust screening procedure in a 384-well format, additional negative control luciferase constructs and an empty vector were tested together with positive controls in three different IUs (75, 85, 100). A satisfying and highly reproducible window between positive and negative controls was achieved with all virus concentrations (Figure 16 A). To exclude a non-specific effect of transduction on IL-10 secretion by MΦ at an IU of 85, I transduced cells without ACM-stimulation. Although I observed significantly reduced IL-10 secretion from unstimulated MΦ when using virus expressing IL-10 shRNA, as could be expected, no drastic alterations with the control constructs or virus containing shRNA against MAPK14/p38 were observed (Figure 16

B). Thus, I decided to perform the primary screen in a 384-well format and an IU of 85 for the controls.

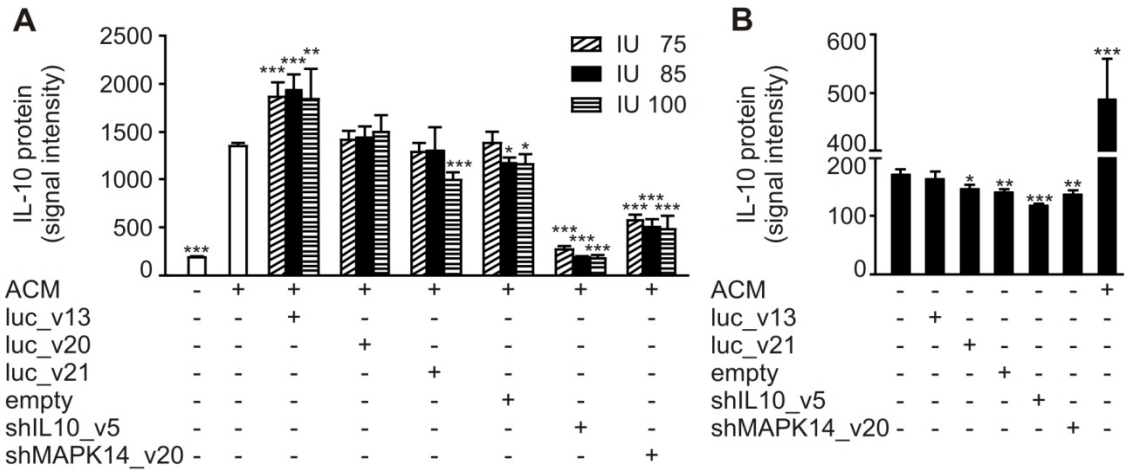

Figure 16: Control virus titration on a HT platform and basal effect on unstimulated MΦ
(A) Experimental procedure was followed as in Figure 14. Additional negative (luc_v13, _v20, _v21, empty) and positive controls were tested at different IUs on a 384-well plate. **(B)** The effect of control viruses on unstimulated MΦ was tested at an IU of 85. For both experiments, IL-10 protein was measured by MSD. Data from one donor are shown as representative result, with 4 – 12 individually obtained data points. Data are means ± SEM. P-values were calculated using two-tailed student's t-test. *, $p \leq 0.05$; **, $p \leq 0.01$; ***, $p \leq 0.001$.

The last question, which had to be answered before proceeding to the screen, was the optimal transduction volume for the library. The average IU of the library was 7 x 10^7/ml. Calculating with the optimal IU of 85 for the controls, 12.14 µl would have been the corresponding transduction volume for the library. Considering that virus repropagation was performed in different formats for the library (96-well plate) and controls (flasks) with possible effects on the properties of the virus suspensions, I tested three different transduction volumes on MΦ to obtain the optimal volume to be used for the screen. Consequently, one random library plate, reformatted to 384-well, was chosen. From this, MΦ cultures were transduced, as duplicate plates, with 4, 8 or 16 µl virus lysate. The experimental procedure was performed as shown in Figure 14. IL-10 protein in the supernatant was assessed by MSD and extinction signals of the replicates were plotted against each other to visualize signal distribution between duplicate plates. No drastic differences were observed between the three transduction volumes (Figure 17 A). Hit calling was performed (please refer to *4.2.14.2*) in order to identify the amount of overlapping hits between the volumes. At the chosen cut-off, to obtain approximately 5% hits per plate (~ 20 hits), the three volumes showed 11

common hits (white bars) and 9 (8 µl, black) to 12 (16 µl, red) hits, which were only found in one or two of the volumes (Figure 17 B).

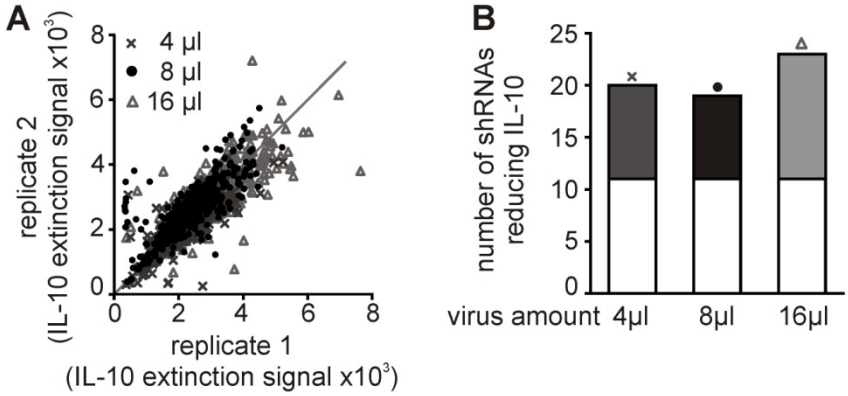

Figure 17: Determination of optimal library transduction volume
One virus library plate served as virus reservoir for transducing MΦ in a 384-well format with three different transduction volumes (4, 8. 16 µl), in duplicate plates. The procedure depicted in Figure 14 was followed. IL-10 was measured by MSD in the supernatant. **(A)** Obtained IL-10 signal intensities of both replicate plates for each transduction volume are plotted. **(B)** Number of shRNA constructs which passed hit calling. White bars: hits correspond between different volumes, shaded: Hits found in one or two of the three transduction volumes.

Thus, four-fold changes in virus concentration did not drastically influence the hits identified, confirming the stability of the experimental system. To be assured not to lose hits, due to low virus load, or to deal with too many unspecific targets, due to toxicity of high virus concentrations, I chose 8 µl as transduction volume of the library.

5.2.2 Screen yields 96 genes involved in IL-10 secretion

Having established controls and optimal virus load for transduction, the screen was performed. 8495 adenoviral shRNA constructs targeting 2825 genes (usually 3 different shRNA sequences/versions (v_) targeting one gene) were screened on duplicate plates, transduced from the same virus source plate (Figure 18). The screen was divided into 3 batches and MΦ from 4 donors were used. Throughout the screen, the percentage of IL-10 inhibition between shIL-10 and negative controls was above 65%, and above 30% for shMAPK14 and negative controls. In the primary screen, 459 out of the screened 8495 shRNA constructs, targeting 434 protein-coding genes, diminished ACM-induced IL-10 release based on the chosen hit calling and quality criteria (refer to *4.2.14.1* and *4.2.14.2*). To substantiate the results, shRNA sequences, which did not unambiguously target a unique protein-coding gene in Ensembl 61, were excluded from further analysis (Ensemble 61 analysis was performed by J.K. Hériché,

EMBL, Heidelberg). In a next step, I used the 459 shRNA virus constructs for a rescreen to validate their ability to inhibit ACM-induced IL-10 production in MΦ from two additional donors. Therefore, the viruses were cherry-picked and formatted on 12 96-well plates for repropagation, which resulted in three 384-well plates for MΦ-transduction. The two outer rows of the 384-well plates were left empty to avoid edge effects and controls were distributed over the plates. Following the formatting, the optimal transduction volume (12 µl) was determined as described for the primary screen. In the rescreen a shRNA construct was considered to reduce IL-10 secretion, when in 2 donors, screened in duplicates (total of 4 data points), 3 data points were below the assigned cut-off. For details on the hit calling procedure, see *4.2.14.2*. 131 shRNA constructs emerged from the rescreen and were validated by sequencing. Additionally, 13 targets were dismissed, as differential shRNAs targeting the same genes showed IL-10 induction in the primary screen. This resulted in the identification of 98 unique targeting sequences that reduced IL-10 release in the used system These 98 sequences corresponded to 96 biological targets, which were required for IL-10 secretion from MΦ stimulated with dying tumor cells (Figure 18).

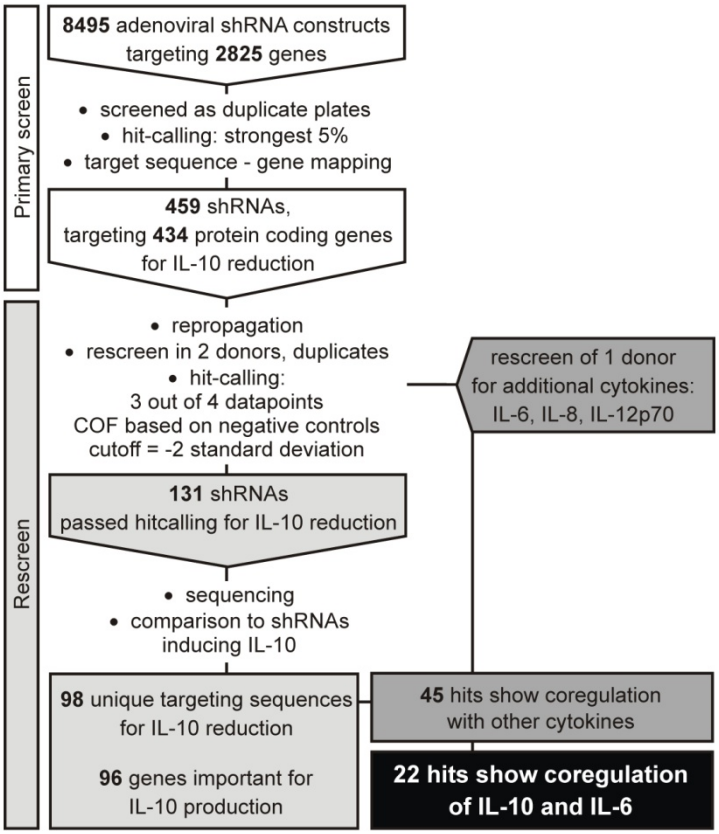

Figure 18: Screening workflow and outcome

In the primary screen, 8495 adenoviral shRNA constructs targeting 2825 individual genes were screened for reduction of ACM-induced IL-10 in primary human MΦ as depicted in Figure 14. The strongest 5% were considered hits and were taken into the rescreen. Constructs were repropagated and screened in MΦ from two additional donors. Hit calling resulted in 131 shRNAs which reduced IL-10 secretion. These were sequenced and compared to shRNAs inducing IL-10 in the primary screen to ensure specificity. 98 unique targeting sequences were found, leading to 96 genes important for IL-10 production. Additionally, three other cytokines (IL-6, IL-8 and IL-12p70) were measured in the supernatant of the rescreened samples, resulting in 45 hits showing coregulation of IL-10 reduction and expression of one or more of the other cytokines. 22 of these shRNAs reduced IL-6 and IL-10.

5.2.3 IL-6 and IL-10 are highly co-regulated in ACM-stimulated macrophages

Tumor-associated macrophages (TAM) produce a variety of tumor-promoting cytokines and chemokines, e.g. IL-10, IL-6 or IL-8, but lack the production of factors potentially inducing protective immunity such as IL-12. This cytokine signature maintains a tumor-promoting milieu, finally supporting tumor outgrowth (97). Thus, identification of a common target globally changing this functional pattern would be desirable. I was therefore interested in clarifying whether the identified targets for IL-10 affected the cytokines mentioned above. Selection of the three cytokines was based on previous findings showing that IL-10, IL-6 and IL-8 were strongly induced in

MΦ interacting with apoptotic cancer cells, whereas IL-12 was repressed ((130), Figure 19).

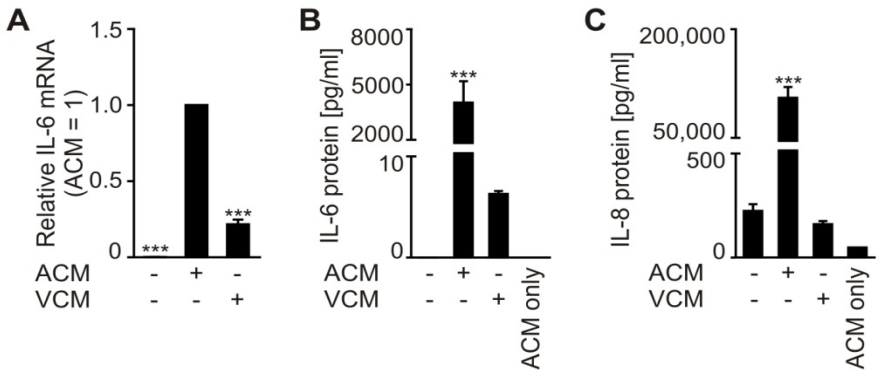

Figure 19: IL-6 and IL-8 induction by ACM

(A) MΦ were treated for 3 h with or without ACM or VCM. IL-6 mRNA and ribosomal 18S RNA were quantified by qRT-PCR. The ratio of IL-6 versus ribosomal 18S in ACM-treated cells was set to 1, n = 10. **(B, C)** ACM, VCM or control medium were incubated on MΦ and IL-6 **(B)** and IL-8 **(C)** protein was measured in supernatant or in ACM alone after 24 h by CBA, n = 4 - 5. All data are means ± SEM and Statistics were performed using one-way ANOVA and Bonferroni's post test. ***, $p \leq 0.001$.

Thus, I determined IL-6, IL-8 and IL-12 contents in the MΦ supernatants from the rescreen, i.e. of MΦ transduced with viruses containing shRNAs that emerged from the primary screen. Within the screening procedure, mean concentrations of cytokines secreted by ACM-stimulated MΦ were 150 pg/ml for IL-10, 10 ng/ml for IL-6, 11 ng/ml for IL-8 and 130 pg/ml for IL-12p70. When I evaluated the expression pattern of IL-6, IL-8 and IL-12 from the supernatants obtained in the rescreen and compared them to regulation of IL-10, I unfortunately was unable to identify a single gene affecting the production of all four cytokines (Figure 20). A major functional pattern of TAM, and regulatory MΦ in general, is high IL-10 expression but repressed release of IL-12 (95). Only few of the targets efficiently reduced IL-10 secretion while simultaneously elevating IL-12 levels. A reason for this might be the absence of a classical pro-inflammatory stimulus in ACM that would be required to trigger IL-12 production, such as IFN-γ (130). However, a prominent co-regulation pattern of IL-10 and IL-6 secretion from ACM-stimulated human MΦ emerged (Figure 20).

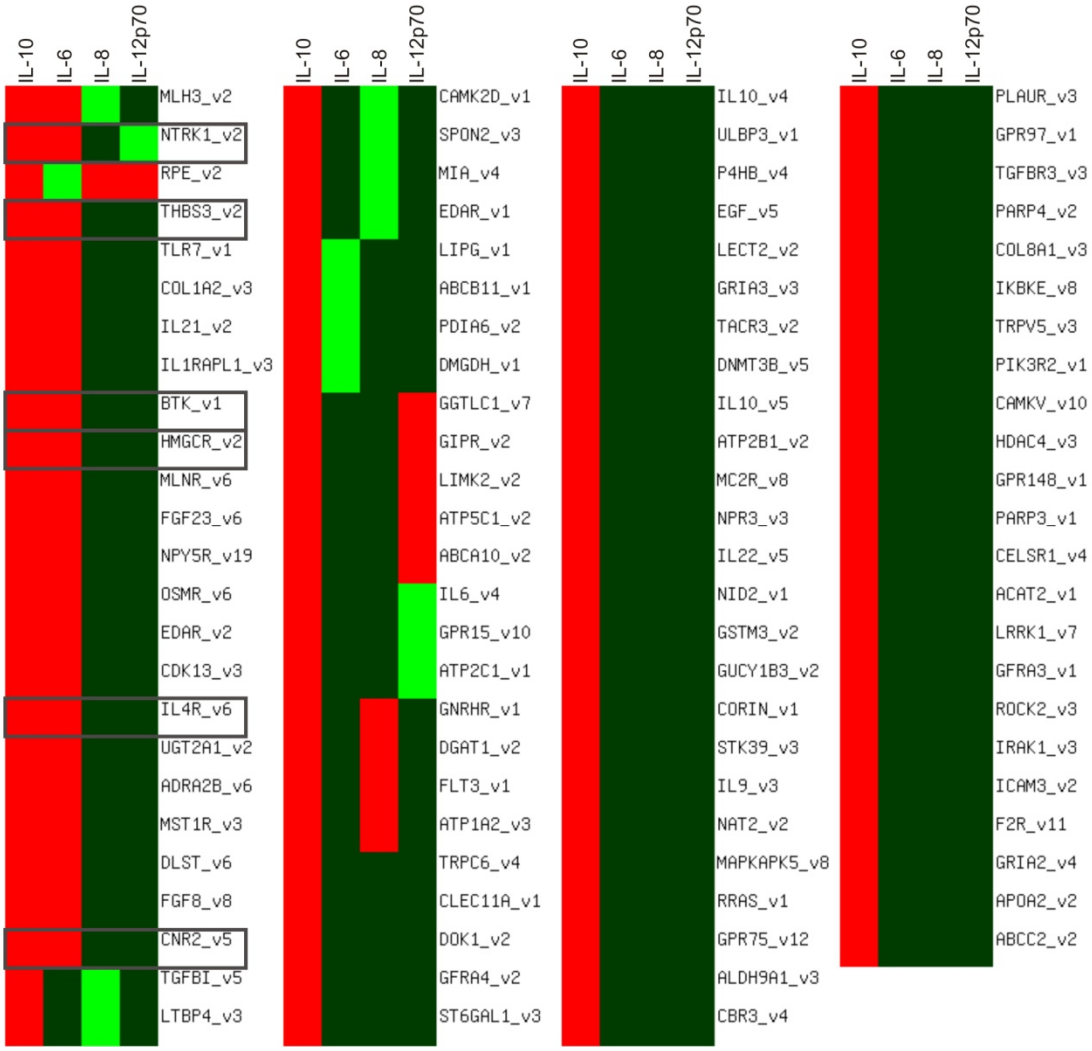

Figure 20: Heat map of final hits of HTS

Cytokine regulation by unique target shRNAs, which passed hit calling criteria for IL–10 reduction in the primary screen and the rescreen. Additional regulation of IL–6, IL–8 and IL–12p70 in supernatants is depicted. Red: cytokine reduction, green: cytokine induction. Boxed shRNAs were verified in subsequent experiments. NTRK1_v2 was validated in detail for IL-10 induction. The heat map was created by J.K. Hériché, EMBL, Heidelberg using clusters obtained with the DBScan algorithm rearranged manually to visualize regulation patterns.

5.2.4 Validation of selected targets co-regulating IL-10 and IL-6

For validation of the screening results, I focused on the pronounced cluster of genes, whose knockdown diminished IL-10 and IL-6 production after ACM-stimulation. This regulation pattern was rather surprising, as a co-regulation of IL-10 and IL-6 is not described in literature. However, both IL-6 and IL-10 are capable of activating STAT3 in cancer cells and in MΦ in an autocrine manner, which is highly linked to tumorigenesis (131). Interrupting this vicious cycle in tumor-associated inflammation might be beneficial for cancer therapy.

Confirmation of the screening results was performed by using a pool of target-specific siRNA (ON-TARGETplus SMARTpool) and/or common pharmacological inhibitors. Furthermore, I validated the screening results not only by applying alternative techniques interfering with the targets, but also by using an alternative MΦ generation protocol. MΦ were selected by adherence and differentiated with AB^+ human serum from different donors, as it was performed for all screen-preceding experiments and subsequent validation assays. I selected 5 targets, which allowed a rational link to IL-10 or IL-6 generation. I chose IL-4 receptor alpha (IL-4RA, IL-4Rα), cannabinoid receptor 2 (CNR2, CB2), 3-hydroxy-3-methylglutaryl coenzyme-A (HMG-CoA) reductase (HMGCR), bruton's tyrosine kinase (BTK) and thrombospondin 3 (THBS3, TSP3). For CBR2 and BTK I applied pharmacological antagonists/inhibitors and for IL-4RA, HMGCR and THBS3 I used a knockdown strategy for evaluation. Primary human MΦ were transfected with target-specific or non-targeting siRNA using Hiperfect for 24 h, followed by stimulation with ACM for 24 h. Knockdown efficacy was evaluated by qRT-PCR in transfected, non-stimulated cells, after harvesting MΦ supernatants. In average, IL4-RA knockdown reached 80%, HMGCR knockdown 69% and THBS3 73% compared to non-targeting siRNA.

By binding to the IL-4 receptor, IL-4 and IL-13 are well established modulators of MΦ biology. IL-4 was the first stimulus described for alternative macrophage activation (74) and accounts for a wound-healing MΦ phenotype with pronounced IL-10 expression (95). As observed in the screen, the knockdown of IL4-RA compared to non-targeting siRNA significantly reduced IL-10 and IL-6 secretion after 24 h of ACM-stimulation (Figure 21 A, B). Regarding the cannabinoid system, CNR2 is primarily expressed by immune cells and anti-inflammatory properties have been assigned to this receptor before. In addition, under inflammatory conditions endocannabinoid synthesis in MΦ has been observed (209-212). Indeed, I was able to confirm the screening results. CNR2 antagonist/reverse agonist AM630 (213) reduced IL-10 and IL-6 secretion at concentrations of 10 µM in ACM-stimulated MΦ (Figure 21 C, D).

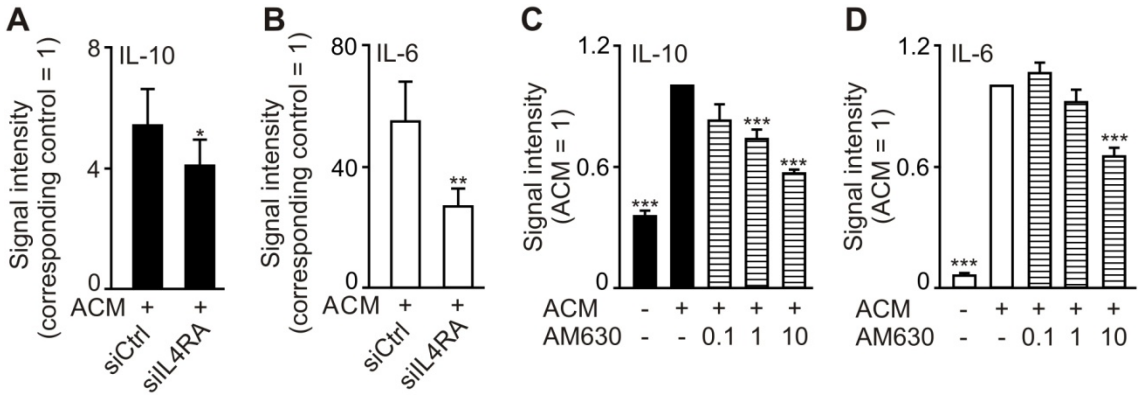

Figure 21: Hit validation: IL-4RA and CNR2 regulate IL-10 and IL-6 expression
(A, B) MΦ were transfected with a target specific pool of siRNAs against human IL-4RA or non-targeting siCtrl for 24 h. After medium exchange, cells were stimulated for additional 24 h with or without ACM and IL-10 and IL-6 protein in the supernatant were measured by ELISA. Transfected (siIL4RA and siCtrl) unstimulated extinction signals were set to 1, n = 11 – 12. **(C, D)** MΦ were left untreated or preincubated for 45 min with AM630 (at given concentrations in µM) and stimulated with ACM with or without AM630 for 24 h. IL-10 and IL-6 protein in the supernatant were measured by ELISA and extinction signals of ACM-treated cells were set to 1, n = 7 – 13. All data are means ± SEM. P-values were calculated using two-tailed student's t-test. *, $p \leq 0.05$; **, $p \leq 0.01$; ***, $p \leq 0.001$.

The third candidate chosen for validation was HMGCR. The reductase is the key enzyme in the mevalonate pathway generating isoprene moieties, which are required for synthesis of steroids, cholesterol, ubiquinones, and prenylation of GTPase proteins, important for cell function and survival (214). Drugs of the statin family inhibit HMGCR. They are widely used in the therapy of hypercholesterolemia and anti-inflammatory effects are reported (215). I did not observe this anti-inflammatory effect of statins with regard to IL-10, as knockdown of HMGCR during the screen, through siRNA or by pharmacological intervention (Cerivastatin and Atorvastatin) diminished IL-10 release in ACM-stimulated MΦ (Figure 22 A, C). Unfortunately, the reduction of IL-6 in the screen was not reproducible by knockdown or statins (Figure 22 B, D).

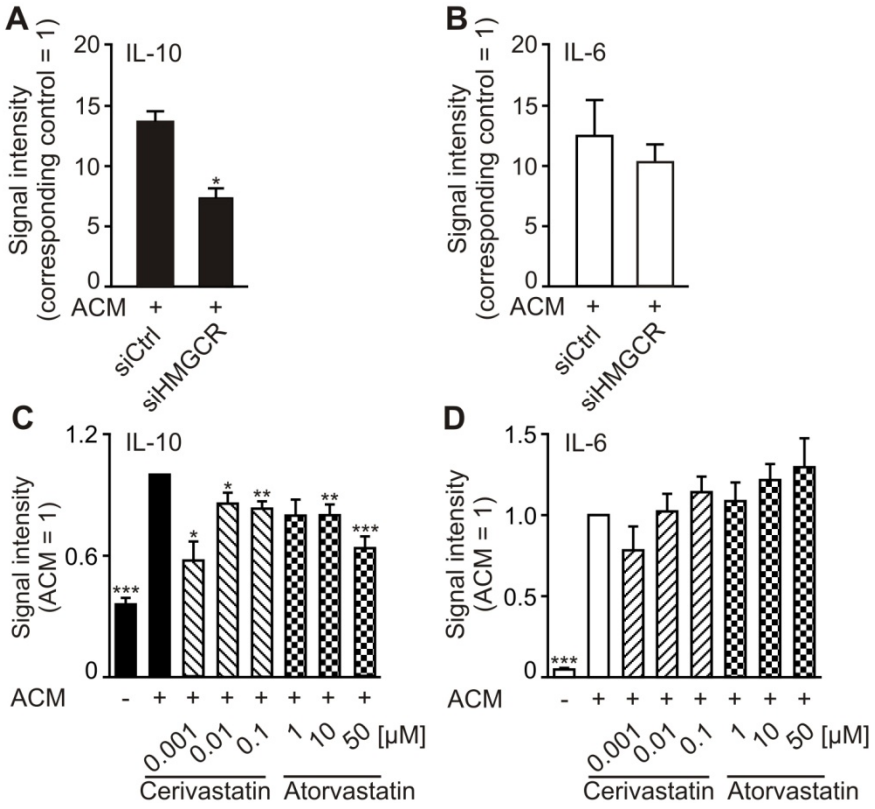

Figure 22: Validation of HMGCR on IL-10 and IL-6 production

(A, B) MΦ were transfected with a target specific pool of siRNAs against human HMGCR or non-targeting siCtrl for 24 h. After medium exchange, cells were stimulated for additional 24 h with or without ACM and cytokines were measured by ELISA, n = 3. Transfected (siHMGCR or siCtrl) unstimulated extinction signals were set to 1. **(C, D)** MΦ were left untreated or preincubated for 45 min with Cerviastatin or Atorvastatin (at given concentrations) and stimulated with ACM with or without statins for 24 h, n = 4 - 11. Cytokines were measured by ELISA and extinction signals of ACM-treated cells were set to 1. All data are means ± SEM. Statistical analysis was performed using two-tailed student's t-test. *, $p \leq 0.05$; **, $p \leq 0.01$; ***, $p \leq 0.001$.

Targeting BTK with the pharmacological inhibitor LFM-A13 drastically reduced IL-6 but had no effect on IL-10 (Figure 23 A, B). I had chosen this candidate, as several reports link the kinase to MΦ function, e.g. HO-1 induction and cytokine production (216, 217). The only chosen candidate that failed validation completely was THBS3, a largely uncharacterized family member of thrombospondins which have been linked to tumor angiogenesis and prognosis (218). Knockdown of THBS3 significantly affected neither IL-10 nor IL-6 (Figure 23 C, D). Although I was not able to reproduce all effects observed in the screen, the level of reproducibility was encouraging for further detailed analysis, especially, as I used differentially generated MΦ for the validation

experiments, which can have an impact on the cell's transcriptome and thus on functionality of the highly versatile human MΦ (219).

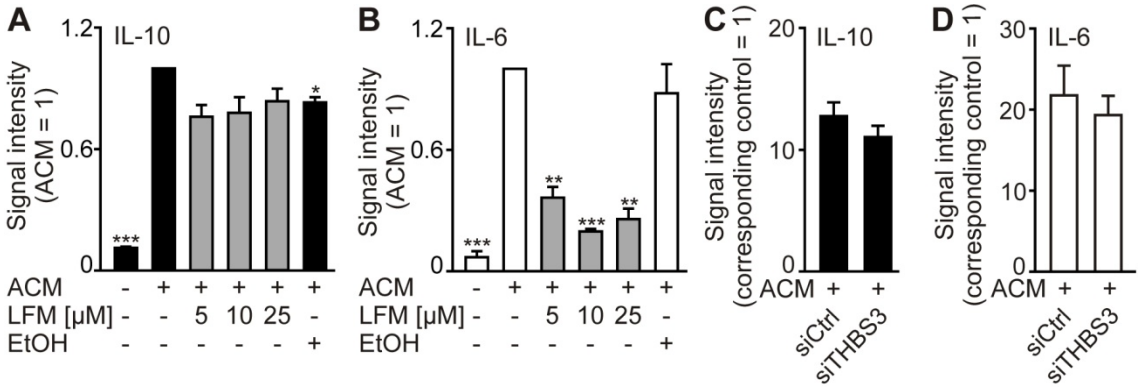

Figure 23: Validation of BTK and THBS3

(A, B) MΦ were left untreated or preincubated for 45 min with LFM-A13 (at given concentrations) and stimulated with ACM with or without LFM-A13 or EtOH as solvent control for 24 h. IL-10 and IL-6 protein in the supernatant were measured by ELISA. Extinction signals of ACM-treated cells were set to 1, n = 3. **(C, D)** MΦ were transfected with a target specific pool of siRNAs against human THBS3 or non-targeting siCtrl for 24 h. After medium exchange, cells were stimulated for additional 24 h with or without ACM and IL-10 and IL-6 protein in the supernatant were measured by ELISA, n = 6. Transfected (siTHBS3 or siCtrl) unstimulated extinction signals were set to 1. All data are means ± SEM. P-values were calculated using two-tailed student's t-test. *, $p \leq 0.05$; **, $p \leq 0.01$; ***, $p \leq 0.001$.

The above mentioned studies brought forward a robust screening assay for primary human MΦ, which are highly resistant to transfection and identified putative targets for intervention with tumor-induced macrophage polarization. One target particularly caught my attention, the nerve growth factor receptor TRKA, which is crucial in neuronal development and which has been linked to tumor growth in a murine breast cancer model (220).

5.3 Detailed validation of TRKA signaling in regard to IL-10 production

Of the targets that reduced IL-10 and IL-6 protein secretion, unexpectedly knockdown of TRKA stood out both regarding the magnitude and reproducibility of IL-10 reduction (~60% compared to negative controls) (Figure 24 A). Reports of TRKA being related to breast cancer progression (220, 221), its described interaction with S1P receptors (222, 223) and studies showing TRKA involvement in inflammatory responses of monocytes/ MΦ (136, 224) strengthened my interest to validate this specific candidate.

To verify the involvement of TRKA in IL-10 regulation by AC, I first asked whether TRKA was activated by ACM. Therefore, I stimulated primary human MΦ with ACM for

30 min and immunoprecipitated TRKA, followed by staining for the specific autophosphorylation-site (Y490) of the receptor. Immature (80 and 110 kDa) and mature forms (140 kDa) of TRKA monomers as well as dimers (225, 226) were detected using the pan-TRKA antibody (ab) in the loading controls. Importantly, following IP a specific band for TRKA autophosphorylation was observed in ACM-treated MΦ at a molecular weight corresponding to TRKA dimers, whereas it was completely absent in unstimulated cells (Figure 24 B).

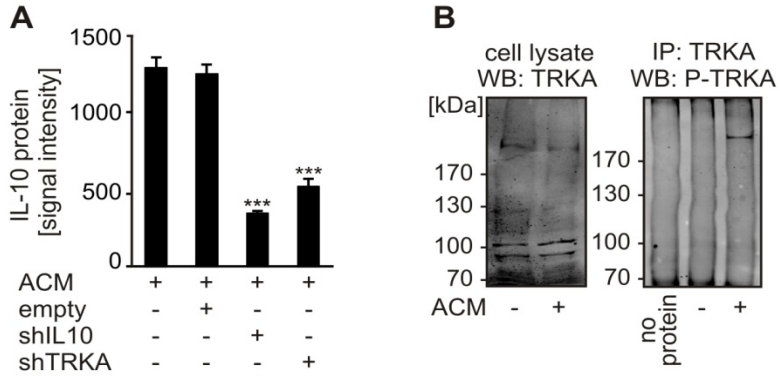

Figure 24: ACM induces TRKA-dependent IL-10 secretion in primary human MΦ
(A) Raw data from the HTS and rescreen. IL-10 signal intensity of ACM with or without adenoviral empty control vector, shIL10 and shTRKA are depicted. 4 donors were screened. Data are means ± SEM. ***, $p \leq 0.001$. Statistics were performed using one-way ANOVA and Bonferroni's post test. **(B)** Human MΦ were stimulated for 30 min with ACM. TRKA was immunoprecipitated from cell lysates, subjected to 6% SDS-PAGE and stained for phospho-TRKA (Y490). Additionally, TRKA was stained in the input controls, n = 3.

Next, I confirmed the involvement of TRKA in IL-10 up-regulation through ACM by using two TRKA inhibitors. K252a, a TRK family inhibitor (227), markedly decreased IL-10 mRNA after 3 h and protein up-regulation induced by ACM after 24 h. This was also achieved when using GW441756, a putatively selective TRKA activity inhibitor (228), although to a lesser degree (Figure 25 A, B).

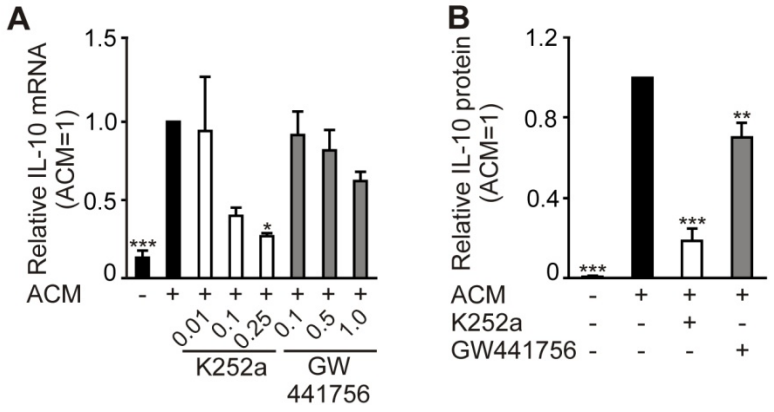

Figure 25: Pharmacological TRKA inhibition verifies screening result

(A) IL-10 mRNA and ribosomal 18S RNA were quantified by qRT-PCR after 3 h of incubation with ACM and the inhibitors K252a, GW441756 (concentrations in µM). The ratio of IL-10 mRNA versus ribosomal 18S RNA in ACM-treated cells was set to 1, $n \geq 6$. **(B)** ACM with or without inhibitors K252a (250 nM), GW441756 (1 µM) was added to MΦ and IL-10 protein was measured in supernatant after 24 h by CBA. Inhibitors were pre-incubated for 45 min before ACM treatment, $n \geq 5$. All data are means ± SEM. Statistical analysis was performed using one-way ANOVA and Bonferroni's post test. *, $p \leq 0.05$; **, $p \leq 0.01$; ***, $p \leq 0.001$.

5.3.1 IL-10 production downstream of TRKA requires PI3K and p38 MAPK

In order to investigate the contribution of TRKA in signaling pathways involved in IL-10 induction (Figure 12), I closely monitored p38 and AKT phosphorylation. Supportive argumentation for these two pathways downstream of TRKA is well established and was summarized in a review by Arevalo and Wu (183). First, I assessed the time kinetics of p38 and AKT phosphorylation in ACM-stimulated MΦ by Western blotting. AKT phosphorylation was rapidly induced by ACM and remained stable over 1 h (Figure 26 A). P38 MAPK phosphorylation was also rapidly initiated, but increased over time (Figure 26 C). At 30 min of ACM stimulation, ACM-induced p38 phosphorylation was reduced to about 50% using the TRK inhibitor K252a, but was unaffected by either src tyrosine kinase or PI3K inhibitors (Figure 26 D). In contrast, phosphorylation of AKT was completely abolished with the src inhibitor PP2 as well as with K252a. The PI3K inhibitor Wortmannin served as positive control (Figure 26 B).

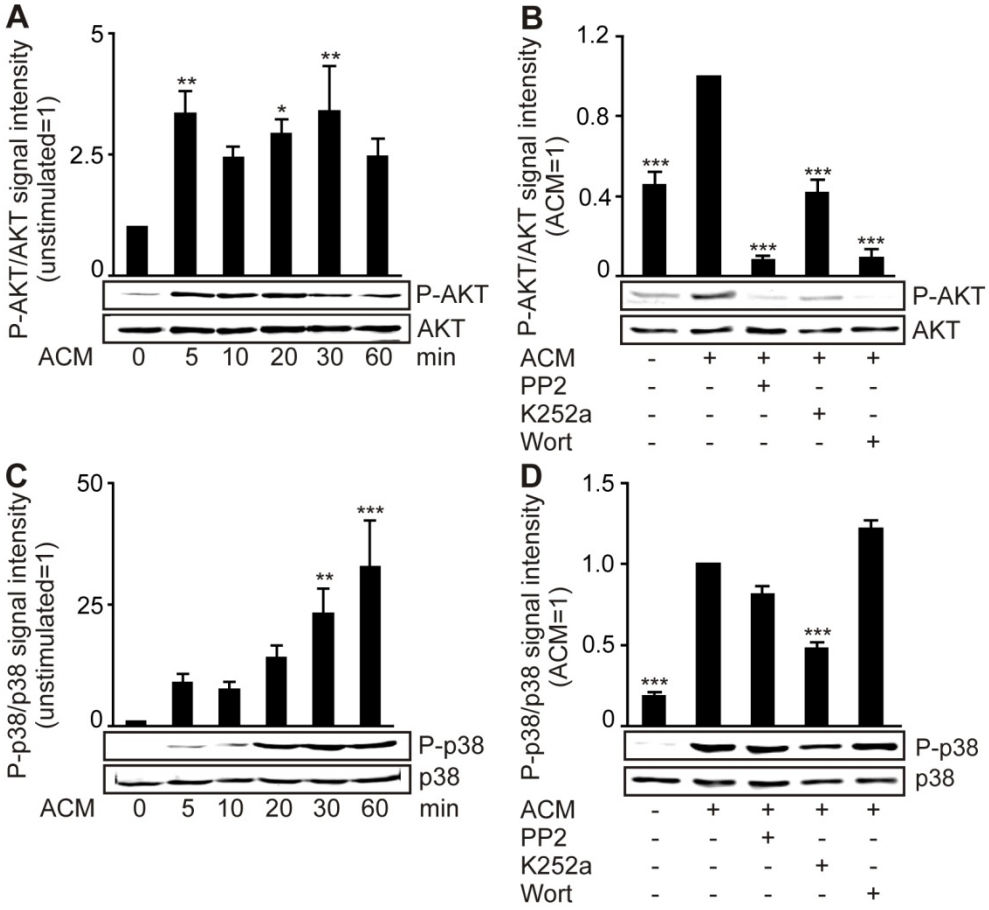

Figure 26: ACM-induced AKT and p38 phosphorylation depends on TRKA
(A, C) MΦ were incubated for indicated times with ACM and Western analysis was performed. Graphs show quantification of ACM-mediated phospho-AKT and phospho-p38 protein expression, with unstimulated control set to 1, $n \geq 11$. **(B, D)** Cells were stimulated for 30 min with ACM and inhibitors PP2 (10 µM), K252a (250 nM), Wortmannin (100 nM). For quantification ACM stimulation was set to 1, $n \geq 4$. Inhibitors were pre-incubated for 45 min before ACM treatment. All data are means ± SEM. Statistics were performed using one-way ANOVA and Bonferroni's post test.*, $p \leq 0.05$; **, $p \leq 0.01$; ***, $p \leq 0.001$.

In summary, p38 phosphorylation was only dependent on TRKA, whereas AKT activation needed functional TRKA and src. This behaviour and the distinct time kinetics argue for differential regulation of the two pathways, with PI3K/AKT being of major importance.

5.3.2 Constitutive NGF secretion takes part in IL-10 induction

In the following experiments I reached out to understand the molecular basis of TRKA activation. Activation of TRKA is reported to depend either on the availability of its ligand NGF and/or transactivation e.g. by other receptor tyrosine kinases without requiring NGF, but may also be regulated by the availability of the receptor itself (183).

In a first approach, I scavenged NGF in ACM and in supernatants of MΦ. Using a neutralizing antibody significantly, but not completely, inhibited ACM-induced IL-10 protein secretion after 24 h compared to isotype control (Figure 27). Thus, I searched for the source of NGF.

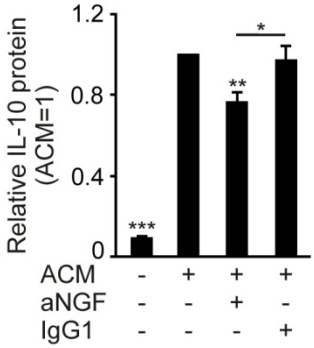

Figure 27: Neutralization of NGF reduces IL-10 secretion
MΦ were incubated for 24 h with ACM and neutralizing anti-NGF ab (aNGF) (5 µg/ml) or control IgG1 (5 µg/ml). ACM was pre-incubated with antibodies for 45 min at 37°C prior to addition to the cells. IL-10 protein was measured in supernatant by CBA and ACM treatment was set to 1, n = 8. Data are means ± SEM. *, $p \leq 0.05$; **, $p \leq 0.01$; ***, $p \leq 0.001$. One-way ANOVA followed by Bonferroni's post test was used for statistical validation.

Existing literature points to cancer cells, as well as monocytes/MΦ, as potential sources of NGF. Especially for breast cancer, strong NGF release has been described (188, 189) and the same holds true for MΦ (194, 229). To investigate whether dying MCF-7 or MΦ were the source of NGF, I performed qRT-PCR for NGF mRNA induction and Western blotting for intracellular protein expression in the course of ACM generation (Figure 28 A and B) or in stimulated MΦ (Figure 28 C and D). Changes in NGF mRNA or protein levels were observed neither in MCF-7 cells nor in MΦ. Interestingly, Western analysis of cell lysates for NGF revealed different maturation states of NGF. MCF-7 lysates showed a pronounced band at the size of the immature pro-NGF form, whereas MΦ revealed a band at the size of matured monomeric NGF (Figure 28 B and D).

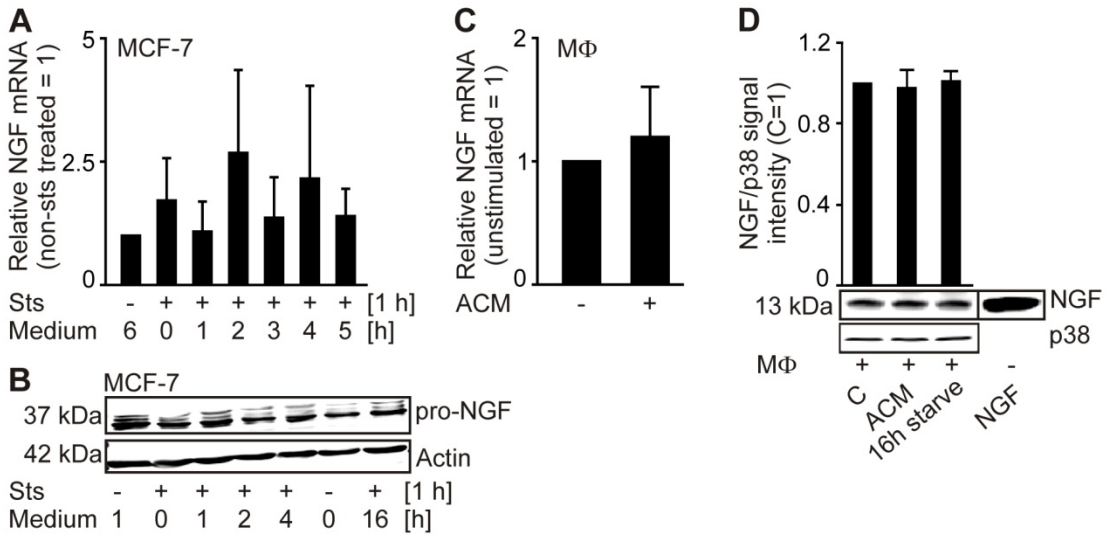

Figure 28: NGF is not induced in MCF-7 nor in MΦ

(A, B) MCF-7 cells were treated as for preparation of ACM with or without induction of apoptosis by staurosporine (Sts). Cells were harvested after different incubation periods with growth medium after Sts treatment. **(A)** NGF mRNA and ribosomal 18S RNA were quantified by qRT-PCR. The ratio of NGF versus ribosomal 18S in non-sts treated cells was set to 1, n = 5. **(B)** Western blotting of MCF-7 cell lysates was performed, n = 1. **(C)** MΦ were stimulated for 3 h with our without ACM. NGF mRNA and ribosomal 18S RNA were quantified by qRT-PCR. The ratio of NGF versus ribosomal 18S in unstimulated cells was set to 1, n = 2. **(D)** MΦ were incubated with ACM or without C for 20 min after medium exchange or no medium exchange took place after 16 h-starvation (16h starve). Whole cell lysate expression of NGF and p38 was followed by Western blotting. Authentic NGF served as control. For quantification the ratio of NGF to p38 was calculated with C set to 1, n = 4. Data are means ± SEM.

It remained elusive, which cell type produced NGF as no induction through stimulation was observed. To clarify this, I analyzed NGF content in ACM, in supernatants of MΦ treated with or without ACM for 20 min, as well as in normal growth medium. The monomeric form as well as the active dimer of NGF was present in ACM in low quantities, but to a similar extent as in growth medium containing the same amount of FCS. However, human MΦ constitutively secreted high levels of NGF as indicated by the presence of the active dimer already 20 min after medium exchange and its prominent accumulation over time in the supernatant of 16 h-starved MΦ. Surprisingly NGF release was not affected by the addition of ACM (Figure 29). Thus, although ACM-induced IL-10 release was clearly dependent on the presence of NGF, the availability of NGF was not the decisive regulatory step.

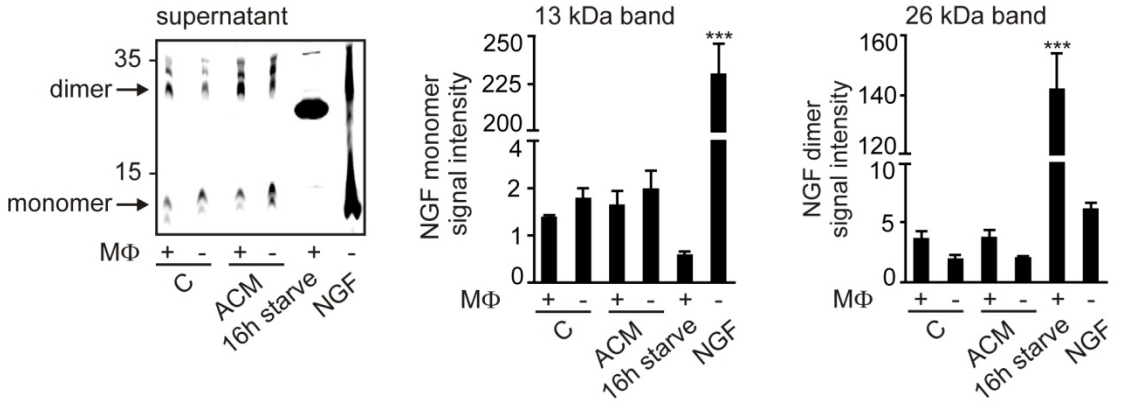

Figure 29: Macrophages constitutively secrete high levels of NGF
NGF was detected in control medium C and ACM alone or after 20 min incubation on starved MΦ. Additionally, supernatant of 16 h-starved MΦ and authentic NGF (100 ng/ml) in control medium were measured by Western blotting. Graphs show quantification of monomeric and dimeric NGF, n = 4. Data are means ± SEM. ***, $p \leq 0.001$. Statistics were performed using one-way ANOVA and Bonferroni's post test.

As the availability of NGF was not the rate-limiting step in TRKA activation, transactivation of TRKA or the availability of TRKA at the plasma membrane had to be considered as potential modes of actions. Transactivation of TRKA is frequently observed and was reported downstream of adrenergic receptor 2A (186), adenosine receptors (230), epidermal growth factor receptor (EGFR), formyle peptide receptor (231) and other receptors. Based on the finding that neutralization of NGF did not completely prevent ACM-induced IL-10 secretion, I suspected transactivation of TRKA to be involved. However, pharmacological inhibition of potential receptors did not significantly interfere with ACM-mediated IL-10 production (Figure 30), although a tendency was observed for the EGFR inhibitor AG1478.

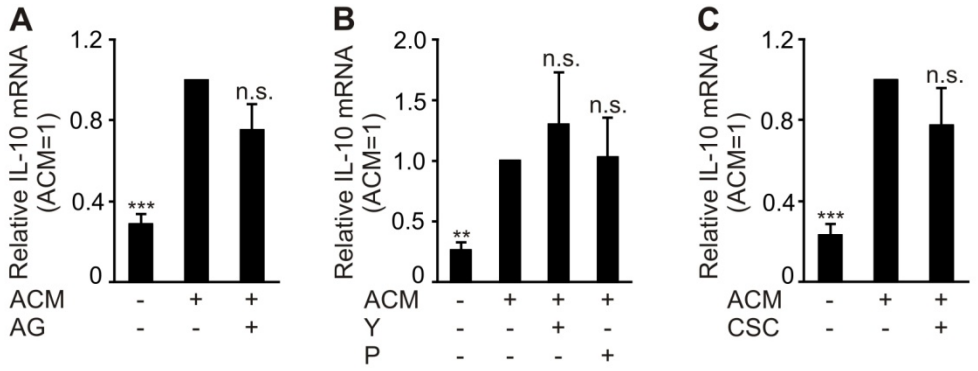

Figure 30: Common transactivation partners of TRKA are not involved in IL-10 production
(**A – C**) MΦ were pre-incubated with inhibitors for 45 min followed by stimulation for 3 h with ACM with or without EGFR inhibitor AG1478 (1 µM), α-adrenoceptor antagonist yohimbine (Y, 10 µM), β-adrenoceptor antagonist propranolol (P, 1 µM), or A2A adenosine receptor antagonist CSC (10 µM). IL-10 mRNA and 18S RNA were quantified by qRT-PCR. The ratio of IL-10 versus 18S RNA in ACM-treated cells was set to 1 and statistics were performed using student's t-test, $n \geq 3$. All data are means ± SEM. *, $p \leq 0.05$; **, $p \leq 0.01$; ***, $p \leq 0.001$.

Finally, I hypothesized that TRKA-dependent increase of IL-10 by ACM might be due to the regulation of TRKA availability in human MΦ. This hypothesis was strengthened by the observation that neither NGF nor any other TRK family member induced IL-10 mRNA in MΦ (Figure 31 A). Furthermore, NGF did not induce phosphorylation of p38 and AKT, while this occured in ACM-treated MΦ (Figure 31 B). In contrast, PC-12 rat pheochromocytoma cells, the gold-standard for investigating TRKA signaling, due to high expression of TRKA at the plasma membrane, responded to both ACM and, although to a lesser extent, also to NGF with phosphorylation of AKT and p38 MAPK (Figure 31 C). This response was specific for NGF, as it was not observed with other neurotrophins (Figure 31 D). These findings suggested that in MΦ, and to a lesser extent in PC-12 cells, ACM increased the bioavailability of TRKA. With the notion that ACM induces a rapid response, I did not expect regulation at the expression level of TRKA. This assumption was preliminarily confirmed at least by the lack of mRNA-increase within 3h of MΦ-stimulation.

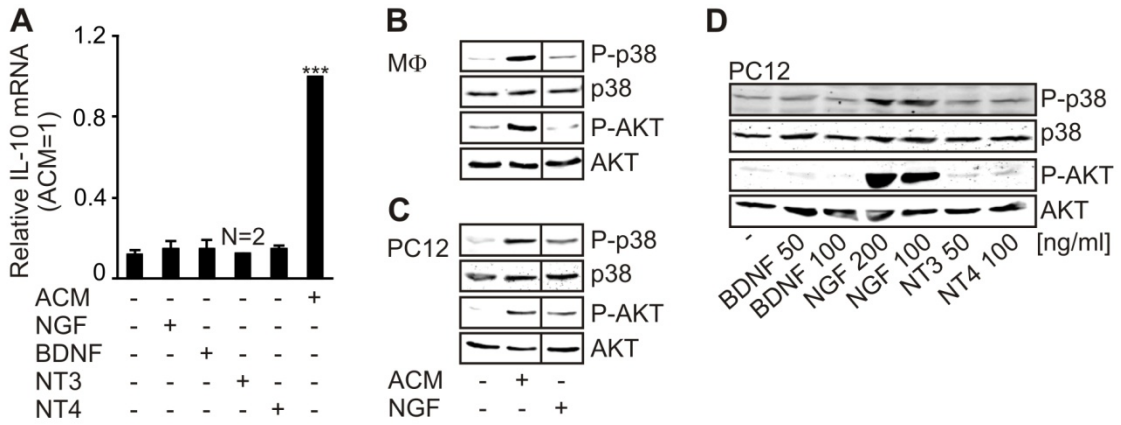

Figure 31: NGF activates p38 and AKT in PC12 cells

(A) MΦ were stimulated for 3 h with NGF (200 ng/ml), BDNF (50 ng/ml), NT3 (20 ng/ml), NT4 (100 ng/ml) or ACM and IL-10 mRNA and ribosomal 18S RNA were quantified by qRT-PCR. The ratio of IL-10 versus ribosomal 18S in ACM-treated cells was set to 1, $n \geq 3$ if not stated otherwise. Data are means ± SEM. ***, $p \leq 0.001$. Statistics were performed using one-way ANOVA and Bonferroni's post test. **(B, C)** MΦ **(B)** and PC-12 cells **(C)** were treated with ACM or NGF (100 ng/ml) for 10 min and relative expression of phosphorylated p38 and AKT to p38 and AKT content was followed by Western blotting, $n \geq 3$. **(D)** PC12 cells were treated for 10 min with neurotrophins NGF, BDNF, NT3 and NT4 at given concentrations. P38 and AKT phosphorylation was analyzed by Western blotting, n = 1.

5.3.3 S1P-dependent redistribution of TRKA to the plasma membrane is required for autocrine NGF signaling

The above described hints pointed to an ACM-induced translocation of TRKA to the plasma membrane for its activation and downstream signaling in MΦ. This assumption was supported by the highly regulated trafficking of TRKA in neurons (232). Therefore, I investigated the localization of TRKA in primary human MΦ before and after stimulation with ACM. Indeed, immunofluorescence staining of TRKA and tubulin, as a cell body marker, revealed a very rapid redistribution of TRKA to the plasma membrane, reaching full manifestation at 10 min of ACM incubation (Figure 32 A). A similar pattern was observed in HEK293 cells overexpressing HA-tagged TRKA (Figure 32 B).

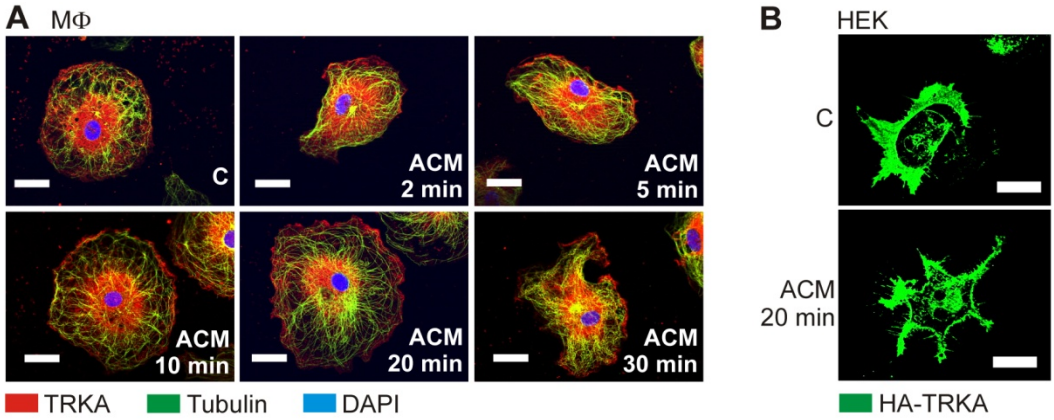

Figure 32: ACM-induced trafficking of TRKA to the plasma membrane
(A) Time kinetics of ACM effect on TRKA localization. MΦ were incubated with or without ACM and stained for TRKA (red), Tubulin (green) and DAPI (blue). Cells from 3 individual donors were used and at least 6 pictures per stimulation were acquired. **(B)** HEK293 cells were transfected with HA-tagged TRKA, stimulated for 20 min with ACM and stained for HA (green). At least 8 pictures per stimulation from 2 individual experiments were acquired and representative pictures are shown. Scale bars represent 10 µm.

With the intention to characterize the cell organelle of TRKA translocation, I used CD36 as membrane marker for the following experiments. By staining for CD36 before permeablization of the cells, I was able to nicely depict the delicate and typical MΦ-pseudopodia and to show potential colocalization of CD36 and TRKA at the plasma membrane. Staining of CD36 and TRKA revealed remarkable differences between unstimulated and ACM-stimulated MΦ. Control cells with pronounced $CD36^{+}$ pseudopodia showed no accumulation of TRKA at the plasma membrane. In contrast, I observed strong TRKA staining at the plasma membrane in ACM-stimulated MΦ, accompanied by remarkably reduced pseudopodia (Figure 33). This effect was abrogated neither by neutralization of NGF nor by the TRK inhibitor K252a (Figure 33), which underscored the assumption of another factor being involved in TRKA functionality in MΦ.

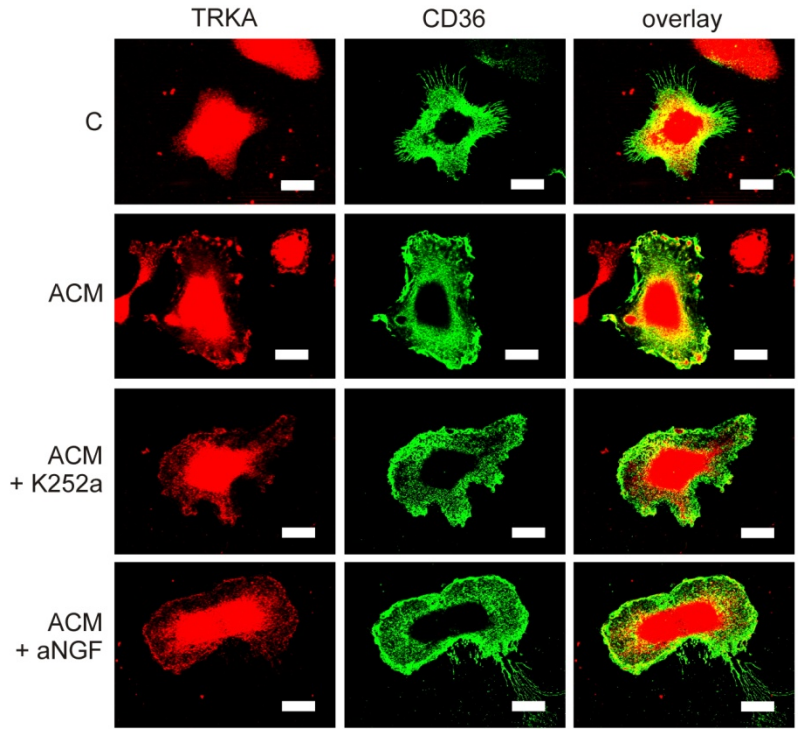

Figure 33: Trafficking of TRKA to the plasma membrane is NGF/TRKA-independent
MΦ were stimulated for 20 min with or without ACM and inhibitor K252a (250 nM) or anti-NGF neutralizing ab (aNGF) (5 µg/ml). K252a was pre-incubated for 45 min on cells and neutralizing ab in ACM before ACM treatment. Cells were stained for CD36 as membrane marker (green) and TRKA (red). Scale bars represent 10 µm, cells from 6 individual donors were used and at least 10 pictures per donor and stimulation were taken.

5.3.3.1 ACM activates S1PR to induce src-dependent TRKA shuttling

The question of the factor responsible for TRKA translocation arose. This led me back to S1P, which had been previously identified to be involved in IL-10 regulation (Figure 11, (130)). S1P and its five receptors are known for their ability to influence and transactivate receptor tyrosine kinases, as exemplified for S1PR4 and human epidermal growth factor receptor 2 (Her2/neu) (233) as well as S1P1 and platelet-derived growth factor receptor (234). Among others, platelet-derived growth factor receptor and TRKA cross-activate S1P1/2 (222, 223). Considering this information, I investigated the effect of pharmacological inhibitors of S1P receptors on ACM-induced IL-10 production, p38 and AKT phosphorylation and finally on trafficking of TRKA.

First, I elucidated the effects of S1P receptor antagonists on ACM-induced IL-10 production. JTE-013, described as a S1P2 antagonist (half maximal inhibitory concentration (IC50) 1.5 µM) and a S1PR4 antagonist (IC50 4.5 µM) (235), reduced ACM-mediated IL-10 production only when used at high concentrations (20 µM *vs.* 1

µM), whereas the S1P1/3 antagonist VPC23019 (236) did not (Figure 34 A). As only high concentrations of JTE-013 showed inhibitory effects, S1PR4 activation is likely required to induce IL-10 secretion from MΦ. This is in line with previous findings showing enhanced IL-10 secretion in T cells via S1PR4 signaling (56). Nevertheless, a synergistic effect with S1PR2 or other S1P receptors cannot be excluded.

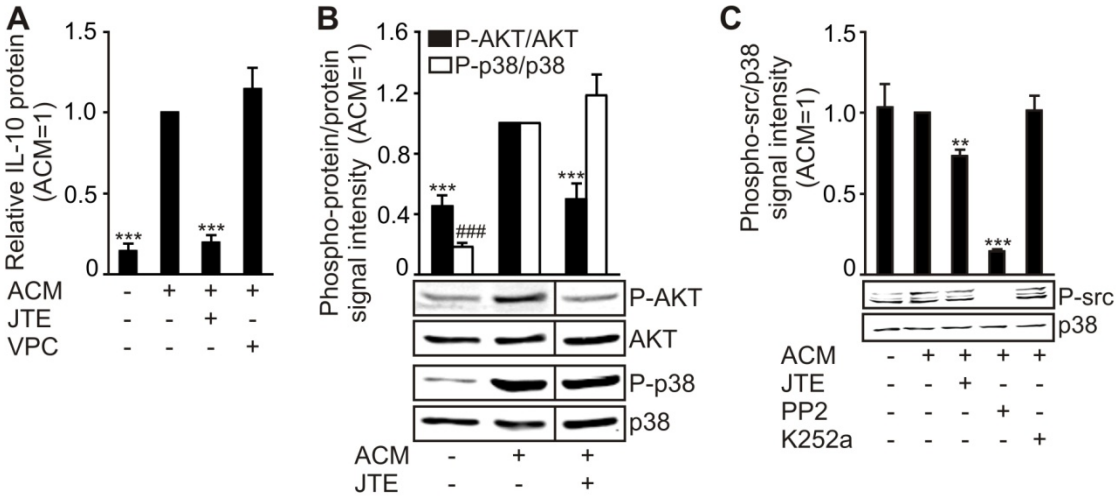

Figure 34: Antagonism of S1PR reduces IL-10, AKT and src phosphorylation
(A) ACM with or without inhibitors JTE-013 (20 µM), VPC23019 (1 µM) was incubated on MΦ and IL-10 protein was measured in supernatant after 24 h by CBA. ACM treatment was set to 1, n ≥ 5. **(B, C)** MΦ were treated with ACM with or without JTE-013 (20 µM), PP2 (10 µM), K252a (250 nM) for 30 min and relative expression of phosphorylated p38, AKT or src to p38 and AKT content was followed by Western blotting. For quantification, ACM treatment was set to 1, n ≥ 5. Inhibitors were pre-incubated for 45 min on cells. Data are means ± SEM and statistics were performed using student's t-test. **, $p \leq 0.01$; ***/###, $p \leq 0.001$.

To further substantiate S1P signaling in IL-10 regulation, I investigated the two required signaling pathways and observed S1PR-dependent AKT phosphorylation (Figure 34 B), which, as described above, was strongly TRKA-dependent (Figure 26 B). Interestingly, JTE-013 had no influence on p38 activation (Figure 34 B). These data corroborate the observation that TRKA inhibition showed weaker effect on p38 phosphorylation compared to AKT (Figure 26 D) and that p38 signaling likely required a yet unidentified protein factor (Figure 13). Prior results had indicated an important role of src in AKT phosphorylation and IL-10 production (Figure 12 C, Figure 26 B). Intriguingly, src phosphorylation was markedly reduced with JTE-013, but not with K252a (Figure 34 C) indicating a putative link involving src between S1PR and TRKA signaling.

In a next step, I was intrigued to know whether TRKA trafficking was influenced by S1PR and src. Indeed, stainings revealed ablated ACM-depended translocation of TRKA to the plasma membrane when S1PR and src were blocked by JTE-013 and PP2 respectively (Figure 35).

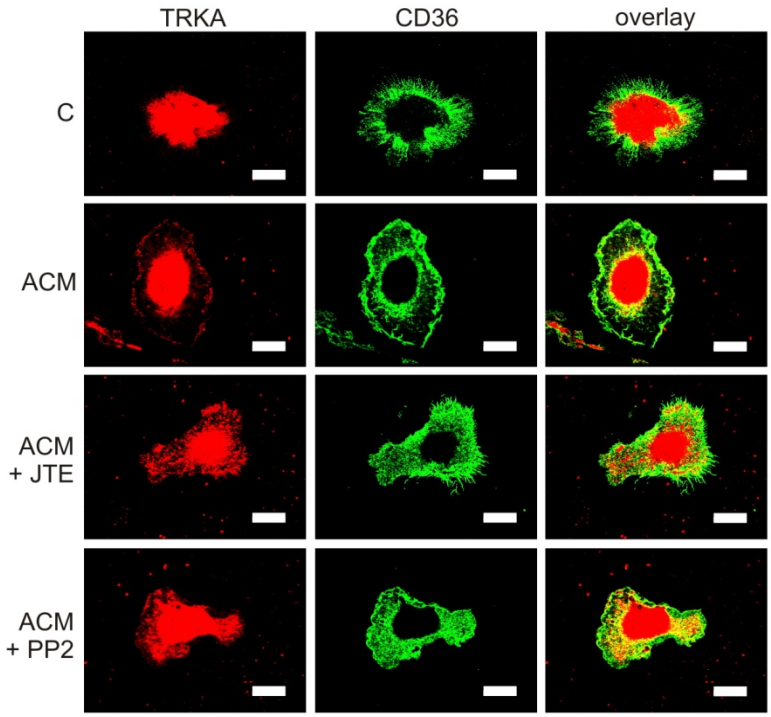

Figure 35: TRKA translocation depends on S1P and src signaling
MΦ were stimulated for 20 min with or without ACM and inhibitors JTE-013 (20 µM), PP2 (10 µM). Inhibitors were pre-incubated for 45 min on cells before ACM treatment. Cells were stained for CD36 as membrane marker (green) and TRKA (red). Scale bars represent 10 µm, cells from 6 individual donors were used and at least 10 pictures per donor and stimulation were taken.

In conclusion and summarized in Figure 42, the here presented data identified a complex regulation of IL-10 secretion from human MΦ. Apoptotic cell-derived S1P activates S1PR. The resulting signaling via src is a requisit for TRKA translocation to the plasma membrane. Membrane-associated TRKA is stimulated by autocrine NGF, which results in induction of IL-10 mainly through PI3K/AKT signaling. However, an unknown ACM-derived factor, signaling through p38, is additionally required for the full MΦ response to ACM

5.4 Regulation of TAM markers of mice and men

5.4.1 ACM induces differentially regulated TAM markers

Within the tumor environment, tumor-associated macrophages express various enzymes, transcription factors, receptors and soluble mediators to establish and maintain a tumor-favourable environment (depicted and summarized in the introduction, Figure 6 and Figure 7). To verify the relevance of my *in vitro* model of ACM-treated MΦ in comparison to the *in vivo* situation of TAM, I screened for induction and regulation of well-described TAM markers in ACM-treated MΦ.

Interestingly, already within 3 h ACM induced a variety of TAM markers and targets of ACM-derived S1P signaling in MΦ (115, 130, 133, 134, 237), such as VEGF, ADORA2A, IDO, IL-8, HIF-1α, and IL-1ra, but had no effect on mRNA expression of mannose receptor 1 (MRC-1) (Figure 36 A).

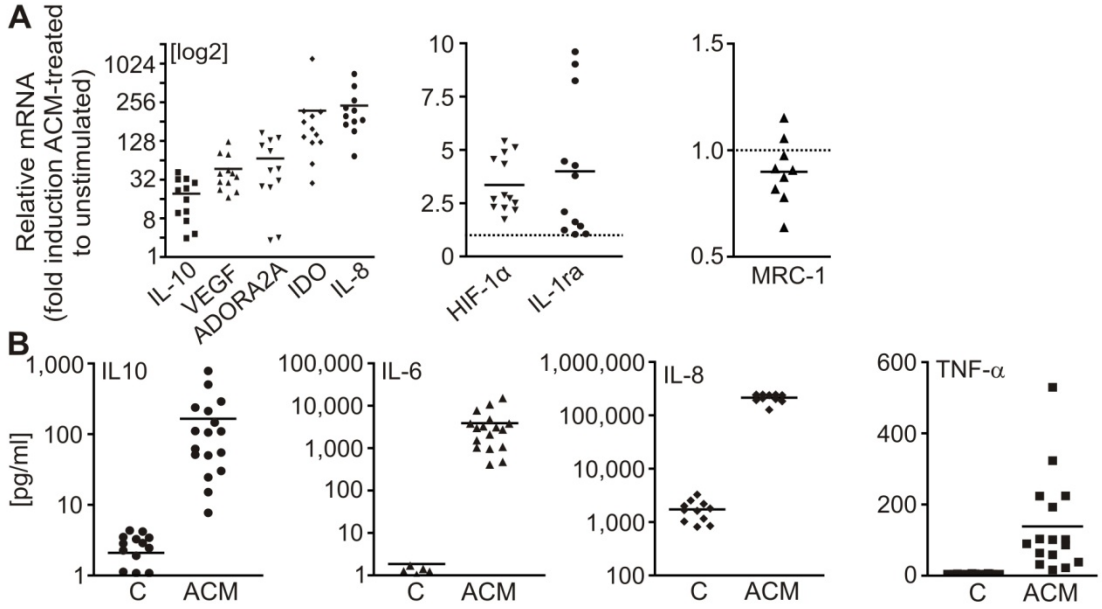

Figure 36: TAM markers in ACM-stimulated MΦ

(A) mRNA regulation of TAM markers IL-10, VEGF, ADORA2A, IDO, IL-8, HIF-1α, IL-1ra and MRC-1 after 3 h stimulation with ACM compared to unstimulated control cells was quantified against ribosomal 18S RNA by qRT-PCR. The ratio of TAM marker mRNA versus ribosomal 18S in ACM-treated cells was set to 1 **(B)** IL-10, IL-6, IL-8 and TNF-α protein was measured in MΦ-supernatants after 24 h-incubation with ACM, using CBA.

In addition to mRNA expression profiles, I noticed drastically enhanced secretion of tumor-promoting cytokines, such as IL-6, IL-8 and TNF-α by ACM treatment, whereas pro-inflammatory, anti-tumoral IL-12p70 was not detectable (Figure 19 and Figure 36 B). Now the question arose whether the augmented TAM markers shared the

regulation patterns I had identified for IL-10. Consequently, I employed inhibitors, which had shown suppressive effects on IL-10 induction. Of note, inhibition of S1P signaling reduced expression of all markers except IL-1ra, which confirmed previous reports for some of the here investigated TAM markers (133, 134). Interestingly, TRKA signaling seemed only to be important for cytokine release (Figure 37), but no marker showed exactly the same response as IL-10.

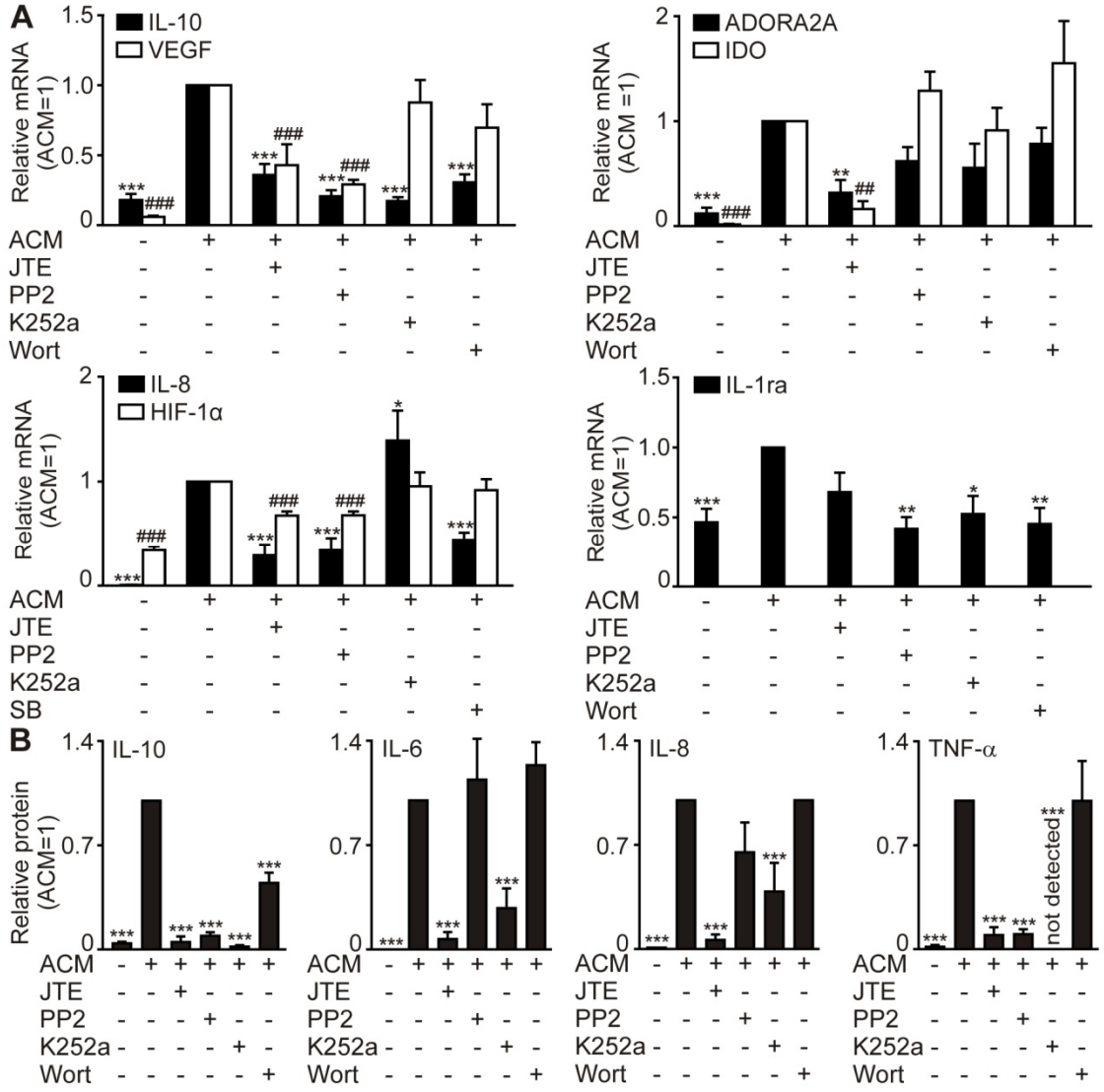

Figure 37: Mechanistic analogy of TAM marker regulation

(A) TAM marker mRNA and 18S RNA were quantified by qRT-PCR after 3 h of incubation with ACM and JTE-013 (20 µM), PP2 (10 µM), K252a (250 nM), Wortmannin (100 nM) or SB203580 (5 µM). The ratio of TAM marker mRNA versus ribosomal 18S in ACM-treated cells was set to 1, $n \geq 3$. **(B)** Cytokines were measured by CBA in MΦ supernatants after 24 h incubation with ACM with or without inhibitors, as in **(A).** ACM treatment was set to 1, $n \geq 5$. Inhibitors were pre-incubated for 45 min. Data are means ± SEM. Statistics were performed using one-way ANOVA and Bonferroni's post test. *, $p \leq 0.05$; **/##, $p \leq 0.01$; ***/###, $p \leq 0.001$.

Of note, although inhibition of S1P signaling reduced secretion of all investigated cytokines, authentic S1P alone or in combination with VCM showed no effect (Figure 38). This again argues for a modulatory function of S1P in combination with other, yet unidentified, AC-derived factors.

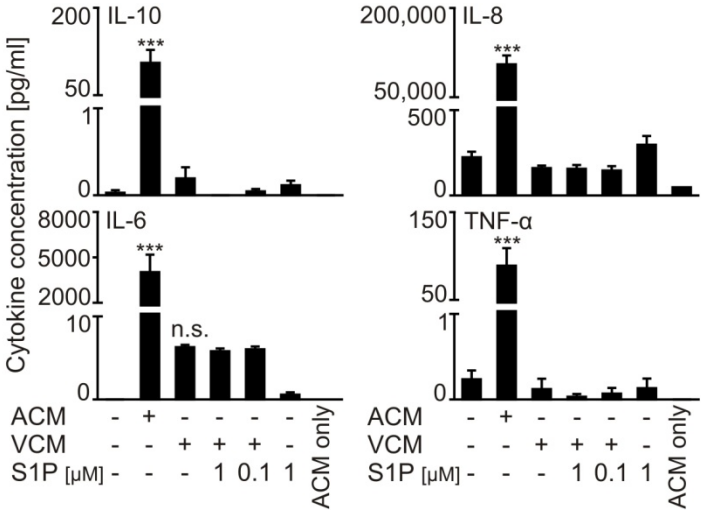

Figure 38: Authentic S1P has no effect on cytokine production
MΦ were stimulated for 24 h with ACM, VCM with or without S1P or S1P alone and secreted IL-10, IL-6, IL-8 and TNF-α were measured in the supernatant by CBA, n = 4 – 5. Statistics were performed using one-way ANOVA and Bonferroni's post test. Data are means ± SEM. n.s., not significant; ***, $p \leq 0.001$.

5.4.2 TRKA signaling is required for cytokine release by murine TAM

I wondered whether the discovered signaling pathway was also active in primary tumor-infiltrating MΦ. Therefore, I isolated TAM from primary murine breast cancer tissue of PyMT transgenic mice and investigated spontaneously secreted cytokines as well as putative mechanistic parallels to human ACM-stimulated MΦ. In a first approach, I isolated $CD11b^+$ cells and exposed them to pharmacological inhibitors used in the ACM/MΦ approach. After 3 and 24 h, supernatants from $CD11b^+$ cells, which were pre-dominantly $CD11b^{high}$, $HLA\text{-}DR^{high}$, $F4/80^{high}$ MΦ (238), were collected and cytokine release (IL-10, IL-6, TNF-α, MCP-1, IL-12p70 and IFN-γ) was assessed. At both time points, the cells produced significant amounts of IL-10, IL-6, TNF-α and MCP-1 without prior stimulation, whereas, as expected, the classical inflammatory IL-12 or IFN-γ were not detectable (Figure 39 A and B). Indeed, K252a and SB203580 markedly suppressed IL-10 release from primary TAM. Although the TRK inhibitor K252a was surprisingly potent in regulating cytokine secretion at 24 h, I exclude toxicity since the inhibitor was as effective when applied for 3 h only, and I did not detect signs of cell

stress. In contrast, src inhibition was only effective at the 24 h time point. This might reflect a situation where TRKA is already localized at the plasma membrane due to activation of CD11b$^+$ cells e.g. by dying tumor cells within the tumor. Compared to IL-10, IL-6 and TNF-α were regulated in a similar manner, being also dependent on TRKA. Interestingly, the PI3K inhibitor Wortmannin did not block cytokine production by CD11b$^+$ cells (Figure 39 C - F), except for MCP-1, contrasting its potent suppression of IL-10 in the human setup (Figure 12 C).

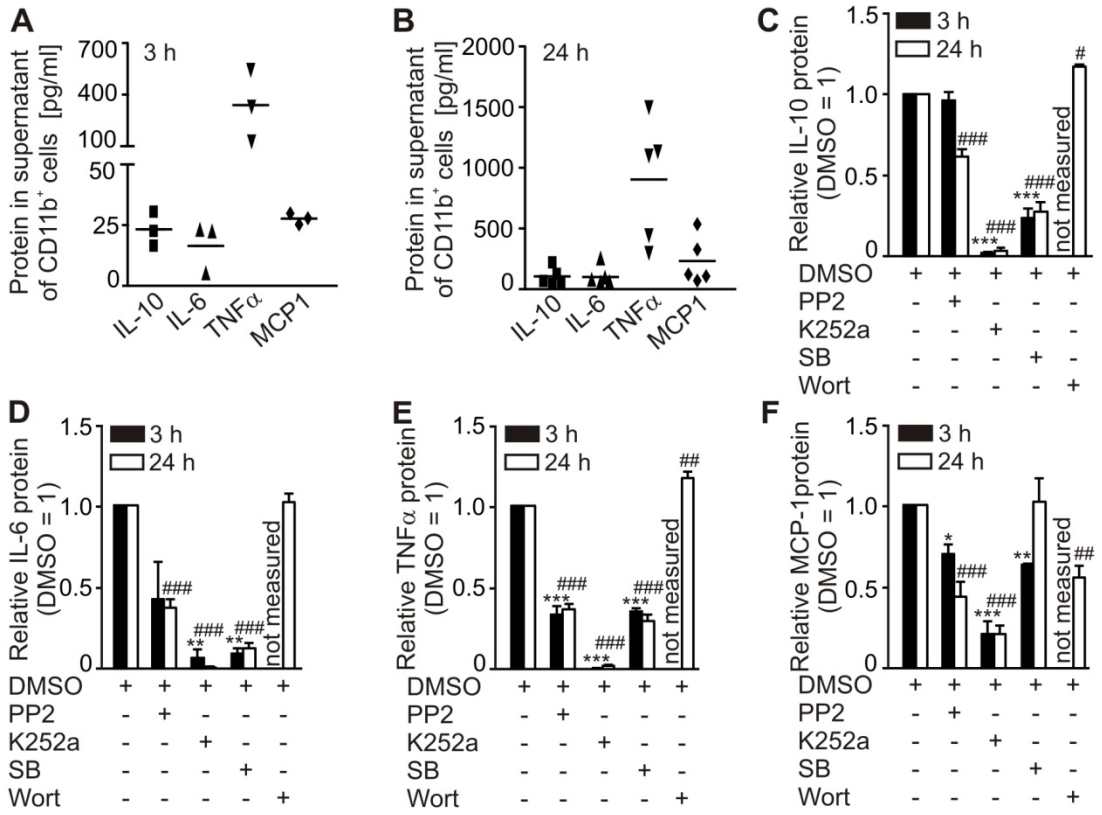

Figure 39: TRKA signaling is operating in murine CD11b$^+$ cells of PyMT tumors

(A, B) CD11b$^+$ cells were isolated from PyMT tumors and cultured for 3 or 24 h. Spontaneous cytokine secretion (IL-10, IL-6, TNF-α, MCP-1, IL-12, IFN-γ) was measured. IL-12 and IFN-γ were not detected. 3 h: n = 3, 24 h: n = 5. **(C-F)** CD11b$^+$ cells were isolated from PyMT tumors and cultured for 3 or 24 h with or without inhibitors PP2 (10 µM), K252a (250 nM), SB203580 (10 µM), Wortmannin (100 nM) and secreted cytokines were measured. For statistical analysis, DMSO (0.1%) solvent-treated cells were set to 1, 3h: n = 3, 24h: n $\geq$ 4. All data are means ± SEM. Statistics were performed using one-way ANOVA and Bonferroni's post test.*$^{/\#}$, p $\leq$ 0.05; **$^{/\#\#}$, p $\leq$ 0.01; ***$^{/\#\#\#}$, p $\leq$ 0.001.

CD11b$^+$ immune cells are not a homogenous cell population, as they are comprised of CD11b$^+$, Ly6G$^+$ granulocytes, CD11b$^+$, F4/80$^-$, HLR-DR$^-$, Ly6C$^+$ monocytes; CD11b$^+$, F4/80$^-$, HLR-DR$^-$, Ly6C$^-$ monocytes and CD11b$^+$, F4/80$^+$, HLR-DR$^+$ TAM, which are all potentially capable of secreting the above measured cytokines. To corroborate

the earlier findings and to verify the importance of TAM in cytokine secretion I sorted the four distinct CD45/CD11b^{high} immune cell sub-populations mentioned above from PyMT tumor single cell suspensions. TAM were the major cell population (~80%) within the sorted CD45/CD11b^{high} cells (Figure 40 A). The four cell populations were seeded at identical densities (6000 cells/well) and 24 h later cytokines were again measured in supernatants. IL-12p70 and IFN-γ were not detected. IL-10 was measured in all four fractions, whereas only TAM showed the previously observed regulation by inhibitors PP2 and K252a. IL-6 and TNF-α secretion was only pronounced by the TAM population and responded to the used inhibitors. When I seeded TAM at higher density (20,000 cells/well) the observed effects were verified and MCP-1 was also detectable, its release being dependent on src and TRKA (Figure 40 B and C).

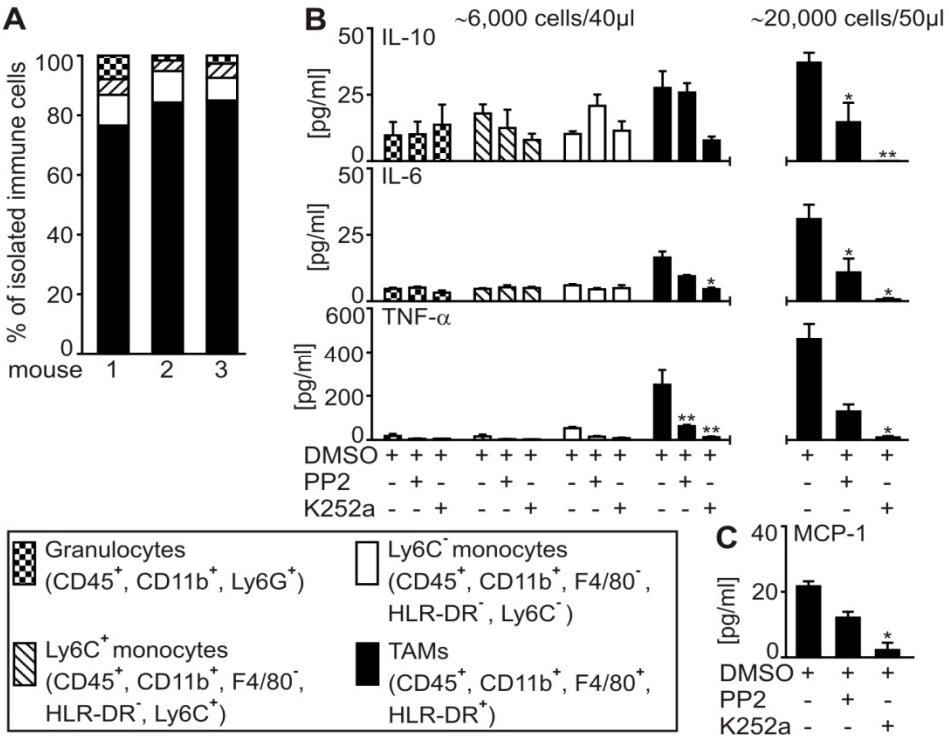

Figure 40: TAM are the main CD11b$^+$ cytokine producing cells in PyMT tumors
(A) Distinct CD45$^+$/CD11b$^+$ immune cell populations were isolated from PyMT tumors and the relative amounts (%) of sub-populations within the CD45$^+$/CD11b$^+$ population are shown. **(B, C)** Cells were cultured at the indicated densities for 24 h with or without inhibitors PP2 (10 µM), K252a (250 nM) and spontaneous cytokine secretion (IL-10, IL-6, TNF-α, MCP-1) was measured. MCP-1 was only detected at higher cell density, n = 3. All data are means ± SEM. Statistics were performed by student's t-test. *, $p \leq 0.05$; **, $p \leq 0.01$.

In conclusion, the combined presented data suggests a very tight and specific regulation of IL-10, as no other investigated marker responded identically.

Additionally, signaling pathways activated downstream of TRKA might be species-specific. However, TRKA was involved in cytokine secretion from both human tumor cell-activated MΦ and isolated murine TAM, which were primed by tumor cells *in vivo*, giving room for further research and possible translation to future cancer therapies.

6 Discussion

The milestone review by Hanahan and Weinberg, 'The Hallmarks of Cancer' (239), summarized six characteristics of cancer cells enabling them to malignantly outgrow. Cancer therapy predominantly focuses on targeting cancer cells directly, and so far not much attention has been paid on the tumor microenvironment as therapeutic target. This gradually changed over the last ten years as marked by the expansion of cancer hallmarks, including new aspects of tumor biology, namely avoiding immune destruction and tumor-promoting inflammation ((103, 240) , Figure 41).

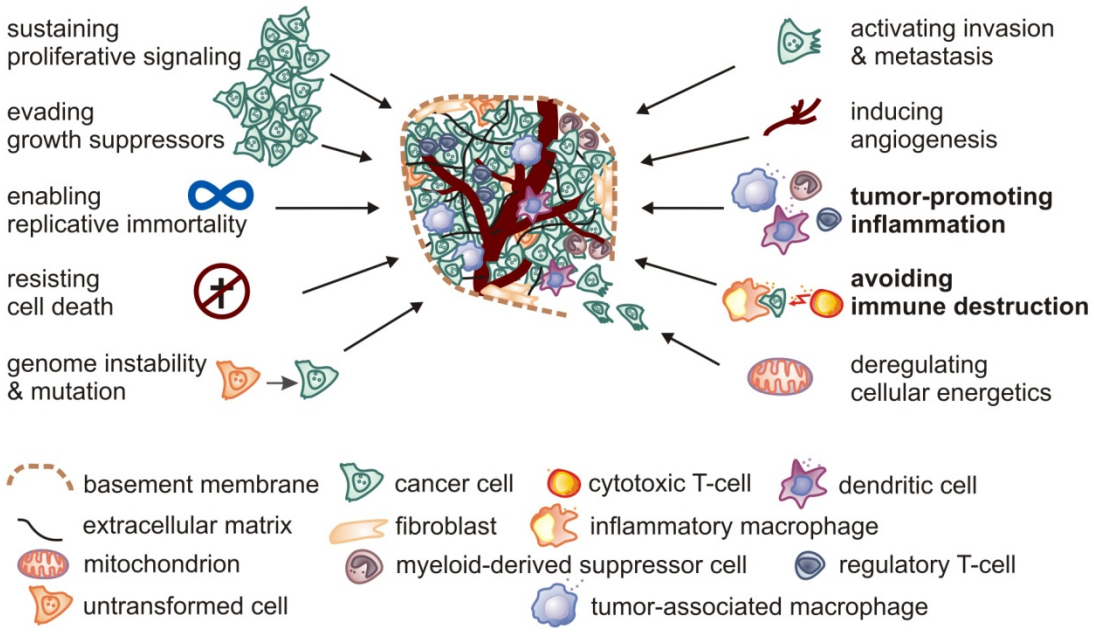

Figure 41: Hallmarks of cancer
Adopted from (240)

Due to a lack of nutrients, diminished oxygen supply, chemotherapy or radiation, a high apoptosis index is found within tumors. The impact of dying cancer cells on fueling cancer growth was recently connected to MΦ polarization in tumors (16, 241, 242). However, as early as 1956, Révész described that inoculation of a mixture of dead and viable cancer cells drastically augmented tumor growth and reduced overall survival in mice compared to viable cells only (243). Mechanistic proof for this observation comes from interaction of apoptotic tumor cells with neighboring cancer cells, as well as immune cells. Cell death and concomitant caspase-3 activation in tumors was recently shown to stimulate growth and survival of tumor cells by the release of PGE2 (244), and vaccination of MΦ with apoptotic but not necrotic cancer

cells acted as a strong priming factor for rapid growth of tumor xenografts in mice (245).

In this scenario, direct cell-cell contact of apoptotic cells and MΦ was not required for phenotypical changes in MΦ (130). Earlier studies from our lab (133-135, 241, 246), as well as the presented data herein, show pronounced induction of tumor-promoting cytokines and expression of well established TAM markers in MΦ challenged with supernatant of apoptotic cancer cells. Since especially in breast cancer, TAM exert powerful tumor-promoting functions by driving immune as well as tumor cells to promote tumor growth (98, 131), I chose dying MCF-7 breast cancer cells for my studies. Of note, supernatant from other solid tumor cell lines, which respond to apoptotic stimuli, e.g. A549 lung cancer cells or DU145 prostate cancer cells, show comparable responses in MΦ. This simplified model to investigate and understand aspects of MΦ activation in tumors certainly does not reflect the complexity of TAM plasticity and diversity in different stages of cancer progression (98, 247) but may serve as an acceptable starting point.

With the intention to characterize the nature of macrophage responses to apoptotic cancer cell supernatant, I investigated in detail the production of the immunosuppressive cytokine IL-10:

1) I started to evaluate the impact of S1P and common intracellular signaling pathways in IL-10 production.
2) Knowing that S1P was not the only ACM-derived factor responsible for MΦ responses, I performed an adenoviral RNAi high-throughput screen to reveal novel regulators of MΦ polarization.
3) Following screen validation of several targets of a distinguished IL-6/IL-10 co-regulatory cluster, I chose TRKA as candidate to perform mechanistic in-depth analysis of IL-10 regulation.
4) Finally, having elucidated the complex S1PR/src/TRKA/AKT-signaling circuit resulting in IL-10 release after ACM stimulation, I investigated the involvement of this signaling axis on other tumor-associated markers in ACM-stimulated human MΦ and in primary murine immune cells infiltrating PyMT mammary carcinoma.

6.1 The facets of S1P signaling in MΦ

The decision to study mechanisms of IL-10 secretion in detail evolved from observations that IL-10 release from MΦ was subject to complex regulation as compared to e.g. IL-8 and TNF-α. Co-cultures of MΦ with cancer cells followed by stimulation with LPS/IFN-γ resulted in enhanced IL-8 and reduced TNF-α production compared to LPS/IFN-γ alone. The effect of co-cultures was dependent on cancer cell death and SK2 in cancer cells. Interestingly, LPS/IFN-γ-induced IL-10 secretion was not influenced by cancer cells, but when treating MΦ with ACM or ACM-siSK2 in the absence of LPS/IFN-γ, IL-10 production was cell death and SK2 dependent (130). I therefore concentrated on ACM-mediated IL-10 induction without further MΦ activation by LPS/IFN-γ. In early experiments, I verified MΦ as the exclusive source of IL-10 in my system, as cancer cells are also capable of IL-10 production (143). Furthermore, I asked whether cancer cell death was necessary to trigger IL-10 release. I was able to reproduce previous results from our lab (130) showing S1P dependancy, but neither authentic S1P alone nor in combination with supernatant from viable cancer cells provoked IL-10 secretion. During that time, we published data from a MCF-7 xenograft study in nude mice, emphasizing the potent role of S1P on MΦ functions within tumors by regulating MΦ polarization but not infiltration. A drastically reduced tumor burden of MCF-7-siSK2 tumors compared to MCF-7-wt tumors was observed, probably due to the inflammatory, anti-tumor MΦ phenotype in siSK2 tumors (207).

S1P is a multipotent signaling molecule and, by binding to its 5 receptors, can activate multiple signaling pathways dependent on expression profiles, interaction with specific signaling molecules and cross-talk with other receptors (see 3.2.2.4 and 5.3.3.1). Of the five receptors, S1PR4 is primarily expressed by immune cells (248) and might be the dominant S1P receptor on human MΦ (129). There are yet few functional studies concerning S1PR4 in immune cells. Interestingly, forced expression of S1PR4 in T cells inhibited proliferation accompanied by reduced secretion of IL-2 and IFN-γ but enhanced IL-10 release (56). In my work, supportive evidence for the importance of S1PR4 emerged from immunofluorescence data. I observed pronounced retraction of pseudopodia following ACM treatment and incubation with the S1PR2/4 inhibitor JTE-013 markedly restored pseudopodia expression. This finding correlates with

observations from Koh et al., who reported that S1P initiates retraction of pseudopodia in NIH3T3 clone 7 cells (249). Furthermore, overexpression of S1PR4 in chinese hamster ovary cells (CHO-K1) stimulated with S1P showed cytoskeleton rearrangement and rounding of cells (250). However, involvement of other S1PRs alone or in combination cannot be excluded, as JTE-013 at concentrations used here not exclusively affects S1PR4. Moreover, previous studies on ACM-stimulated MΦ have shown involvement of other S1PRs. In murine MΦ, S1PR2 accounted for ACM-induced arginase-2 expression (135), and S1PR1 led to augmented heme oxygenase-1 in ACM-stimulated human MΦ (133). Authentic S1P was sufficient to reproduce ACM-mediated HO-1 (133), Arg-2 (135), Bcl-2 and Bcl-xl expression, protected MΦ from chemotherapeutic-induced cell death and repressed NFκB activity (34). On the other hand, HIF-1α expression (134) and, regarding the here presented data, overall cytokine production were S1P-dependent but required an additional yet unidentified factor (*6.4.1*).

6.2 Validation of IL-6/IL-10 co-regulation

To affect MΦ polarization during tumor development, the goal must be to identify regulators impinging on more than one phenotypical and preferable functional aspect of these cells. Therefore, after completion of the HTS on IL-10 regulation, I screened for additional cytokines (IL-6, IL-8, IL-12), which are positively (IL-6, IL-8) or negatively (IL-12) associated with macrophage-dependent tumor promotion (97). Interestingly, a pronounced cluster of shRNAs, reducing both IL-10 and IL-6 secretion was identified.

This revealed co-regulation spurred my interest, as IL-10 and IL-6 signal through STAT3 (251) to promote tumor outgrowth, although by different mechanisms. IL-10 is usually connected to suppression of anti-tumor immune responses. IL-6 is rather associated with promoting survival and proliferation of tumor cells as well as tumor angiogenesis (252, 253). Therefore, targeting a common regulator of tumor-associated production of these cytokines might be advisable. Focusing on this cluster, I verified five of the identified targets in a different set-up *in vitro*, one being IL-4Rα, which has been described to contribute to TAM generation in mouse models (110, 254). However, I also identified a multitude of new genes that were not previously linked to TAM generation or MΦ polarization. During validation, two out of five targets affected

release of IL-10 and IL-6, two targets influenced either IL-10 or IL-6, whereas one target was not confirmed. Keeping in mind the complex screening procedure using primary cells and the different selection and maturation stimuli for MΦ ($CD14^+$ selection and M-CSF vs. selection by adherence and human serum), the comparatively high level of reproducibility strengthens the credibility of the identified genes regulating cytokine expression in this particular setting. Nevertheless, the putative targets identified in the HTS require independent validation *in vitro* as well as *in vivo* in relevant assays in the future.

6.2.1 IL-4 receptor alpha

One of the identified IL-10 and IL-6 co-regulators was IL-4Rα/IL-4RA, one subunit of the receptor for both IL-4 and IL-13 (255). These two cytokines play pivotal roles in MΦ phenotyping relevant for wound healing and allergic inflammatory diseases. Additionally, both cytokines are established inducers of IL-10 (95, 256). However, the source and the identity of the ligand for IL-4Rα was unknown, since IL-4 was produced by neither MCF-7 cells nor MΦ stimulated with ACM. Interestingly, human MΦ produced low levels of IL-13 (80 pg/ml). Therefore, IL-13 released by MΦ themselves (257) rather than cancer cells (258) might trigger IL-10 and IL-6 in an autocrine fashion (Figure 43). A possible intermediate in this mechanism might be IL-13-dependent TGF-β production (255) augmenting IL-6, which has been described for PBMCs and endothelial cells (259, 260). In line, TGFBR3, TGFBI and other TGF-related genes in connection with IL-10 production emerged from the screen (refer to *6.4.1*). Identification of the well known IL-4RA-dependent IL-10 production can be regarded as verification of the screening approach. In addition, diminished IL-6 production, which was to my knowledge not described before, adds novelty.

6.2.2 Cannabinoid receptor 2

Besides IL-4RA, I validated the cannabinoid receptor 2 (CBR2) to be involved in IL-10 and IL-6 secretion by ACM-stimulated MΦ. Endocannabinoids are potent regulators of immune responses (261). Under inflammatory conditions they may provoke anti-inflammatory effects in MΦ and are described to be directly synthesized by MΦ (212, 262). It was shown that in murine MΦ, cannabinoids reduced oxLDL-mediated inflammatory responses (263). Additionally, LPS/IFN-γ activated murine MΦ (264) and

glia cells replied to endocannabinoids with enhanced IL-10 secretion (265). Regarding IL-6 regulation, CBR2-dependent suppressive effects have been reported (212), but respective experiments were consistently being performed using inflammatory LPS-stimulated MΦ (266) and are therefore not directly comparable to my approach. Importantly, ACM-stimulated MΦ did not produce enhanced levels of endocannabinoids, as determined in preliminary experiments in our lab using lipid mass spectrometry. Therefore, the ligand for CBR2 must be generated by the tumor cells (Figure 43). With regard to lipids as signaling molecules, cannabinoids were shown to induce S1P synthesis, and S1P itself functionally interacts with CBR2 (267). On the other hand, sphingosine was shown to antagonize cannabinoid receptor 1 signaling (268). An interaction of the cannabinoid- and S1P-signaling system might be one of the regulatory circuits in ACM-stimulated MΦ. Although I did not identify S1PRs in the screening procedure, S1PR4 was associated with IL-10 induction in the primary screen, but failed to score in the rescreen. One might argue for activation of multiple S1P receptors on MΦ by ACM but also an interaction with the CBR system might be possible, which would explain the absence of S1PRs in the final hitlist.

6.2.3 HMG-CoA reductase

Unexpectedly, 3-hydroxy-3-methylglutaryl coenzyme-A (HMG-CoA) reductase (HMGCR) was identified as a regulator of IL-10 and IL-6 in the screen and was validated for regulating IL-10 in ACM-stimulated primary human MΦ using a knockdown approach. HMGCR is the rate-limiting enzyme for mevalonate synthesis, essential for production of steroids, cholesterol, ubiquinones, and prenylation of GTPase proteins (214). I wondered whether statins, widely used HMGCR inhibitors, would reproduce the effect of the HMGCR knockdown. However, the two statins cerivastatin and atorvastatin, mimicked the effect of the HMGCR knockdown only at certain concentrations. This might be explained by off-target side-effects of these drugs, which curb the potential benefit of interfering with HMGCR via statins for interfering with cancer. As opposed to my limited and defined system, primarily anti-inflammatory effects of statins were observed in large clinical trials (215), and statins were shown to reduce radiotherapy-induced pro-inflammatory cytokines and DNA damage (214). On the other hand, zoledronic acid, a nitrogen-containing bisphosphonate used therapeutically against bone resorption, inhibits the farnesyl pyrophosphate synthase

in the mevalonate pathway. Zoledronic acid was shown to repolarize anti-inflammatory TAM towards an inflammatory anti-tumor M1 phenotype with reduced IL-10 secretion, augmented IFN-γ, iNOS and NFκB activation (269). This report correlates with my findings where statins reduce IL-10 secretion by ACM-stimulated MΦ. Thus, it seems that effects of statins might largely depend on the studied cell type, stress stimulus or disease. However, interfering with HMGCR might potently impact immunological processes, which have to be closely investigated, as statins are widely used and often by patients with multiple morbidities.

6.3 TRKA involvement in IL-10 production

An extensive part of my studies focused on the elucidation of TRKA involvement in MΦ polarization by ACM (Figure 42). I had chosen TRKA as a target for detailed validation of the IL-6/IL-10 cluster. TRKA and its ligand NGF were previously controversially associated with supporting and suppressing tumor growth (187, 220), and especially breast cancer cells can benefit from NGF signaling (177, 188, 189, 220). Furthermore, TRKA was shown to modulate immune cell function, but until now only a handful of studies have been performed investigating NGF effects on murine and human monocytes and MΦ. Inflammatory properties of TRKA activation by NGF are described for murine MΦ, as enhanced NO and TNF-α production were reported (270). Murine peritoneal MΦ showed increased phagocytosis in response to NGF stimulation as well as enhanced killing of ingested pathogens (271). Moreover, NGF treatment of mouse peritoneal MΦ increased IL-1β release. However, these effects were not observed in human MΦ (272). Importantly, with regard to my studies, TRKA was shown to be highly expressed on human monocytes but largely down-regulated upon differentiation to MΦ (273). Under unstimulated conditions, my experiments revealed that TRKA is not associated with the plasma membrane of MΦ. This observation is corroborated by the assumption that low TRKA expression in mature MΦ compared to monocytes might enhance the sensitivity of TRKA activity regulation, since TRKA is prone to auto-activation when highly expressed (274). Interestingly, in human monocytes and monocyte-derived dendritic cells, NGF seems to elicit anti-inflammatory properties. Bracci-Laudiero et al. showed that LPS-stimulated human monocytes responded to neutralization of endogenous NGF with reduced IL-10

secretion (224). Along this line, NGF alone was sufficient to induce IL-10 in human monocyte-derived dendritic cells (275), which I did not observe in human MΦ. Thus, limited availability of TRKA might regulate its signaling in MΦ, as I observed pronounced constitutive NGF secretion by unstimulated MΦ, which therefore cannot be the limiting factor. Contrary to my observations, Samah et al. previously reported enhanced gene expression of NGF upon virtually any kind of activation, but no detectable secreted protein in M-CSF/GM-CSF-differentiated human MΦ (272). These data point to a macrophage-specific receptor regulation among human myeloid cells, which might be sensitive to different MΦ differentiation protocols.

My data on TRKA biology reinforce the importance of S1P in MΦ polarization. Immunofluorenscence stainings strongly support S1PR/src-mediated shuttling of TRKA to the plasma membrane of human MΦ. This finding might be of relevance not only with regard to MΦ activation by dying tumor cells. Activation of sphingosine kinase 1 by LPS or other pro-inflammatory stimuli in monocytes/MΦ is well established (123, 276). Thereby, newly generated S1P might be transported to the outside of cells and thus, induce shuttling of TRKA to the plasma membrane, finally modulating the response to LPS.

All five S1P receptors have been linked to activation of the PI3K/AKT pathway, which was rapidly activated after ACM stimulation. Direct S1P/S1PR signaling could partially explain fast AKT phosphorylation in MΦ already 5 min after activation with ACM. As TRKA translocation to the plasma membrane reached its amplitude after 10 min, the rapid AKT phosphorylation was unrelated to TRKA activation and thus, not related to the studied IL-10 induction. However, as seen by phosphorylation-sensitive Western blot analysis and the use of pharmacological inhibitors, AKT phosphorylation/activation at 30 min, after TRKA shuttling had occurred, was clearly dependent on S1PR, src and TRKA signaling; the same pathways that were critically involved in IL-10 induction by ACM. These findings strongly suggest that the autocrine NGF loop and the preceding S1PR/src-dependent translocation of TRKA were necessary for AKT phosphorylation. Literature reinforces this src-mediated interaction as src kinases are known to be important mediators between G protein-coupled receptors and tyrosine kinase receptors, where they associate with the latter to influence functional responses. Furthermore, src/TRKA interaction was shown to

facilitate and enhance NGF signaling (277). My data add a different facet to this important interaction by showing that TRKA shuttling depends on src kinases. In analogy, fibroblast growth factor receptor 1, another tyrosine kinase receptor, also requires src for endosomal activation, trafficking to the plasma membrane and signaling (278).

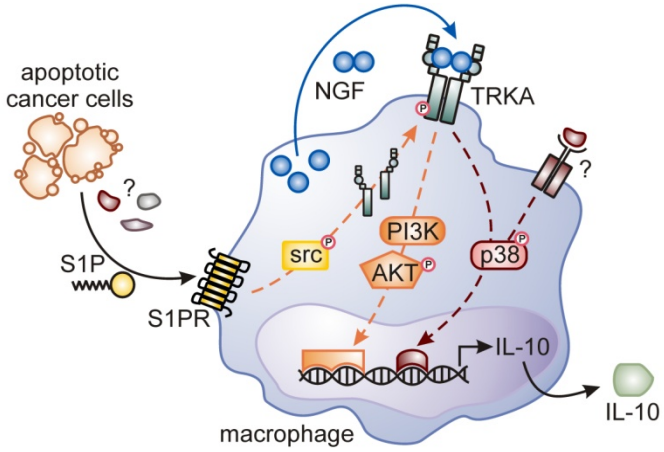

Figure 42: Scheme of IL-10 induction by ACM in macrophages
S1P, generated by apoptotic cells, induces src-dependent TRKA translocation to the plasma membrane, where autocrine NGF accesses its receptor to signal through PI3K/AKT and p38 provoking IL-10 production. Besides S1P, at least one other factor signaling through p38 is necessary for IL-10 induction. Abbreviations: AKT, protein kinase B; IL, interleukin; NGF, nerve growth factor; p38, mitogen-activated protein kinase p38; PI3K, phosphoinositide 3-kinase; S1P, sphingosine-1-phosphate; S1PR, S1P receptor; src, sarcoma tyrosine kinase; TRKA, tyrosine kinase receptor A.

Another interesting aspect of S1P/NGF interaction is their shared chemotactic potential. NGF increases chemotaxis in murine and human MΦ (272, 279), which has also been reported for S1P (33, 128, 280). One might speculate that S1P, derived from damaged tissue, potentiates NGF-dependent recruitment of MΦ to sites of tissue damage and both synergistically promote tissue regeneration or, in the case of neoplastic lesions, cancer outgrowth. Thus, NGF as well as S1P influences functional properties of MΦ depending on the local microenvironment.

6.4 Differential regulation of TAM marker in mice and men

Although most TAM attributes correlate with an *in vitro* M2 phenotype, clear differences are described in literature. Recent investigations showed heterogeneous activation states of MΦ in cutaneous squamous cell carcinoma, where MΦ expressed traditional M1 and M2 marker (96). This observation stresses the differences of *in vivo*

compared to *in vitro* work on MΦ polarization. The model used here has an advantage over other *in vitro* models as it uses crude cancer cell supernatant, i.e. ACM, imitating multiple stimuli present in the micro-environment of a tumor. This explains why my data and others show up-regulation of inflammatory (TNF-a) as well as anti-inflammatory mediators (IL-10) together with multiple other factors important in pro-tumoral functions of TAM, e.g. IL-6, IL-8, PGE2, VEGF ((133, 246), Figure 43). The question arose whether the investigated cytokines (IL-10, IL-6, IL-8, TNF-α) and the induced mRNA of other TAM-associated markers (VEGF, ADORA2A, IDO, HIF-1α, IL-8 and IL-1ra) were regulated by the same ACM-derived factors and signaling pathways. As observed in the screen, this did not seem to be the case as no shRNA reduced IL-10, IL-6 and IL-8. Indeed, when looking closely at the detailed pathway of IL-10 regulation, i.e. the S1P/src/TRKA/PI3K/AKT-axis, use of respective inhibitors did not reveal a similar regulation pattern for any of the investigated markers. Nevertheless, TRKA inhibition was affecting cytokine secretion, and S1P signaling seemed to be necessary for induction of all markers, whereas PI3K/AKT signaling appeared to be restricted to IL-10 induction. In line, S1P-neutralizing antibodies resulted in reduced VEGF-mediated blood vessel formation in mice (65). In contrast to my data, neuronal cells showed requirement of NGF/TRKA signaling for HIF-1α-dependent VEGF induction (281). This might be due to analysis at different time points and cell type-specific regulation patterns, as I had observed for MΦ and neuronal progenitor PC-12 cells.

To validate my results obtained in ACM-stimulated human MΦ and to corroborate my data in a more physiological context, I used $CD11b^+$ cells freshly isolated from PyMT mammary tumors. These cells were primarily TAM, as observed by FACS staining and FACS-based cell sorting. After 24 h-culture, I analyzed secreted cytokines and found a similar regulation pattern as in ACM-stimulated human MΦ. One major difference was the PI3K/AKT-independent regulation of IL-10. However, all measured cytokines (IL-10, IL-6, MCP-1 and TNF-α) were dependent on src and TRKA signaling.

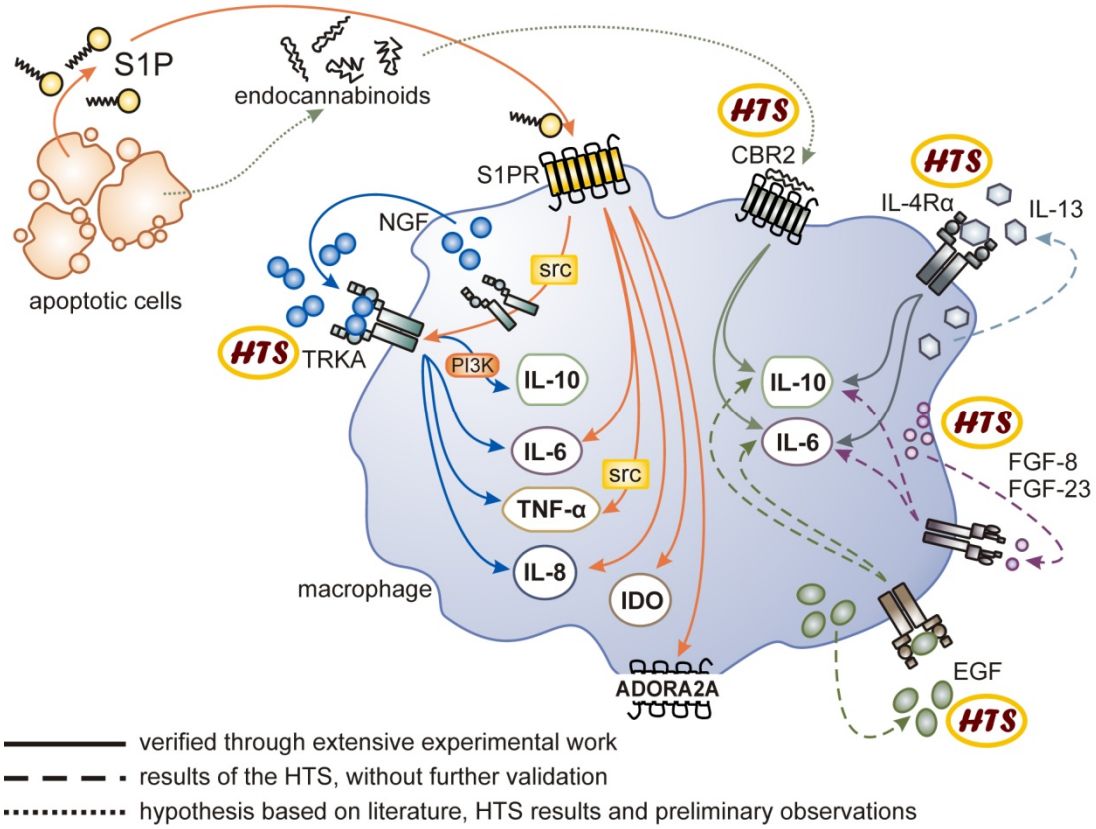

Figure 43: Summary of TAM marker regulation and autocrine factors
Apoptotic cancer cells secrete S1P and potentially endocannabinoids to induce TAM markers in primary human macrophages. Besides S1P signaling, NGF/TRKA, as well as CBR2, IL-4Rα and likely autocrine factors such as IL-13, FGF and EGF are involved. Factors, receptors marked with 'HTS', were discovered in the RNAi screening procedure. Abbreviations: ADORA2A, adenosine receptor A2A; CBR2, cannabinoid receptor 2; EGF, epidermal growth factor; FGF, fibroblast growth factor; HTS, high-throughput screen; IDO, indolamine 2,3-dioxygenase; IL, interleukin; IL-4Rα, interleukin 4 receptor-alpha; NGF, nerve growth factor; PI3K, phosphoinositide 3-kinase; S1P, sphingosine-1-phosphate; S1PR, S1P receptor; src, sarcoma tyrosine kinase; TNF-α, tumor necrosis factor-alpha; TRKA, tyrosine kinase receptor A.

The complexity of the tumor environment and even of ACM is until now not fully understood, and the interaction of the various factors either secreted by viable, apoptotic or necrotic cancer cells or by the associated immune cells themselves represent a challenge for further in-depth research. My obtained data grant an inside into the regulation of MΦ function. MΦ themselves are effective producers of growth factors (e.g. EGF, FGF, VEGF, IL-8) influencing tumor cell function and possibly possess autocrine activity (119, 282), as shown herein for NGF. In the HTS, the IL-6/IL-10 cluster contained fibroblast growth factors (FGF) 8 and 23 and knockdown of EGF and pharmacological inhibition of EGFR, although not reaching statistical significance, resulted in IL-10 reduction (Figure 43). These autocrine signals could account for the

distinct regulation patterns of TAM markers, which are observed besides overall importance on S1P signaling. In addition to that, S1P receptors are well known to interact with several growth factor receptors, controlling and fine-tuning their responses. For instance, extensive data on interaction of S1P and EGF signaling has been published (please refer to *3.2.2.4* and *5.3.3.1*).

6.4.1 TGF-β - the missing AC-derived protein factor?

Opposed to AKT, p38 phosphorylation was only mildly reduced by the TRK inhibitor and independent of S1PR and src. Hereby, p38 might signal from activated TRKA in endosomes, whereas AKT activation preferably occurs at the plasma membrane, which is well-described for AKT and ERK activation downstream of TRKA and other tyrosine kinase growth factor receptors (232, 283). Additionally, it is plausible that p38 signaling is mediated by a so far unidentified AC-derived protein factor, as I had observed a pronounced reduction of IL-10 mRNA when using deproteinated ACM, which resulted in comparable IL-10 levels as ACM in combination with p38 inhibitor SB203580.

It is difficult to speculate about the identity of this factor. To name a few critical questions, which have to be answered: Besides S1P, is there only one more factor necessary to establish the phenotype I observed in ACM-treated MΦ? If there is more than one factor involved, how do they interact? Do they all depend on apoptotic cell death or are some constitutively secreted by cancer cells? Do the factors need subsequent processing after release? And finally, besides NGF, are there additional autocrine secreted factors from MΦ necessary for the full response? Furthermore, none of the ACM-induced TAM markers showed the same regulation as IL-10. Which leads to the final question, whether there is really another “global player” comparable to S1P?

Well-established protein factors released by apoptotic cells, as discussed under 3.1.2.1, are TGF-β and lactoferrin. Chemotactic and immunomodulatory responses are established for lactoferrin (reviewed in (284)). It was shown that lactoferrin has a strong affinity to LPS and modulates TLR4 responses (285). Therefore experimental data on lactoferrin are difficult to interpret as LPS contaminations often cannot be excluded, and obtained results show high variability (286). On account of the conflicting literature and the results of the preformed HTS, where no evidence for

lactoferrin, TLR4, and fortunately LPS involvement was observed, I exclude lactoferrin as a potential mediator of the response to ACM in the presented set-up.

Regarding TGF-β, Herr et al. have previously identified a role of S1P and TGF-β in HIF-1α induction in ACM-stimulated MΦ, although the factors were not sufficient to induce HIF-1α when added exogenously, and it remained unclear, whether TGF-β was produced by apoptotic cancer cells or by MΦ themselves (134). This fact as well as hints from the HTS point to TGF-β or a member of the TGF-β superfamily to contribute to the powerful effects of ACM on MΦ. TGF-β is secreted as part of an inactive complex consisting of the homodimer TGF-β, a latency-associated dimeric propeptide (LAP) and a latent TGF-β binding protein (LTBP). The TGF-β-LAP complex is sufficient for TGF-β release from cells and function. Nevertheless, in the presence of LTBP, secretion as well as correct disulfide bond formation of TGF-β is enhanced. Additionally, by binding of LTBP to the extracellular matrix, the complex serves as a TGF-β reservoir, and LTBPs may regulate the sequestration of the TGF-β-LAP complex and thereby TGF-β function. The complex can be cleaved by plasmin, matrix metalloproteinases (MMP)-2, -9, thrombospondin 1 and integrin αvβ6 to make TGF-β available for receptor binding (287, 288). In line with my hypothesis, TNF-α-dependent MMP-2 and MMP-9 production was shown in MΦ co-cultured with cancer cells (289), and the HTS revealed urokinase plasminogen activator receptor (UPAR, PLAUR) to be necessary for ACM-induced IL-10 production. In regard to TGF-β activation, UPAR is necessary for activation of plasmin and MMPs (290) and was shown to be induced by NGF and was required for NGF-dependent cell differentiation (291). Concomitantly to LTBP-4 and PLAUR, knockdown of TGF-β receptor 3 (TGFBR3), also known as betaglycan, suppressed ACM-induced IL-10 production during the HTS. TGFBR3 binds LTBP-4-released TGF-β as well as other activating or inhibiting TGF-β superfamily members, e.g. inhibin or bone morphogenetic proteins (BMPs). Lacking a signaling domain, TGFBR3 presents the bound ligand to TGFBR2, which subsequently forms the signaling complex with TGFBR1. As TGFBR3 binds different classes of the TGF-β superfamily ligands, it takes part in the fine-tuning of cellular responses, and its functional impact depends on receptor expression and ligand availability (292). Furthermore, S1P has been shown to transactivate TGFBR and induce SMAD activation in renal mesangial cells (293). This transactivation might also occur in MΦ. To further

speculate, S1P might sensitize TGFBRs or release TGFBR3 from suppressive effectors such as inhibins.

Artemin and persephin are members of the glia cell line-derived neurotrophic factor (GDNF) family, a distant member of the TGF-β superfamily. Work on artemin postulates its oncogenic potential in various cancer types, and especially in breast cancer patients, its expression correlates with decreased overall survival (294). The two neurotrophic factors bind to the glycosylphosphatidylinositol (GPI)-anchored GDNF family receptor α (GFRA) 3 and 4, respectively. The receptors share the trans-membrane tyrosine kinase receptor RET (295) and signal via multiple pathways including src, PI3K/AKT and p38 (296, 297). As reported, GDNF family members show similar effects as NGF on neuronal development and survival (298, 299), which might also be true for functions on MΦ. In the HTS, IL-10 production was dependent on GFRA3 as well as GFRA4. Interestingly, GDNF-family members were described to require TGF-β as co-factor for RET-dependent signaling (300-302), and NGF/TRKA signaling was shown to activate RET tyrosine kinase receptors (303). The hypotheses are summarized in Figure 44.

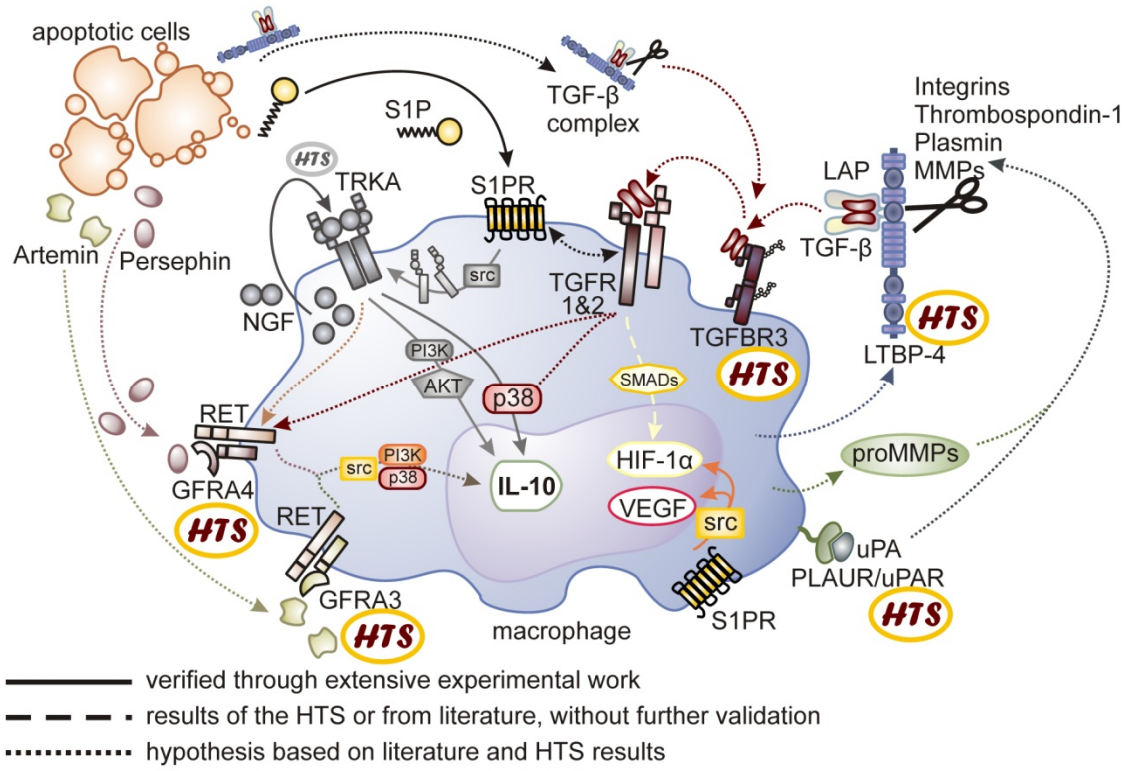

Figure 44: Theoretical regulation in regard to TGF-β signaling

TGF-β is secreted in a latent complex from apoptotic cancer cells or macrophages. Several proteases are known to free TGF-β for binding to TGFBR3, with subsequent activation of TGFR1/2-signaling, potentially inducing IL-10 via p38. In addition, interactions of S1PR or GFRA3/4 with TGFBR1/2 are hypothesized to regulate intracellular signaling and NGF/TRKA signaling potentially activates RET. Artemin and Persephin, derived from cancer cells potentially bind GFRA3/4 to induce IL-10. Furthermore, TGF-β as well as S1P signaling leads to HIF-1α and VEGF induction. In-depth validated IL-10 regulation is depicted in gray, and factors/receptors marked with 'HTS' were discovered in the RNAi screening procedure. Abbreviations: AKT, protein kinase B; GFRA, glycosylphosphatidylinositol (GPI)-anchored glia cell line neurotrophic factor (GDNF) family receptor α; HIF-1α, hypoxia inducible factor-1alpha; HTS, high-throughput screen; IL, interleukin; LAP, latency-associated dimeric propeptide; LTBP, latent TGF-β binding protein; MMP, matrix metalloproteinase; NGF, nerve growth factor; PI3K, phosphoinositide 3-kinase; PLAUR/UPAR, urokinase plasminogen activator receptor; RET, rearranged during transfection;S1P, sphingosine-1-phosphate; S1PR, S1P receptor; src, sarcoma tyrosine kinase; TGF-β, transforming growth factor-beta; TGFBR, TGF-β receptor; TRKA, tyrosine kinase receptor A; VEGF, vascular endothelial growth factor.

6.5 Future cancer therapies

Classical cancer therapies - namely surgery, radiation and chemotherapy - are to a great extent limited in their ability to target metastatic and minimal residual cancer. Immunotherapy employing monoclonal antibodies or small molecule tyrosine kinase inhibitors is an evolving field, which will hopefully improve existing conventional

therapies to target cancer cells. Furthermore, over the last years, the tumor-microenvironment gained acceptance as putative therapeutic target with the goal to overcome tumor-mediated immunosuppression and to activate potent and well directed cytotoxic immune responses. In this respect, targeting the inhibitory cytotoxic T-lymphocyte-associated antigen 4 (CTLA-4) with ipilimumab (Yervoy®) to potentiate antitumor T cell responses was recently approved by the U.S. Food and Drug Administration (FDA) and European Medicines Agency (EMA) for patients with unresectable melanoma (304).

Focusing on MΦ, efforts have been undertaken to define gene expression profiles of TAM in different mouse models of cancer (305-307). However, functional conclusions are often difficult to draw when looking at gene expression signatures. This strengthens my approach of looking at functional readouts to elucidate important mediators in TAM biology. Interestingly, a few studies indicate that these functional properties of TAM can be reversed to promote anti-tumor immunity leading to tumor regression (308, 309). In a recent phase 1 trial, an agonistic CD40 monoclonal antibody in combination with gemcitabine was tested on surgically incurable pancreatic ductal adenocarcinoma patients. CD40 is a co-stimulatory protein on antigen-presenting cells, important for their activation. The authors of the study observed CD40-dependent tumor regress in some patients, in line with their hypothesis of CD40-mediated T cell-dependent antitumor responses. Surprisingly, by subsequent mechanistic analysis in mouse models, the group discovered CD40-activated infiltrating anti-tumor MΦ to be the effector cells. These MΦ were characterized by enhance MHC II expression and elevated levels of IL-12 and TNF-α, but not IL-10 (309). This study highlights the potential of new immuno-based therapies activating the innate immune system, not only as an initiator of cytotoxic T-cell responses, but as a powerful primary effector. These promising results on the recruitment and functional properties of MΦ as targets in cancer therapy may give rise to further clinical studies on these cells as they are highly abundant in a variety of solid human tumors, and their presence is often associated with poor patient survival (310-312).

In regard to the here presented work, multiple aspects of S1P and NGF/TRKA biology are under current investigation for innovative therapies. ASONEP (sonepcizumab), a S1P-neutralizing antibody from LPath, Inc is scheduled to advance to

phase 2 trials against renal cell carcinoma (as stated on www.lpath.com), and Safingol, a multikinase inhibitor targeting sphingosine kinase 1, was recently tested for its safety in a clinical phase 1 trial. It was well tolerated and reduced S1P levels in patients' blood (313). This opens the way for further trials on SK/S1P-mediated tumor-promoting effects, both on cancer as well as cancer-associated immune cells. In the field of small molecule tyrosine kinase inhibitors, Milciclib (PHA-848125), a TRKA/CDK (cyclin-dependent kinases) inhibitor, drastically reduces xenograft growth of various solid tumor cell lines (314). Concomitantly, a phase 1 PHA-848125AC tolerability and pharmacokinetics study in patients with advanced/metastatic solid tumors (315) was performed and a phase 2 trial on thymic carcinoma patients is recruiting at the moment (www.clinicaltrials.gov). Additionally, Pfizer is recruiting bone metastases pain patients for a clinical phase 2 trial with the anti-NGF antibody Tanezumab (www.clinicaltrials.gov), although in summer 2010, all trials on Tanezumab against osteoarthritis pain were stopped due to cases of arthritis worsening (316). Thus, S1P as well as NGF hold great potential as novel therapeutic targets in cancer and other diseases, simultaneously addressing tumor and immune cell biology.

6.6 Concluding remarks

In summary, the here presented study emphasizes the complex and tightly regulated biology of MΦ function. The highly versatile cells respond to their environment by activation of divers signaling pathways, which are often interlinked. Supernatant of apoptotic breast cancer cells, as the tumor microenvironment, contains a variety of signaling molecules of lipid and protein origin. The performed adenoviral shRNA screen brought forward a list of until now underappreciated gene products involved in the corresponding MΦ answer. The exact characterization and identification of the secreted factors and their functions on MΦ provides much potential for further studies of mechanistic and potential therapeutic interest. Moreover, the functional assay might have significant benefits over microarray gene expression studies, which usually provide only information concerning expression of genes on mRNA level at a given time point, without considering a functional aspect.

The detailed analysis of TRKA signaling, with regard to IL-10 production in macrophages contributes to the growing body of evidence concerning the importance of NGF/TRKA signaling in cancer. Whereas an impact of this signaling axis on tumor cell

survival *in vitro* is known (317), its impact on the microenvironment has not yet been defined. My work provides first important findings to the involvement of NGF/TRKA in MΦ function in a TAM-like model. Thus, further studies are justified to dissect the impact of NGF on tumor-infiltrating immune cells. This might be of great value for cancer therapy, by providing a common target on both cancer cells and the tumor-supportive microenvironment.

7 References

1. Vogt C. Untersuchungen über die Entwicklungsgeschichte der Geburtshelferkroete (Alytes obstetricans). Jent und Gassman, Solothurn, 1842. : 130.
2. Clarke P G and Clarke S. Nineteenth century research on naturally occurring cell death and related phenomena. Anat Embryol (Berl), 1996. 193(2): 81-99.
3. Turner W. The cell theory, past and present. J Anat Physiol, 1889. 24: 253-287.
4. Kroemer G, Galluzzi L, Vandenabeele P, Abrams J, Alnemri E S, Baehrecke E H, Blagosklonny M V, El-Deiry W S, et al. Classification of cell death: recommendations of the Nomenclature Committee on Cell Death 2009. Cell Death Differ, 2009. 16(1): 3-11.
5. Golstein P and Kroemer G. Cell death by necrosis: towards a molecular definition. Trends Biochem Sci, 2007. 32(1): 37-43.
6. Festjens N, Vanden Berghe T, and Vandenabeele P. Necrosis, a well-orchestrated form of cell demise: signalling cascades, important mediators and concomitant immune response. Biochim Biophys Acta, 2006. 1757(9-10): 1371-1387.
7. Kerr J F, Wyllie A H, and Currie A R. Apoptosis: a basic biological phenomenon with wide-ranging implications in tissue kinetics. Br J Cancer, 1972. 26(4): 239-257.
8. MacFarlane M and Williams A C. Apoptosis and disease: a life or death decision. EMBO Rep, 2004. 5(7): 674-678.
9. Hengartner M O. The biochemistry of apoptosis. Nature, 2000. 407(6805): 770-776.
10. Rossi D and Gaidano G. Messengers of cell death: apoptotic signaling in health and disease. Haematologica, 2003. 88(2): 212-218.
11. Bader M and Steller H. Regulation of cell death by the ubiquitin-proteasome system. Curr Opin Cell Biol, 2009. 21(6): 878-884.
12. Burlacu A. Regulation of apoptosis by Bcl-2 family proteins. J Cell Mol Med, 2003. 7(3): 249-257.
13. Gatzka M and Walsh C M. Apoptotic signal transduction and T cell tolerance. Autoimmunity, 2007. 40(6): 442-452.
14. Ait-Oufella H, Kinugawa K, Zoll J, Simon T, Boddaert J, Heeneman S, Blanc-Brude O, Barateau V, et al. Lactadherin deficiency leads to apoptotic cell accumulation and accelerated atherosclerosis in mice. Circulation, 2007. 115(16): 2168-2177.
15. Savill J, Dransfield I, Gregory C, and Haslett C. A blast from the past: clearance of apoptotic cells regulates immune responses. Nat Rev Immunol, 2002. 2(12): 965-975.
16. Gregory C D and Pound J D. Cell death in the neighbourhood: direct microenvironmental effects of apoptosis in normal and neoplastic tissues. J Pathol, 2011. 223(2): 177-194.
17. Bournazou I, Pound J D, Duffin R, Bournazos S, Melville L A, Brown S B, Rossi A G, and Gregory C D. Apoptotic human cells inhibit migration of granulocytes via release of lactoferrin. J Clin Invest, 2009. 119(1): 20-32.
18. Zitvogel L, Kepp O, Senovilla L, Menger L, Chaput N, and Kroemer G. Immunogenic tumor cell death for optimal anticancer therapy: the calreticulin exposure pathway. Clin Cancer Res, 2010. 16(12): 3100-3104.
19. Ravichandran K S and Lorenz U. Engulfment of apoptotic cells: signals for a good meal. Nat Rev Immunol, 2007. 7(12): 964-974.

20. Gregory C D and Pound J D. Microenvironmental influences of apoptosis in vivo and in vitro. Apoptosis, 2010. 15(9): 1029-1049.
21. Weigert A, Weichand B, and Brune B. S1P Regulation of Macrophage Functions in The Context of Cancer. Anticancer Agents Med Chem, 2011. 9(11).
22. Zhang H, Desai N N, Olivera A, Seki T, Brooker G, and Spiegel S. Sphingosine-1-phosphate, a novel lipid, involved in cellular proliferation. J Cell Biol, 1991. 114(1): 155-167.
23. Murata N, Sato K, Kon J, Tomura H, Yanagita M, Kuwabara A, Ui M, and Okajima F. Interaction of sphingosine-1-phosphate with plasma components, including lipoproteins, regulates the lipid receptor-mediated actions. Biochem J, 2000. 352 Pt 3: 809-815.
24. Chi H. Sphingosine-1-phosphate and immune regulation: trafficking and beyond. Trends Pharmacol Sci, 2011. 32(1): 16-24.
25. Spiegel S and Milstien S. Sphingosine-1-phosphate: an enigmatic signalling lipid. Nat Rev Mol Cell Biol, 2003. 4(5): 397-407.
26. Hait N C, Oskeritzian C A, Paugh S W, Milstien S, and Spiegel S. Sphingosine kinases, sphingosine-1-phosphate, apoptosis and diseases. Biochim Biophys Acta, 2006. 1758(12): 2016-2026.
27. Pyne S and Pyne N J. Translational aspects of sphingosine-1-phosphate biology. Trends Mol Med, 2011. 17(8): 463-472.
28. Alvarez S E, Milstien S, and Spiegel S. Autocrine and paracrine roles of sphingosine-1-phosphate. Trends Endocrinol Metab, 2007.
29. Kobayashi N, Nishi T, Hirata T, Kihara A, Sano T, Igarashi Y, and Yamaguchi A. Sphingosine-1-phosphate is released from the cytosol of rat platelets in a carrier-mediated manner. J Lipid Res, 2006. 47(3): 614-621.
30. Mitra P, Oskeritzian C A, Payne S G, Beaven M A, Milstien S, and Spiegel S. Role of ABCC1 in export of sphingosine-1-phosphate from mast cells. Proc Natl Acad Sci U S A, 2006. 103(44): 16394-16399.
31. Takabe K, Kim R H, Allegood J C, Mitra P, Ramachandran S, Nagahashi M, Harikumar K B, Hait N C, et al. Estradiol induces export of sphingosine-1-phosphate from breast cancer cells via ABCC1 and ABCG2. J Biol Chem, 2010. 285(14): 10477-10486.
32. Hisano Y, Kobayashi N, Kawahara A, Yamaguchi A, and Nishi T. The sphingosine-1-phosphate transporter, SPNS2, functions as a transporter of the phosphorylated form of the immunomodulating agent FTY720. J Biol Chem, 2011. 286(3): 1758-1766.
33. Gude D R, Alvarez S E, Paugh S W, Mitra P, Yu J, Griffiths R, Barbour S E, Milstien S, et al. Apoptosis induces expression of sphingosine kinase 1 to release sphingosine-1-phosphate as a "come-and-get-me" signal. Faseb J, 2008.
34. Weigert A, Johann A M, von Knethen A, Schmidt H, Geisslinger G, and Brune B. Apoptotic cells promote macrophage survival by releasing the antiapoptotic mediator sphingosine-1-phosphate. Blood, 2006. 108(5): 1635-1642.
35. Weigert A, Cremer S, Schmidt M V, von Knethen A, Angioni C, Geisslinger G, and Brune B. Cleavage of sphingosine kinase 2 by caspase-1 provokes its release from apoptotic cells. Blood, 2010. 115(17): 3531-3540.
36. Venkataraman K, Thangada S, Michaud J, Oo M L, Ai Y, Lee Y M, Wu M, Parikh N S, et al. Extracellular export of sphingosine kinase-1a contributes to the vascular S1P gradient. Biochem J, 2006. 397(3): 461-471.

37. Tani M, Ito M, and Igarashi Y. Ceramide/sphingosine/sphingosine-1-phosphate metabolism on the cell surface and in the extracellular space. Cell Signal, 2007. 19(2): 229-237.
38. Weigert A, Weis N, and Brune B. Regulation of macrophage function by sphingosine-1-phosphate. Immunobiology, 2009. 214(9-10): 748-760.
39. Cuvillier O, Pirianov G, Kleuser B, Vanek P G, Coso O A, Gutkind S, and Spiegel S. Suppression of ceramide-mediated programmed cell death by sphingosine-1-phosphate. Nature, 1996. 381(6585): 800-803.
40. Mizugishi K, Yamashita T, Olivera A, Miller G F, Spiegel S, and Proia R L. Essential role for sphingosine kinases in neural and vascular development. Mol Cell Biol, 2005. 25(24): 11113-11121.
41. Alvarez S E, Harikumar K B, Hait N C, Allegood J, Strub G M, Kim E Y, Maceyka M, Jiang H, et al. Sphingosine-1-phosphate is a missing cofactor for the E3 ubiquitin ligase TRAF2. Nature, 2010. 465(7301): 1084-1088.
42. Hait N C, Allegood J, Maceyka M, Strub G M, Harikumar K B, Singh S K, Luo C, Marmorstein R, et al. Regulation of histone acetylation in the nucleus by sphingosine-1-phosphate. Science, 2009. 325(5945): 1254-1257.
43. Hla T, Lee M J, Ancellin N, Paik J H, and Kluk M J. Lysophospholipids--receptor revelations. Science, 2001. 294(5548): 1875-1878.
44. Kono M, Mi Y, Liu Y, Sasaki T, Allende M L, Wu Y P, Yamashita T, and Proia R L. The sphingosine-1-phosphate receptors S1P1, S1P2, and S1P3 function coordinately during embryonic angiogenesis. J Biol Chem, 2004. 279(28): 29367-29373.
45. Sanna M G, Liao J, Jo E, Alfonso C, Ahn M Y, Peterson M S, Webb B, Lefebvre S, et al. Sphingosine-1-phosphate (S1P) receptor subtypes S1P1 and S1P3, respectively, regulate lymphocyte recirculation and heart rate. J Biol Chem, 2004. 279(14): 13839-13848.
46. Graler M H, Bernhardt G, and Lipp M. EDG6, a novel G-protein-coupled receptor related to receptors for bioactive lysophospholipids, is specifically expressed in lymphoid tissue. Genomics, 1998. 53(2): 164-169.
47. Walzer T, Chiossone L, Chaix J, Calver A, Carozzo C, Garrigue-Antar L, Jacques Y, Baratin M, et al. Natural killer cell trafficking in vivo requires a dedicated sphingosine-1-phosphate receptor. Nat Immunol, 2007. 8(12): 1337-1344.
48. Idzko M, Hammad H, van Nimwegen M, Kool M, Muller T, Soullie T, Willart M A, Hijdra D, et al. Local application of FTY720 to the lung abrogates experimental asthma by altering dendritic cell function. J Clin Invest, 2006. 116(11): 2935-2944.
49. Terai K, Soga T, Takahashi M, Kamohara M, Ohno K, Yatsugi S, Okada M, and Yamaguchi T. Edg-8 receptors are preferentially expressed in oligodendrocyte lineage cells of the rat CNS. Neuroscience, 2003. 116(4): 1053-1062.
50. Pyne N J and Pyne S. Sphingosine-1-phosphate and cancer. Nat Rev Cancer, 2010. 10(7): 489-503.
51. Young N and Van Brocklyn J R. Roles of sphingosine-1-phosphate (S1P) receptors in malignant behavior of glioma cells. Differential effects of S1P2 on cell migration and invasiveness. Exp Cell Res, 2007. 313(8): 1615-1627.
52. Rosen H, Gonzalez-Cabrera P J, Sanna M G, and Brown S. Sphingosine-1-phosphate receptor signaling. Annu Rev Biochem, 2009. 78: 743-768.

53. Sanchez T and Hla T. Structural and functional characteristics of S1P receptors. J Cell Biochem, 2004. 92(5): 913-922.
54. Allende M L and Proia R L. Sphingosine-1-phosphate receptors and the development of the vascular system. Biochim Biophys Acta, 2002. 1582(1-3): 222-227.
55. Pappu R, Schwab S R, Cornelissen I, Pereira J P, Regard J B, Xu Y, Camerer E, Zheng Y W, et al. Promotion of lymphocyte egress into blood and lymph by distinct sources of sphingosine-1-phosphate. Science, 2007. 316(5822): 295-298.
56. Wang W, Graeler M H, and Goetzl E J. Type 4 sphingosine-1-phosphate G protein-coupled receptor (S1P4) transduces S1P effects on T cell proliferation and cytokine secretion without signaling migration. Faseb J, 2005. 19(12): 1731-1733.
57. Cohen J A and Chun J. Mechanisms of fingolimod's efficacy and adverse effects in multiple sclerosis. Ann Neurol, 2011. 69(5): 759-777.
58. Eigenbrod S, Derwand R, Jakl V, Endres S, and Eigler A. Sphingosine kinase and sphingosine-1-phosphate regulate migration, endocytosis and apoptosis of dendritic cells. Immunol Invest, 2006. 35(2): 149-165.
59. Rolin J and Maghazachi A A. Effects of Lysophospholipids on Tumor Microenvironment. Cancer Microenviron, 2011.
60. Sabbadini R A. Sphingosine-1-phosphate antibodies as potential agents in the treatment of cancer and age-related macular degeneration. Br J Pharmacol, 2011. 162(6): 1225-1238.
61. Le Stunff H, Mikami A, Giussani P, Hobson J P, Jolly P S, Milstien S, and Spiegel S. Role of sphingosine-1-phosphate phosphatase 1 in epidermal growth factor-induced chemotaxis. J Biol Chem, 2004. 279(33): 34290-34297.
62. Hait N C, Bellamy A, Milstien S, Kordula T, and Spiegel S. Sphingosine kinase type 2 activation by ERK-mediated phosphorylation. J Biol Chem, 2007. 282(16): 12058-12065.
63. Hsieh H L, Sun C C, Wu C B, Wu C Y, Tung W H, Wang H H, and Yang C M. Sphingosine-1-phosphate induces EGFR expression via Akt/NF-kappaB and ERK/AP-1 pathways in rat vascular smooth muscle cells. J Cell Biochem, 2008. 103(6): 1732-1746.
64. Shida D, Kitayama J, Yamaguchi H, Yamashita H, Mori K, Watanabe T, Yatomi Y, and Nagawa H. Sphingosine-1-phosphate transactivates c-Met as well as epidermal growth factor receptor (EGFR) in human gastric cancer cells. FEBS Lett, 2004. 577(3): 333-338.
65. Visentin B, Vekich J A, Sibbald B J, Cavalli A L, Moreno K M, Matteo R G, Garland W A, Lu Y, et al. Validation of an anti-sphingosine-1-phosphate antibody as a potential therapeutic in reducing growth, invasion, and angiogenesis in multiple tumor lineages. Cancer Cell, 2006. 9(3): 225-238.
66. Liu Q, Zhao X, Frissora F, Ma Y, Santhanam R, Jarjoura D, Lehman A, Perrotti D, et al. FTY720 demonstrates promising preclinical activity for chronic lymphocytic leukemia and lymphoblastic leukemia/lymphoma. Blood, 2008. 111(1): 275-284.
67. Lucas da Silva L B, Ribeiro D A, Cury P M, Cordeiro J A, and Bueno V. FTY720 treatment in experimentally urethane-induced lung tumors. J Exp Ther Oncol, 2008. 7(1): 9-15.
68. Azuma H, Horie S, Muto S, Otsuki Y, Matsumoto K, Morimoto J, Gotoh R, Okuyama A, et al. Selective cancer cell apoptosis induced by FTY720; evidence

for a Bcl-dependent pathway and impairment in ERK activity. Anticancer Res, 2003. 23(4): 3183-3193.
69. LaMontagne K, Littlewood-Evans A, Schnell C, O'Reilly T, Wyder L, Sanchez T, Probst B, Butler J, et al. Antagonism of sphingosine-1-phosphate receptors by FTY720 inhibits angiogenesis and tumor vascularization. Cancer Res, 2006. 66(1): 221-231.
70. Schmid G, Guba M, Ischenko I, Papyan A, Joka M, Schrepfer S, Bruns C J, Jauch K W, et al. The immunosuppressant FTY720 inhibits tumor angiogenesis via the sphingosine-1-phosphate receptor 1. J Cell Biochem, 2007. 101(1): 259-270.
71. Nagaoka Y, Otsuki K, Fujita T, and Uesato S. Effects of phosphorylation of immunomodulatory agent FTY720 (fingolimod) on antiproliferative activity against breast and colon cancer cells. Biol Pharm Bull, 2008. 31(6): 1177-1181.
72. Medzhitov R. Origin and physiological roles of inflammation. Nature, 2008. 454(7203): 428-435.
73. Murphy K, Travers P, and Walport M, Janeway's Immunobiology. 7th ed. 2007, New York: Garland Science.
74. Gordon S. Alternative activation of macrophages. Nat Rev Immunol, 2003. 3(1): 23-35.
75. Kawane K, Fukuyama H, Kondoh G, Takeda J, Ohsawa Y, Uchiyama Y, and Nagata S. Requirement of DNase II for definitive erythropoiesis in the mouse fetal liver. Science, 2001. 292(5521): 1546-1549.
76. Pollard J W. Trophic macrophages in development and disease. Nat Rev Immunol, 2009. 9(4): 259-270.
77. Lynch M A. The multifaceted profile of activated microglia. Mol Neurobiol, 2009. 40(2): 139-156.
78. Kupper T S and Fuhlbrigge R C. Immune surveillance in the skin: mechanisms and clinical consequences. Nat Rev Immunol, 2004. 4(3): 211-222.
79. Fantin A, Vieira J M, Gestri G, Denti L, Schwarz Q, Prykhozhij S, Peri F, Wilson S W, et al. Tissue macrophages act as cellular chaperones for vascular anastomosis downstream of VEGF-mediated endothelial tip cell induction. Blood, 2010. 116(5): 829-840.
80. Rescigno M, Lopatin U, and Chieppa M. Interactions among dendritic cells, macrophages, and epithelial cells in the gut: implications for immune tolerance. Curr Opin Immunol, 2008. 20(6): 669-675.
81. Williams T M, Little M H, and Ricardo S D. Macrophages in renal development, injury, and repair. Semin Nephrol, 2010. 30(3): 255-267.
82. Ishibashi H, Nakamura M, Komori A, Migita K, and Shimoda S. Liver architecture, cell function, and disease. Semin Immunopathol, 2009. 31(3): 399-409.
83. O'Brien J, Lyons T, Monks J, Lucia M S, Wilson R S, Hines L, Man Y G, Borges V, et al. Alternatively activated macrophages and collagen remodeling characterize the postpartum involuting mammary gland across species. Am J Pathol, 2010. 176(3): 1241-1255.
84. Gouon-Evans V, Lin E Y, and Pollard J W. Requirement of macrophages and eosinophils and their cytokines/chemokines for mammary gland development. Breast Cancer Res, 2002. 4(4): 155-164.
85. Wu R, Van der Hoek K H, Ryan N K, Norman R J, and Robker R L. Macrophage contributions to ovarian function. Hum Reprod Update, 2004. 10(2): 119-133.

86. Banaei-Bouchareb L, Gouon-Evans V, Samara-Boustani D, Castellotti M C, Czernichow P, Pollard J W, and Polak M. Insulin cell mass is altered in Csf1op/Csf1op macrophage-deficient mice. J Leukoc Biol, 2004. 76(2): 359-367.
87. Nagamatsu T and Schust D J. The immunomodulatory roles of macrophages at the maternal-fetal interface. Reprod Sci, 2010. 17(3): 209-218.
88. Timmons B, Akins M, and Mahendroo M. Cervical remodeling during pregnancy and parturition. Trends Endocrinol Metab, 2010. 21(6): 353-361.
89. Stout R D and Suttles J. Functional plasticity of macrophages: reversible adaptation to changing microenvironments. J Leukoc Biol, 2004. 76(3): 509-513.
90. Mackaness G B. Cellular immunity and the parasite. Adv Exp Med Biol, 1977. 93: 65-73.
91. Trautmann A. Extracellular ATP in the immune system: more than just a "danger signal". Sci Signal, 2009. 2(56): pe6.
92. Apetoh L, Ghiringhelli F, Tesniere A, Criollo A, Ortiz C, Lidereau R, Mariette C, Chaput N, et al. The interaction between HMGB1 and TLR4 dictates the outcome of anticancer chemotherapy and radiotherapy. Immunol Rev, 2007. 220: 47-59.
93. Stein M, Keshav S, Harris N, and Gordon S. Interleukin 4 potently enhances murine macrophage mannose receptor activity: a marker of alternative immunologic macrophage activation. J Exp Med, 1992. 176(1): 287-292.
94. Mantovani A, Sica A, Sozzani S, Allavena P, Vecchi A, and Locati M. The chemokine system in diverse forms of macrophage activation and polarization. Trends Immunol, 2004. 25(12): 677-686.
95. Mosser D M and Edwards J P. Exploring the full spectrum of macrophage activation. Nat Rev Immunol, 2008. 8(12): 958-969.
96. Pettersen J S, Fuentes-Duculan J, Suarez-Farinas M, Pierson K C, Pitts-Kiefer A, Fan L, Belkin D A, Wang C Q, et al. Tumor-associated macrophages in the cutaneous SCC microenvironment are heterogeneously activated. J Invest Dermatol, 2011. 131(6): 1322-1330.
97. Biswas S K and Mantovani A. Macrophage plasticity and interaction with lymphocyte subsets: cancer as a paradigm. Nat Immunol, 2010. 11(10): 889-896.
98. Qian B Z and Pollard J W. Macrophage diversity enhances tumor progression and metastasis. Cell, 2010. 141(1): 39-51.
99. Ehrlich P. Über den jetzigen Stand der Karzinomforschung. Ned. Tijdschr. Geneeskd, 1909(5): 273-290.
100. Vesely M D, Kershaw M H, Schreiber R D, and Smyth M J. Natural innate and adaptive immunity to cancer. Annu Rev Immunol, 2011. 29: 235-271.
101. Schreiber R D, Old L J, and Smyth M J. Cancer immunoediting: integrating immunity's roles in cancer suppression and promotion. Science, 2011. 331(6024): 1565-1570.
102. Dunn G P, Old L J, and Schreiber R D. The three Es of cancer immunoediting. Annu Rev Immunol, 2004. 22: 329-360.
103. Mantovani A and Sica A. Macrophages, innate immunity and cancer: balance, tolerance, and diversity. Curr Opin Immunol, 2010. 22(2): 231-237.
104. Aguirre-Ghiso J A. Models, mechanisms and clinical evidence for cancer dormancy. Nature Reviews Cancer, 2007. 7(11): 834-846.
105. Bingle L, Brown N J, and Lewis C E. The role of tumour-associated macrophages in tumour progression: implications for new anticancer therapies. J Pathol, 2002. 196(3): 254-265.

106. Smith H O, Anderson P S, Kuo D Y, Goldberg G L, DeVictoria C L, Boocock C A, Jones J G, Runowicz C D, et al. The role of colony-stimulating factor 1 and its receptor in the etiopathogenesis of endometrial adenocarcinoma. Clin Cancer Res, 1995. 1(3): 313-325.
107. Scholl S M, Pallud C, Beuvon F, Hacene K, Stanley E R, Rohrschneider L, Tang R, Pouillart P, et al. Anti-colony-stimulating factor-1 antibody staining in primary breast adenocarcinomas correlates with marked inflammatory cell infiltrates and prognosis. J Natl Cancer Inst, 1994. 86(2): 120-126.
108. Saji H, Koike M, Yamori T, Saji S, Seiki M, Matsushima K, and Toi M. Significant correlation of monocyte chemoattractant protein-1 expression with neovascularization and progression of breast carcinoma. Cancer, 2001. 92(5): 1085-1091.
109. Negus R P, Stamp G W, Relf M G, Burke F, Malik S T, Bernasconi S, Allavena P, Sozzani S, et al. The detection and localization of monocyte chemoattractant protein-1 (MCP-1) in human ovarian cancer. J Clin Invest, 1995. 95(5): 2391-2396.
110. DeNardo D G, Barreto J B, Andreu P, Vasquez L, Tawfik D, Kolhatkar N, and Coussens L M. CD4(+) T cells regulate pulmonary metastasis of mammary carcinomas by enhancing protumor properties of macrophages. Cancer Cell, 2009. 16(2): 91-102.
111. Cools N, Ponsaerts P, Van Tendeloo V F, and Berneman Z N. Regulatory T cells and human disease. Clin Dev Immunol, 2007. 2007: 89195.
112. Wilson W R and Hay M P. Targeting hypoxia in cancer therapy. Nat Rev Cancer, 2011. 11(6): 393-410.
113. Munn D H and Mellor A L. Indoleamine 2,3-dioxygenase and tumor-induced tolerance. J Clin Invest, 2007. 117(5): 1147-1154.
114. Johnson B A, 3rd, Baban B, and Mellor A L. Targeting the immunoregulatory indoleamine 2,3 dioxygenase pathway in immunotherapy. Immunotherapy, 2009. 1(4): 645-661.
115. Allavena P, Sica A, Solinas G, Porta C, and Mantovani A. The inflammatory micro-environment in tumor progression: the role of tumor-associated macrophages. Crit Rev Oncol Hematol, 2008. 66(1): 1-9.
116. Coussens L M, Tinkle C L, Hanahan D, and Werb Z. MMP-9 supplied by bone marrow-derived cells contributes to skin carcinogenesis. Cell, 2000. 103(3): 481-490.
117. Mantovani A, Schioppa T, Porta C, Allavena P, and Sica A. Role of tumor-associated macrophages in tumor progression and invasion. Cancer Metastasis Rev, 2006. 25(3): 315-322.
118. Sica A, Allavena P, and Mantovani A. Cancer related inflammation: the macrophage connection. Cancer Lett, 2008. 267(2): 204-215.
119. Pollard J W. Tumour-educated macrophages promote tumour progression and metastasis. Nat Rev Cancer, 2004. 4(1): 71-78.
120. Martinez F O, Gordon S, Locati M, and Mantovani A. Transcriptional profiling of the human monocyte-to-macrophage differentiation and polarization: new molecules and patterns of gene expression. J Immunol, 2006. 177(10): 7303-7311.
121. Edwards J P, Zhang X, Frauwirth K A, and Mosser D M. Biochemical and functional characterization of three activated macrophage populations. J Leukoc Biol, 2006. 80(6): 1298-1307.

122. Pchejetski D, Nunes J, Coughlan K, Lall H, Pitson S M, Waxman J, and Sumbayev V V. The involvement of sphingosine kinase 1 in LPS-induced Toll-like receptor 4-mediated accumulation of HIF-1alpha protein, activation of ASK1 and production of the pro-inflammatory cytokine IL-6. Immunol Cell Biol. 89(2): 268-274.
123. Zhi L, Leung B P, and Melendez A J. Sphingosine kinase 1 regulates pro-inflammatory responses triggered by TNFalpha in primary human monocytes. J Cell Physiol, 2006. 208(1): 109-115.
124. Nayak D, Huo Y, Kwang W X, Pushparaj P N, Kumar S D, Ling E A, and Dheen S T. Sphingosine kinase 1 regulates the expression of proinflammatory cytokines and nitric oxide in activated microglia. Neuroscience, 2010. 166(1): 132-144.
125. Xia P, Wang L, Moretti P A, Albanese N, Chai F, Pitson S M, D'Andrea R J, Gamble J R, et al. Sphingosine kinase interacts with TRAF2 and dissects tumor necrosis factor-alpha signaling. J Biol Chem, 2002. 277(10): 7996-8003.
126. Fyrst H and Saba J D. An update on sphingosine-1-phosphate and other sphingolipid mediators. Nat Chem Biol, 2010. 6(7): 489-497.
127. Hughes J E, Srinivasan S, Lynch K R, Proia R L, Ferdek P, and Hedrick C C. Sphingosine-1-Phosphate Induces an Antiinflammatory Phenotype in Macrophages. Circ Res, 2008. 102(8): 950-958.
128. Keul P, Lucke S, von Wnuck Lipinski K, Bode C, Graler M, Heusch G, and Levkau B. Sphingosine-1-phosphate receptor 3 promotes recruitment of monocyte/macrophages in inflammation and atherosclerosis. Circ Res, 2011. 108(3): 314-323.
129. Duong C Q, Bared S M, Abu-Khader A, Buechler C, Schmitz A, and Schmitz G. Expression of the lysophospholipid receptor family and investigation of lysophospholipid-mediated responses in human macrophages. Biochim Biophys Acta, 2004. 1682(1-3): 112-119.
130. Weigert A, Tzieply N, von Knethen A, Johann A M, Schmidt H, Geisslinger G, and Brune B. Tumor cell apoptosis polarizes macrophages role of sphingosine-1-phosphate. Mol Biol Cell, 2007. 18(10): 3810-3819.
131. Yu H, Pardoll D, and Jove R. STATs in cancer inflammation and immunity: a leading role for STAT3. Nat Rev Cancer, 2009. 9(11): 798-809.
132. Lee H, Deng J, Kujawski M, Yang C, Liu Y, Herrmann A, Kortylewski M, Horne D, et al. STAT3-induced S1PR1 expression is crucial for persistent STAT3 activation in tumors. Nat Med, 2010. 16(12): 1421-1428.
133. Weis N, Weigert A, von Knethen A, and Brune B. Heme oxygenase-1 contributes to an alternative macrophage activation profile induced by apoptotic cell supernatants. Mol Biol Cell, 2009. 20(5): 1280-1288.
134. Herr B, Zhou J, Werno C, Menrad H, Namgaladze D, Weigert A, Dehne N, and Brune B. The supernatant of apoptotic cells causes transcriptional activation of hypoxia-inducible factor-1alpha in macrophages via sphingosine-1-phosphate and transforming growth factor-beta. Blood, 2009. 114(10): 2140-2148.
135. Barra V, Kuhn A M, von Knethen A, Weigert A, and Brune B. Apoptotic cell-derived factors induce arginase II expression in murine macrophages by activating ERK5/CREB. Cell Mol Life Sci, 2011. 68(10): 1815-1827.
136. Ley S, Weigert A, and Brune B. Neuromediators in inflammation--a macrophage/nerve connection. Immunobiology, 2010. 215(9-10): 674-684.
137. Bystrom J, Evans I, Newson J, Stables M, Toor I, van Rooijen N, Crawford M, Colville-Nash P, et al. Resolution-phase macrophages possess a unique

inflammatory phenotype that is controlled by cAMP. Blood, 2008. 112(10): 4117-4127.
138. Wang F, Okamoto Y, Inoki I, Yoshioka K, Du W, Qi X, Takuwa N, Gonda K, et al. Sphingosine-1-phosphate receptor-2 deficiency leads to inhibition of macrophage proinflammatory activities and atherosclerosis in apoE-deficient mice. J Clin Invest, 2010. 120(11): 3979-3995.
139. Skoura A, Michaud J, Im D S, Thangada S, Xiong Y, Smith J D, and Hla T. Sphingosine-1-phosphate receptor-2 function in myeloid cells regulates vascular inflammation and atherosclerosis. Arterioscler Thromb Vasc Biol, 2011. 31(1): 81-85.
140. Seruga B, Zhang H, Bernstein L J, and Tannock I F. Cytokines and their relationship to the symptoms and outcome of cancer. Nat Rev Cancer, 2008. 8(11): 887-899.
141. Akdis M, Burgler S, Crameri R, Eiwegger T, Fujita H, Gomez E, Klunker S, Meyer N, et al. Interleukins, from 1 to 37, and interferon-gamma: receptors, functions, and roles in diseases. J Allergy Clin Immunol, 2011. 127(3): 701-721 e701-770.
142. Fiorentino D F, Bond M W, and Mosmann T R. Two types of mouse T helper cell. IV. Th2 clones secrete a factor that inhibits cytokine production by Th1 clones. J Exp Med, 1989. 170(6): 2081-2095.
143. Mosser D M and Zhang X. Interleukin-10: new perspectives on an old cytokine. Immunol Rev, 2008. 226: 205-218.
144. Moore K W, Vieira P, Fiorentino D F, Trounstine M L, Khan T A, and Mosmann T R. Homology of cytokine synthesis inhibitory factor (IL-10) to the Epstein-Barr virus gene BCRFI. Science, 1990. 248(4960): 1230-1234.
145. Vieira P, de Waal-Malefyt R, Dang M N, Johnson K E, Kastelein R, Fiorentino D F, deVries J E, Roncarolo M G, et al. Isolation and expression of human cytokine synthesis inhibitory factor cDNA clones: homology to Epstein-Barr virus open reading frame BCRFI. Proc Natl Acad Sci U S A, 1991. 88(4): 1172-1176.
146. Donnelly R P, Dickensheets H, and Finbloom D S. The interleukin-10 signal transduction pathway and regulation of gene expression in mononuclear phagocytes. J Interferon Cytokine Res, 1999. 19(6): 563-573.
147. Kuhn R, Lohler J, Rennick D, Rajewsky K, and Muller W. Interleukin-10-deficient mice develop chronic enterocolitis. Cell, 1993. 75(2): 263-274.
148. Glocker E O, Kotlarz D, Boztug K, Gertz E M, Schaffer A A, Noyan F, Perro M, Diestelhorst J, et al. Inflammatory bowel disease and mutations affecting the interleukin-10 receptor. N Engl J Med, 2009. 361(21): 2033-2045.
149. Bettelli E, Das M P, Howard E D, Weiner H L, Sobel R A, and Kuchroo V K. IL-10 is critical in the regulation of autoimmune encephalomyelitis as demonstrated by studies of IL-10- and IL-4-deficient and transgenic mice. J Immunol, 1998. 161(7): 3299-3306.
150. Couper K N, Blount D G, and Riley E M. IL-10: the master regulator of immunity to infection. J Immunol, 2008. 180(9): 5771-5777.
151. Moore K W, de Waal Malefyt R, Coffman R L, and O'Garra A. Interleukin-10 and the interleukin-10 receptor. Annu Rev Immunol, 2001. 19: 683-765.
152. Redpath S, Ghazal P, and Gascoigne N R. Hijacking and exploitation of IL-10 by intracellular pathogens. Trends Microbiol, 2001. 9(2): 86-92.

153. de Waal Malefyt R, Abrams J, Bennett B, Figdor C G, and de Vries J E. Interleukin 10(IL-10) inhibits cytokine synthesis by human monocytes: an autoregulatory role of IL-10 produced by monocytes. J Exp Med, 1991. 174(5): 1209-1220.
154. Coffelt S B, Tal A O, Scholz A, De Palma M, Patel S, Urbich C, Biswas S K, Murdoch C, et al. Angiopoietin-2 regulates gene expression in TIE2-expressing monocytes and augments their inherent proangiogenic functions. Cancer Res, 2010. 70(13): 5270-5280.
155. Ozao-Choy J, Ma G, Kao J, Wang G X, Meseck M, Sung M, Schwartz M, Divino C M, et al. The novel role of tyrosine kinase inhibitor in the reversal of immune suppression and modulation of tumor microenvironment for immune-based cancer therapies. Cancer Res, 2009. 69(6): 2514-2522.
156. Hasko G, Linden J, Cronstein B, and Pacher P. Adenosine receptors: therapeutic aspects for inflammatory and immune diseases. Nat Rev Drug Discov, 2008. 7(9): 759-770.
157. Chung E Y, Liu J, Homma Y, Zhang Y, Brendolan A, Saggese M, Han J, Silverstein R, et al. Interleukin-10 Expression in Macrophages during Phagocytosis of Apoptotic Cells Is Mediated by Homeodomain Proteins Pbx1 and Prep-1. Immunity, 2007. 27(6): 952-964.
158. Voll R E, Herrmann M, Roth E A, Stach C, Kalden J R, and Girkontaite I. Immunosuppressive effects of apoptotic cells. Nature, 1997. 390(6658): 350-351.
159. Saraiva M and O'Garra A. The regulation of IL-10 production by immune cells. Nat Rev Immunol, 2010. 10(3): 170-181.
160. Pengal R A, Ganesan L P, Wei G, Fang H, Ostrowski M C, and Tridandapani S. Lipopolysaccharide-induced production of interleukin-10 is promoted by the serine/threonine kinase Akt. Mol Immunol, 2006. 43(10): 1557-1564.
161. Benkhart E M, Siedlar M, Wedel A, Werner T, and Ziegler-Heitbrock H W. Role of Stat3 in lipopolysaccharide-induced IL-10 gene expression. J Immunol, 2000. 165(3): 1612-1617.
162. Staples K J, Smallie T, Williams L M, Foey A, Burke B, Foxwell B M, and Ziegler-Heitbrock L. IL-10 induces IL-10 in primary human monocyte-derived macrophages via the transcription factor Stat3. J Immunol, 2007. 178(8): 4779-4785.
163. Tone M, Powell M J, Tone Y, Thompson S A, and Waldmann H. IL-10 gene expression is controlled by the transcription factors Sp1 and Sp3. J Immunol, 2000. 165(1): 286-291.
164. Brightbill H D, Plevy S E, Modlin R L, and Smale S T. A prominent role for Sp1 during lipopolysaccharide-mediated induction of the IL-10 promoter in macrophages. J Immunol, 2000. 164(4): 1940-1951.
165. Norkina O, Dolganiuc A, Shapiro T, Kodys K, Mandrekar P, and Szabo G. Acute alcohol activates STAT3, AP-1, and Sp-1 transcription factors via the family of Src kinases to promote IL-10 production in human monocytes. J Leukoc Biol, 2007. 82(3): 752-762.
166. Csoka B, Nemeth Z H, Virag L, Gergely P, Leibovich S J, Pacher P, Sun C X, Blackburn M R, et al. A2A adenosine receptors and C/EBP{beta} are crucially required for IL-10 production by macrophages exposed to Escherichia coli. Blood, 2007. 110(7): 2685-2695.
167. Brenner S, Prosch S, Schenke-Layland K, Riese U, Gausmann U, and Platzer C. cAMP-induced Interleukin-10 promoter activation depends on CCAAT/enhancer-

binding protein expression and monocytic differentiation. J Biol Chem, 2003. 278(8): 5597-5604.
168. Platzer C, Docke W, Volk H, and Prosch S. Catecholamines trigger IL-10 release in acute systemic stress reaction by direct stimulation of its promoter/enhancer activity in monocytic cells. J Neuroimmunol, 2000. 105(1): 31-38.
169. Lucas M, Zhang X, Prasanna V, and Mosser D M. ERK activation following macrophage FcgammaR ligation leads to chromatin modifications at the IL-10 locus. J Immunol, 2005. 175(1): 469-477.
170. Meisel C, Vogt K, Platzer C, Randow F, Liebenthal C, and Volk H D. Differential regulation of monocytic tumor necrosis factor-alpha and interleukin-10 expression. Eur J Immunol, 1996. 26(7): 1580-1586.
171. Asadullah K, Sterry W, and Volk H D. Interleukin-10 therapy--review of a new approach. Pharmacol Rev, 2003. 55(2): 241-269.
172. Zeni E, Mazzetti L, Miotto D, Lo Cascio N, Maestrelli P, Querzoli P, Pedriali M, De Rosa E, et al. Macrophage expression of interleukin-10 is a prognostic factor in nonsmall cell lung cancer. Eur Respir J, 2007. 30(4): 627-632.
173. O'Garra A, Barrat F J, Castro A G, Vicari A, and Hawrylowicz C. Strategies for use of IL-10 or its antagonists in human disease. Immunol Rev, 2008. 223: 114-131.
174. Guiducci C, Vicari A P, Sangaletti S, Trinchieri G, and Colombo M P. Redirecting in vivo elicited tumor infiltrating macrophages and dendritic cells towards tumor rejection. Cancer Res, 2005. 65(8): 3437-3446.
175. Kaplan D R and Miller F D. Neurotrophin signal transduction in the nervous system. Curr Opin Neurobiol, 2000. 10(3): 381-391.
176. Brodeur G M, Minturn J E, Ho R, Simpson A M, Iyer R, Varela C R, Light J E, Kolla V, et al. Trk receptor expression and inhibition in neuroblastomas. Clin Cancer Res, 2009. 15(10): 3244-3250.
177. Lagadec C, Meignan S, Adriaenssens E, Foveau B, Vanhecke E, Romon R, Toillon R A, Oxombre B, et al. TrkA overexpression enhances growth and metastasis of breast cancer cells. Oncogene, 2009. 28(18): 1960-1970.
178. Freund-Michel V and Frossard N. The nerve growth factor and its receptors in airway inflammatory diseases. Pharmacol Ther, 2008. 117(1): 52-76.
179. De Santi L, Annunziata P, Sessa E, and Bramanti P. Brain-derived neurotrophic factor and TrkB receptor in experimental autoimmune encephalomyelitis and multiple sclerosis. J Neurol Sci, 2009. 287(1-2): 17-26.
180. Cirulli F and Alleva E. The NGF saga: from animal models of psychosocial stress to stress-related psychopathology. Front Neuroendocrinol, 2009. 30(3): 379-395.
181. Caporali A and Emanueli C. Cardiovascular actions of neurotrophins. Physiol Rev, 2009. 89(1): 279-308.
182. Lee R, Kermani P, Teng K K, and Hempstead B L. Regulation of cell survival by secreted proneurotrophins. Science, 2001. 294(5548): 1945-1948.
183. Arevalo J C and Wu S H. Neurotrophin signaling: many exciting surprises! Cell Mol Life Sci, 2006. 63(13): 1523-1537.
184. Chao M V. Neurotrophins and their receptors: a convergence point for many signalling pathways. Nat Rev Neurosci, 2003. 4(4): 299-309.
185. Lee F S, Rajagopal R, and Chao M V. Distinctive features of Trk neurotrophin receptor transactivation by G protein-coupled receptors. Cytokine Growth Factor Rev, 2002. 13(1): 11-17.

186. Karkoulias G and Flordellis C. Delayed transactivation of the receptor for nerve growth factor is required for sustained signaling and differentiation by alpha2-adrenergic receptors in transfected PC12 cells. Cell Signal, 2007. 19(5): 945-957.
187. Kruttgen A, Schneider I, and Weis J. The dark side of the NGF family: neurotrophins in neoplasias. Brain Pathol, 2006. 16(4): 304-310.
188. Romon R, Adriaenssens E, Lagadec C, Germain E, Hondermarck H, and Le Bourhis X. Nerve growth factor promotes breast cancer angiogenesis by activating multiple pathways. Mol Cancer, 2010. 9: 157.
189. Dolle L, El Yazidi-Belkoura I, Adriaenssens E, Nurcombe V, and Hondermarck H. Nerve growth factor overexpression and autocrine loop in breast cancer cells. Oncogene, 2003. 22(36): 5592-5601.
190. Kogner P, Barbany G, Dominici C, Castello M A, Raschella G, and Persson H. Coexpression of messenger RNA for TRK protooncogene and low affinity nerve growth factor receptor in neuroblastoma with favorable prognosis. Cancer Res, 1993. 53(9): 2044-2050.
191. Suzuki T, Bogenmann E, Shimada H, Stram D, and Seeger R C. Lack of high-affinity nerve growth factor receptors in aggressive neuroblastomas. J Natl Cancer Inst, 1993. 85(5): 377-384.
192. Aoyama M, Asai K, Shishikura T, Kawamoto T, Miyachi T, Yokoi T, Togari H, Wada Y, et al. Human neuroblastomas with unfavorable biologies express high levels of brain-derived neurotrophic factor mRNA and a variety of its variants. Cancer Lett, 2001. 164(1): 51-60.
193. Kerschensteiner M, Stadelmann C, Dechant G, Wekerle H, and Hohlfeld R. Neurotrophic cross-talk between the nervous and immune systems: implications for neurological diseases. Ann Neurol, 2003. 53(3): 292-304.
194. Vega J A, Garcia-Suarez O, Hannestad J, Perez-Perez M, and Germana A. Neurotrophins and the immune system. J Anat, 2003. 203(1): 1-19.
195. Soule H D, Vazguez J, Long A, Albert S, and Brennan M. A human cell line from a pleural effusion derived from a breast carcinoma. J Natl Cancer Inst, 1973. 51(5): 1409-1416.
196. Giard D J, Aaronson S A, Todaro G J, Arnstein P, Kersey J H, Dosik H, and Parks W P. In vitro cultivation of human tumors: establishment of cell lines derived from a series of solid tumors. J Natl Cancer Inst, 1973. 51(5): 1417-1423.
197. Stone K R, Mickey D D, Wunderli H, Mickey G H, and Paulson D F. Isolation of a human prostate carcinoma cell line (DU 145). Int J Cancer, 1978. 21(3): 274-281.
198. Graham F L, Smiley J, Russell W C, and Nairn R. Characteristics of a human cell line transformed by DNA from human adenovirus type 5. J Gen Virol, 1977. 36(1): 59-74.
199. Greene L A and Tischler A S. Establishment of a noradrenergic clonal line of rat adrenal pheochromocytoma cells which respond to nerve growth factor. Proc Natl Acad Sci U S A, 1976. 73(7): 2424-2428.
200. Fallaux F J, Bout A, van der Velde I, van den Wollenberg D J, Hehir K M, Keegan J, Auger C, Cramer S J, et al. New helper cells and matched early region 1-deleted adenovirus vectors prevent generation of replication-competent adenoviruses. Hum Gene Ther, 1998. 9(13): 1909-1917.
201. Guy C T, Cardiff R D, and Muller W J. Induction of mammary tumors by expression of polyomavirus middle T oncogene: a transgenic mouse model for metastatic disease. Mol Cell Biol, 1992. 12(3): 954-961.

202. Bibel M, Hoppe E, and Barde Y A. Biochemical and functional interactions between the neurotrophin receptors trk and p75NTR. EMBO J, 1999. 18(3): 616-622.
203. Gantner F, Kupferschmidt R, Schudt C, Wendel A, and Hatzelmann A. In vitro differentiation of human monocytes to macrophages: change of PDE profile and its relationship to suppression of tumour necrosis factor-alpha release by PDE inhibitors. Br J Pharmacol, 1997. 121(2): 221-231.
204. Michiels F, van Es H, van Rompaey L, Merchiers P, Francken B, Pittois K, van der Schueren J, Brys R, et al. Arrayed adenoviral expression libraries for functional screening. Nat Biotechnol, 2002. 20(11): 1154-1157.
205. Lowry O H, Rosebrough N J, Farr A L, and Randall R J. Protein measurement with the Folin phenol reagent. J Biol Chem, 1951. 193(1): 265-275.
206. Viera A J and Garrett J M. Understanding interobserver agreement: the kappa statistic. Fam Med, 2005. 37(5): 360-363.
207. Weigert A, Schiffmann S, Sekar D, Ley S, Menrad H, Werno C, Grosch S, Geisslinger G, et al. Sphingosine kinase 2 deficient tumor xenografts show impaired growth and fail to polarize macrophages towards an anti-inflammatory phenotype. Int J Cancer, 2009. 125(9): 2114-2121.
208. Arts G J, Langemeijer E, Tissingh R, Ma L, Pavliska H, Dokic K, Dooijes R, Mesic E, et al. Adenoviral vectors expressing siRNAs for discovery and validation of gene function. Genome Res, 2003. 13(10): 2325-2332.
209. Di Marzo V, Bisogno T, De Petrocellis L, Melck D, Orlando P, Wagner J A, and Kunos G. Biosynthesis and inactivation of the endocannabinoid 2-arachidonoylglycerol in circulating and tumoral macrophages. Eur J Biochem, 1999. 264(1): 258-267.
210. Stella N. Cannabinoid signaling in glial cells. Glia, 2004. 48(4): 267-277.
211. Nagarkatti P, Pandey R, Rieder S A, Hegde V L, and Nagarkatti M. Cannabinoids as novel anti-inflammatory drugs. Future Med Chem, 2009. 1(7): 1333-1349.
212. Burstein S H and Zurier R B. Cannabinoids, endocannabinoids, and related analogs in inflammation. AAPS J, 2009. 11(1): 109-119.
213. Pertwee R G, Howlett A C, Abood M E, Alexander S P, Di Marzo V, Elphick M R, Greasley P J, Hansen H S, et al. International Union of Basic and Clinical Pharmacology. LXXIX. Cannabinoid receptors and their ligands: beyond CB and CB. Pharmacol Rev, 2010. 62(4): 588-631.
214. Fritz G, Henninger C, and Huelsenbeck J. Potential use of HMG-CoA reductase inhibitors (statins) as radioprotective agents. Br Med Bull, 2011. 97: 17-26.
215. Jain M K and Ridker P M. Anti-inflammatory effects of statins: clinical evidence and basic mechanisms. Nat Rev Drug Discov, 2005. 4(12): 977-987.
216. Vijayan V, Baumgart-Vogt E, Naidu S, Qian G, and Immenschuh S. Bruton's tyrosine kinase is required for TLR-dependent heme oxygenase-1 gene activation via Nrf2 in macrophages. J Immunol, 2011. 187(2): 817-827.
217. Mukhopadhyay S, Mohanty M, Mangla A, George A, Bal V, Rath S, and Ravindran B. Macrophage effector functions controlled by Bruton's tyrosine kinase are more crucial than the cytokine balance of T cell responses for microfilarial clearance. J Immunol, 2002. 168(6): 2914-2921.
218. Kazerounian S, Yee K O, and Lawler J. Thrombospondins in cancer. Cell Mol Life Sci, 2008. 65(5): 700-712.

219. Fleetwood A J, Lawrence T, Hamilton J A, and Cook A D. Granulocyte-macrophage colony-stimulating factor (CSF) and macrophage CSF-dependent macrophage phenotypes display differences in cytokine profiles and transcription factor activities: implications for CSF blockade in inflammation. J Immunol, 2007. 178(8): 5245-5252.
220. Adriaenssens E, Vanhecke E, Saule P, Mougel A, Page A, Romon R, Nurcombe V, Le Bourhis X, et al. Nerve growth factor is a potential therapeutic target in breast cancer. Cancer Res, 2008. 68(2): 346-351.
221. Romon R, Adriaenssens E, Lagadec C, Germain E, Hondermarck H, and Le Bourhis X. Nerve growth factor promotes breast cancer angiogenesis by activating multiple pathways. Mol Cancer. 9: 157.
222. Hobson J P, Rosenfeldt H M, Barak L S, Olivera A, Poulton S, Caron M G, Milstien S, and Spiegel S. Role of the sphingosine-1-phosphate receptor EDG-1 in PDGF-induced cell motility. Science, 2001. 291(5509): 1800-1803.
223. Toman R E, Payne S G, Watterson K R, Maceyka M, Lee N H, Milstien S, Bigbee J W, and Spiegel S. Differential transactivation of sphingosine-1-phosphate receptors modulates NGF-induced neurite extension. J Cell Biol, 2004. 166(3): 381-392.
224. Bracci-Laudiero L, Aloe L, Caroleo M C, Buanne P, Costa N, Starace G, and Lundeberg T. Endogenous NGF regulates CGRP expression in human monocytes, and affects HLA-DR and CD86 expression and IL-10 production. Blood, 2005. 106(10): 3507-3514.
225. Jullien J, Guili V, Reichardt L F, and Rudkin B B. Molecular kinetics of nerve growth factor receptor trafficking and activation. J Biol Chem, 2002. 277(41): 38700-38708.
226. Muragaki Y, Timothy N, Leight S, Hempstead B L, Chao M V, Trojanowski J Q, and Lee V M. Expression of trk receptors in the developing and adult human central and peripheral nervous system. J Comp Neurol, 1995. 356(3): 387-397.
227. Tapley P, Lamballe F, and Barbacid M. K252a is a selective inhibitor of the tyrosine protein kinase activity of the trk family of oncogenes and neurotrophin receptors. Oncogene, 1992. 7(2): 371-381.
228. Jung E J, Kim C W, and Kim D R. Cytosolic accumulation of gammaH2AX is associated with tropomyosin-related kinase A-induced cell death in U2OS cells. Exp Mol Med, 2008. 40(3): 276-285.
229. Caroleo M C, Costa N, Bracci-Laudiero L, and Aloe L. Human monocyte/macrophages activate by exposure to LPS overexpress NGF and NGF receptors. J Neuroimmunol, 2001. 113(2): 193-201.
230. Lee F S and Chao M V. Activation of Trk neurotrophin receptors in the absence of neurotrophins. Proc Natl Acad Sci U S A, 2001. 98(6): 3555-3560.
231. El Zein N, D'Hondt S, and Sariban E. Crosstalks between the receptors tyrosine kinase EGFR and TrkA and the GPCR, FPR, in human monocytes are essential for receptors-mediated cell activation. Cell Signal, 2010. 22(10): 1437-1447.
232. Moises T, Dreier A, Flohr S, Esser M, Brauers E, Reiss K, Merken D, Weis J, et al. Tracking TrkA's trafficking: NGF receptor trafficking controls NGF receptor signaling. Mol Neurobiol, 2007. 35(2): 151-159.
233. Long J S, Fujiwara Y, Edwards J, Tannahill C L, Tigyi G, Pyne S, and Pyne N J. Sphingosine-1-phosphate receptor 4 uses HER2 (ERBB2) to regulate extracellular

signal regulated kinase-1/2 in MDA-MB-453 breast cancer cells. J Biol Chem, 2010. 285(46): 35957-35966.
234. Pyne N J and Pyne S. Sphingosine-1-phosphate, lysophosphatidic acid and growth factor signaling and termination. Biochim Biophys Acta, 2008. 1781(9): 467-476.
235. Wetter J A, Revankar C, and Hanson B J. Utilization of the Tango beta-arrestin recruitment technology for cell-based EDG receptor assay development and interrogation. J Biomol Screen, 2009. 14(9): 1134-1141.
236. Davis M D, Clemens J J, Macdonald T L, and Lynch K R. Sphingosine-1-phosphate analogs as receptor antagonists. J Biol Chem, 2005. 280(11): 9833-9841.
237. Mantovani A, Sozzani S, Locati M, Allavena P, and Sica A. Macrophage polarization: tumor-associated macrophages as a paradigm for polarized M2 mononuclear phagocytes. Trends Immunol, 2002. 23(11): 549-555.
238. Movahedi K, Laoui D, Gysemans C, Baeten M, Stange G, Van den Bossche J, Mack M, Pipeleers D, et al. Different tumor microenvironments contain functionally distinct subsets of macrophages derived from Ly6C(high) monocytes. Cancer Res, 2010. 70(14): 5728-5739.
239. Hanahan D and Weinberg R A. The hallmarks of cancer. Cell, 2000. 100(1): 57-70.
240. Hanahan D and Weinberg R A. Hallmarks of cancer: the next generation. Cell, 2011. 144(5): 646-674.
241. Weigert A, Jennewein C, and Brune B. The liaison between apoptotic cells and macrophages - the end programs the beginning. Biol Chem, 2009. 390(5-6): 379-390.
242. Shiao S L, Ganesan A P, Rugo H S, and Coussens L M. Immune microenvironments in solid tumors: new targets for therapy. Genes Dev, 2011. 25(24): 2559-2572.
243. Revesz L. Effect of tumour cells killed by x-rays upon the growth of admixed viable cells. Nature, 1956. 178(4547): 1391-1392.
244. Huang Q, Li F, Liu X, Li W, Shi W, Liu F F, O'Sullivan B, He Z, et al. Caspase 3-mediated stimulation of tumor cell repopulation during cancer radiotherapy. Nat Med, 2011. 17(7): 860-866.
245. Gough M J, Melcher A A, Ahmed A, Crittenden M R, Riddle D S, Linardakis E, Ruchatz A N, Emiliusen L M, et al. Macrophages orchestrate the immune response to tumor cell death. Cancer Res, 2001. 61(19): 7240-7247.
246. Brecht K, Weigert A, Hu J, Popp R, Fisslthaler B, Korff T, Fleming I, Geisslinger G, et al. Macrophages programmed by apoptotic cells promote angiogenesis via prostaglandin E2. Faseb J, 2011. 25(7): 2408-2417.
247. Biswas S K, Sica A, and Lewis C E. Plasticity of macrophage function during tumor progression: regulation by distinct molecular mechanisms. J Immunol, 2008. 180(4): 2011-2017.
248. Rivera J, Proia R L, and Olivera A. The alliance of sphingosine-1-phosphate and its receptors in immunity. Nat Rev Immunol, 2008. 8(10): 753-763.
249. Koh E, Clair T, Hermansen R, Bandle R W, Schiffmann E, Roberts D D, and Stracke M L. Sphingosine-1-phosphate initiates rapid retraction of pseudopodia by localized RhoA activation. Cell Signal, 2007. 19(6): 1328-1338.
250. Graler M H, Grosse R, Kusch A, Kremmer E, Gudermann T, and Lipp M. The sphingosine-1-phosphate receptor S1P4 regulates cell shape and motility via coupling to Gi and G12/13. J Cell Biochem, 2003. 89(3): 507-519.
251. Murray P J. The JAK-STAT signaling pathway: input and output integration. J Immunol, 2007. 178(5): 2623-2629.

252. Hodge D R, Hurt E M, and Farrar W L. The role of IL-6 and STAT3 in inflammation and cancer. Eur J Cancer, 2005. 41(16): 2502-2512.
253. Naugler W E and Karin M. The wolf in sheep's clothing: the role of interleukin-6 in immunity, inflammation and cancer. Trends Mol Med, 2008. 14(3): 109-119.
254. Gocheva V, Wang H W, Gadea B B, Shree T, Hunter K E, Garfall A L, Berman T, and Joyce J A. IL-4 induces cathepsin protease activity in tumor-associated macrophages to promote cancer growth and invasion. Genes Dev, 2010. 24(3): 241-255.
255. Terabe M, Park J M, and Berzofsky J A. Role of IL-13 in regulation of anti-tumor immunity and tumor growth. Cancer Immunol Immunother, 2004. 53(2): 79-85.
256. Hansbro P M, Kaiko G E, and Foster P S. Cytokine/anti-cytokine therapy - novel treatments for asthma? Br J Pharmacol, 2011. 163(1): 81-95.
257. Kim E Y, Battaile J T, Patel A C, You Y, Agapov E, Grayson M H, Benoit L A, Byers D E, et al. Persistent activation of an innate immune response translates respiratory viral infection into chronic lung disease. Nat Med, 2008. 14(6): 633-640.
258. Todaro M, Lombardo Y, Francipane M G, Alea M P, Cammareri P, Iovino F, Di Stefano A B, Di Bernardo C, et al. Apoptosis resistance in epithelial tumors is mediated by tumor-cell-derived interleukin-4. Cell Death Differ, 2008. 15(4): 762-772.
259. Turner M, Chantry D, and Feldmann M. Transforming growth factor beta induces the production of interleukin 6 by human peripheral blood mononuclear cells. Cytokine, 1990. 2(3): 211-216.
260. McGee D W, Beagley K W, Aicher W K, and McGhee J R. Transforming growth factor-beta enhances interleukin-6 secretion by intestinal epithelial cells. Immunology, 1992. 77(1): 7-12.
261. Basu S and Dittel B N. Unraveling the complexities of cannabinoid receptor 2 (CB2) immune regulation in health and disease. Immunol Res, 2011. 51(1): 26-38.
262. Bisogno T, Maurelli S, Melck D, De Petrocellis L, and Di Marzo V. Biosynthesis, uptake, and degradation of anandamide and palmitoylethanolamide in leukocytes. J Biol Chem, 1997. 272(6): 3315-3323.
263. Hao M X, Jiang L S, Fang N Y, Pu J, Hu L H, Shen L H, Song W, and He B. The cannabinoid WIN55,212-2 protects against oxidized LDL-induced inflammatory response in murine macrophages. J Lipid Res, 2010. 51(8): 2181-2190.
264. Correa F, Mestre L, Docagne F, and Guaza C. Activation of cannabinoid CB2 receptor negatively regulates IL-12p40 production in murine macrophages: role of IL-10 and ERK1/2 kinase signaling. Br J Pharmacol, 2005. 145(4): 441-448.
265. Correa F, Hernangomez M, Mestre L, Loria F, Spagnolo A, Docagne F, Di Marzo V, and Guaza C. Anandamide enhances IL-10 production in activated microglia by targeting CB(2) receptors: roles of ERK1/2, JNK, and NF-kappaB. Glia, 2010. 58(2): 135-147.
266. Chang Y H, Lee S T, and Lin W W. Effects of cannabinoids on LPS-stimulated inflammatory mediator release from macrophages: involvement of eicosanoids. J Cell Biochem, 2001. 81(4): 715-723.
267. Mair K M, Robinson E, Kane K A, Pyne S, Brett R R, Pyne N J, and Kennedy S. Interaction between anandamide and sphingosine-1-phosphate in mediating vasorelaxation in rat coronary artery. Br J Pharmacol, 2010. 161(1): 176-192.

268. Paugh S W, Cassidy M P, He H, Milstien S, Sim-Selley L J, Spiegel S, and Selley D E. Sphingosine and its analog, the immunosuppressant 2-amino-2-(2-[4-octylphenyl]ethyl)-1,3-propanediol, interact with the CB1 cannabinoid receptor. Mol Pharmacol, 2006. 70(1): 41-50.
269. Coscia M, Quaglino E, Iezzi M, Curcio C, Pantaleoni F, Riganti C, Holen I, Monkkonen H, et al. Zoledronic acid repolarizes tumour-associated macrophages and inhibits mammary carcinogenesis by targeting the mevalonate pathway. J Cell Mol Med, 2010. 14(12): 2803-2815.
270. Barouch R, Kazimirsky G, Appel E, and Brodie C. Nerve growth factor regulates TNF-alpha production in mouse macrophages via MAP kinase activation. J Leukoc Biol, 2001. 69(6): 1019-1026.
271. Susaki Y, Shimizu S, Katakura K, Watanabe N, Kawamoto K, Matsumoto M, Tsudzuki M, Furusaka T, et al. Functional properties of murine macrophages promoted by nerve growth factor. Blood, 1996. 88(12): 4630-4637.
272. Samah B, Porcheray F, and Gras G. Neurotrophins modulate monocyte chemotaxis without affecting macrophage function. Clin Exp Immunol, 2008. 151(3): 476-486.
273. Ehrhard P B, Ganter U, Stalder A, Bauer J, and Otten U. Expression of functional trk protooncogene in human monocytes. Proc Natl Acad Sci U S A, 1993. 90(12): 5423-5427.
274. Schecterson L C and Bothwell M. Neurotrophin receptors: Old friends with new partners. Dev Neurobiol, 2010. 70(5): 332-338.
275. Noga O, Peiser M, Altenahr M, Knieling H, Wanner R, Hanf G, Grosse R, and Suttorp N. Differential activation of dendritic cells by nerve growth factor and brain-derived neurotrophic factor. Clin Exp Allergy, 2007. 37(11): 1701-1708.
276. Melendez A J. Sphingosine kinase signalling in immune cells: potential as novel therapeutic targets. Biochim Biophys Acta, 2008. 1784(1): 66-75.
277. Tsuruda A, Suzuki S, Maekawa T, and Oka S. Constitutively active Src facilitates NGF-induced phosphorylation of TrkA and causes enhancement of the MAPK signaling in SK-N-MC cells. FEBS Lett, 2004. 560(1-3): 215-220.
278. Sandilands E, Akbarzadeh S, Vecchione A, McEwan D G, Frame M C, and Heath J K. Src kinase modulates the activation, transport and signalling dynamics of fibroblast growth factor receptors. EMBO Rep, 2007. 8(12): 1162-1169.
279. Kobayashi H and Mizisin A P. Nerve growth factor and neurotrophin-3 promote chemotaxis of mouse macrophages in vitro. Neurosci Lett, 2001. 305(3): 157-160.
280. Michaud J, Im D S, and Hla T. Inhibitory role of sphingosine-1-phosphate receptor 2 in macrophage recruitment during inflammation. J Immunol, 2010. 184(3): 1475-1483.
281. Nakamura K, Tan F, Li Z, and Thiele C J. NGF activation of TrkA induces vascular endothelial growth factor expression via induction of hypoxia-inducible factor-1alpha. Mol Cell Neurosci, 2011. 46(2): 498-506.
282. O'Sullivan C, Lewis C E, Harris A L, and McGee J O. Secretion of epidermal growth factor by macrophages associated with breast carcinoma. Lancet, 1993. 342(8864): 148-149.
283. Zweifel L S, Kuruvilla R, and Ginty D D. Functions and mechanisms of retrograde neurotrophin signalling. Nat Rev Neurosci, 2005. 6(8): 615-625.
284. Legrand D, Elass E, Carpentier M, and Mazurier J. Lactoferrin: a modulator of immune and inflammatory responses. Cell Mol Life Sci, 2005. 62(22): 2549-2559.

285. Appelmelk B J, An Y Q, Geerts M, Thijs B G, de Boer H A, MacLaren D M, de Graaff J, and Nuijens J H. Lactoferrin is a lipid A-binding protein. Infect Immun, 1994. 62(6): 2628-2632.
286. Legrand D and Mazurier J. A critical review of the roles of host lactoferrin in immunity. Biometals, 2010. 23(3): 365-376.
287. Hyytiainen M, Penttinen C, and Keski-Oja J. Latent TGF-beta binding proteins: extracellular matrix association and roles in TGF-beta activation. Crit Rev Clin Lab Sci, 2004. 41(3): 233-264.
288. Yoshinaga K, Obata H, Jurukovski V, Mazzieri R, Chen Y, Zilberberg L, Huso D, Melamed J, et al. Perturbation of transforming growth factor (TGF)-beta1 association with latent TGF-beta binding protein yields inflammation and tumors. Proc Natl Acad Sci U S A, 2008. 105(48): 18758-18763.
289. Hagemann T, Robinson S C, Schulz M, Trumper L, Balkwill F R, and Binder C. Enhanced invasiveness of breast cancer cell lines upon co-cultivation with macrophages is due to TNF-alpha dependent up-regulation of matrix metalloproteases. Carcinogenesis, 2004. 25(8): 1543-1549.
290. Smith H W and Marshall C J. Regulation of cell signalling by uPAR. Nat Rev Mol Cell Biol, 2010. 11(1): 23-36.
291. Farias-Eisner R, Vician L, Silver A, Reddy S, Rabbani S A, and Herschman H R. The urokinase plasminogen activator receptor (UPAR) is preferentially induced by nerve growth factor in PC12 pheochromocytoma cells and is required for NGF-driven differentiation. J Neurosci, 2000. 20(1): 230-239.
292. Bilandzic M and Stenvers K L. Betaglycan: a multifunctional accessory. Mol Cell Endocrinol, 2011. 339(1-2): 180-189.
293. Xin C, Ren S, Kleuser B, Shabahang S, Eberhardt W, Radeke H, Schafer-Korting M, Pfeilschifter J, et al. Sphingosine-1-phosphate cross-activates the Smad signaling cascade and mimics transforming growth factor-beta-induced cell responses. J Biol Chem, 2004. 279(34): 35255-35262.
294. Kang J, Perry J K, Pandey V, Fielder G C, Mei B, Qian P X, Wu Z S, Zhu T, et al. Artemin is oncogenic for human mammary carcinoma cells. Oncogene, 2009. 28(19): 2034-2045.
295. Saarma M. GDNF - a stranger in the TGF-beta superfamily? Eur J Biochem, 2000. 267(24): 6968-6971.
296. Encinas M, Tansey M G, Tsui-Pierchala B A, Comella J X, Milbrandt J, and Johnson E M, Jr. c-Src is required for glial cell line-derived neurotrophic factor (GDNF) family ligand-mediated neuronal survival via a phosphatidylinositol-3 kinase (PI-3K)-dependent pathway. J Neurosci, 2001. 21(5): 1464-1472.
297. Morandi A, Plaza-Menacho I, and Isacke C M. RET in breast cancer: functional and therapeutic implications. Trends Mol Med, 2011. 17(3): 149-157.
298. Stewart A L, Anderson R B, Kobayashi K, and Young H M. Effects of NGF, NT-3 and GDNF family members on neurite outgrowth and migration from pelvic ganglia from embryonic and newborn mice. BMC Dev Biol, 2008. 8: 73.
299. Andres R, Forgie A, Wyatt S, Chen Q, de Sauvage F J, and Davies A M. Multiple effects of artemin on sympathetic neurone generation, survival and growth. Development, 2001. 128(19): 3685-3695.
300. Schober A, Hertel R, Arumae U, Farkas L, Jaszai J, Krieglstein K, Saarma M, and Unsicker K. Glial cell line-derived neurotrophic factor rescues target-deprived

sympathetic spinal cord neurons but requires transforming growth factor-beta as cofactor in vivo. J Neurosci, 1999. 19(6): 2008-2015.
301. Krieglstein K, Henheik P, Farkas L, Jaszai J, Galter D, Krohn K, and Unsicker K. Glial cell line-derived neurotrophic factor requires transforming growth factor-beta for exerting its full neurotrophic potential on peripheral and CNS neurons. J Neurosci, 1998. 18(23): 9822-9834.
302. Roussa E, Oehlke O, Rahhal B, Heermann S, Heidrich S, Wiehle M, and Krieglstein K. Transforming growth factor beta cooperates with persephin for dopaminergic phenotype induction. Stem Cells, 2008. 26(7): 1683-1694.
303. Tsui-Pierchala B A, Milbrandt J, and Johnson E M, Jr. NGF utilizes c-Ret via a novel GFL-independent, inter-RTK signaling mechanism to maintain the trophic status of mature sympathetic neurons. Neuron, 2002. 33(2): 261-273.
304. Hodi F S, O'Day S J, McDermott D F, Weber R W, Sosman J A, Haanen J B, Gonzalez R, Robert C, et al. Improved survival with ipilimumab in patients with metastatic melanoma. N Engl J Med, 2010. 363(8): 711-723.
305. Ojalvo L S, King W, Cox D, and Pollard J W. High-density gene expression analysis of tumor-associated macrophages from mouse mammary tumors. Am J Pathol, 2009. 174(3): 1048-1064.
306. Biswas S K, Gangi L, Paul S, Schioppa T, Saccani A, Sironi M, Bottazzi B, Doni A, et al. A distinct and unique transcriptional program expressed by tumor-associated macrophages (defective NF-kappaB and enhanced IRF-3/STAT1 activation). Blood, 2006. 107(5): 2112-2122.
307. Ojalvo L S, Whittaker C A, Condeelis J S, and Pollard J W. Gene expression analysis of macrophages that facilitate tumor invasion supports a role for Wnt-signaling in mediating their activity in primary mammary tumors. J Immunol, 2010. 184(2): 702-712.
308. Weigert A, Sekar D, and Brüne B. Tumor-associated macrophages as targets for tumor immunotherapy. Immunotherapy, 2009. 1(1): 83-95.
309. Beatty G L, Chiorean E G, Fishman M P, Saboury B, Teitelbaum U R, Sun W, Huhn R D, Song W, et al. CD40 agonists alter tumor stroma and show efficacy against pancreatic carcinoma in mice and humans. Science, 2011. 331(6024): 1612-1616.
310. Qian B Z, Li J, Zhang H, Kitamura T, Zhang J, Campion L R, Kaiser E A, Snyder L A, et al. CCL2 recruits inflammatory monocytes to facilitate breast-tumour metastasis. Nature, 2011. 475(7355): 222-225.
311. Steidl C, Lee T, Shah S P, Farinha P, Han G, Nayar T, Delaney A, Jones S J, et al. Tumor-associated macrophages and survival in classic Hodgkin's lymphoma. N Engl J Med, 2010. 362(10): 875-885.
312. Fujiwara T, Fukushi J, Yamamoto S, Matsumoto Y, Setsu N, Oda Y, Yamada H, Okada S, et al. Macrophage infiltration predicts a poor prognosis for human ewing sarcoma. Am J Pathol, 2011. 179(3): 1157-1170.
313. Dickson M A, Carvajal R D, Merrill A H, Jr., Gonen M, Cane L M, and Schwartz G K. A phase I clinical trial of safingol in combination with cisplatin in advanced solid tumors. Clin Cancer Res, 2011. 17(8): 2484-2492.
314. Albanese C, Alzani R, Amboldi N, Avanzi N, Ballinari D, Brasca M G, Festuccia C, Fiorentini F, et al. Dual targeting of CDK and tropomyosin receptor kinase families by the oral inhibitor PHA-848125, an agent with broad-spectrum antitumor efficacy. Mol Cancer Ther, 2010. 9(8): 2243-2254.

315. Weiss G J, Hidalgo M, Borad M J, Laheru D, Tibes R, Ramanathan R K, Blaydorn L, Jameson G, et al. Phase I study of the safety, tolerability and pharmacokinetics of PHA-848125AC, a dual tropomyosin receptor kinase A and cyclin-dependent kinase inhibitor, in patients with advanced solid malignancies. Invest New Drugs, 2011.
316. Garber K. Fate of novel painkiller mAbs hangs in balance. Nat Biotechnol, 2011. 29(3): 173-174.
317. Descamps S, Toillon R A, Adriaenssens E, Pawlowski V, Cool S M, Nurcombe V, Le Bourhis X, Boilly B, et al. Nerve growth factor stimulates proliferation and survival of human breast cancer cells through two distinct signaling pathways. J Biol Chem, 2001. 276(21): 17864-17870.

8 Appendix

Buffers for cell biology

Erythrocyte lysis buffer	
NH_4Cl	155 mM
$KHCO_3$	10 mM
EDTA	0.1 mM

Leukocyte running buffer	
EDTA	2 mM
BSA	0.5% (w/v)
in PBS	

Leukcocyte washing buffer	
EDTA	2 mM
in PBS	

Phosphate buffered saline (PBS)	
NaCl	137 mM
KCl	2.7 mM
Na_2HPO_4	8.1 mM
KH_2PO_4	1.5 mM
pH	7.4

Tumor lysis buffer	
Collagenase 1A	3 mg/ml
DNAse 1	1 U/ml
in DMEM	

Buffers and solutions for Immunoprecipitation and Western analysis

BSA-TBS buffer	
BSA	5% (w/v)
in TBS	

10 x blotting buffer	
Tris/HCl	250 mM
Glycine	1.9 M
pH	8.3

1 x blotting buffer	
10 x blotting buffer	10% (v/v)
Methanol	20% or 30%

IP buffer	
Tween-20	0,02% (v/v)
in PBS	

Milk-TBS buffer	
Milk powder	5% (w/v)
in TBS	

4 x SDS-PAGE sample buffer	
Tris-HCL	125 mM
SDS	2% (w/v)
Glycerin	50% (v/v)
Mercaptoethanol	10% (v/v)
Bromphenol blue	0.002% (w/v)
pH	6.9

SDS-running buffer	
Tris/HCl	25 mM
Glycine	190 mM
SDS	3.5 mM
pH	8.3

1 x TBS	
Tris/HCl	50 mM
NaCl	140 mM
pH	7.4

TTBS	pH 7.4
Tris-HCl	50 mM
NaCl	140 mM
Tween-20	0.05% (v/v)

NP40 Cell Lysis Buffer, Invitrogen

Tris/HCl	50 mM
Nonidet P40	1% (v/v)
NaCl	250 mM
EDTA	5 mM
NaF	50 mM
Na_3VO_4	1 mM
NaN_3	0.02% (w/v)
Freshly added prior to use:	
PMSF	1 mM
PIM	1 x
PhosSTOP	2 x

Urea lysis buffer

Tris-HCL pH 6,8	10 mM
Urea	6.65 M
Glycine	10% (w/v)
SDS	1% (w/v)
pH	7.4
Add freshly prior use:	
PIM	1 x
Mercaptoethanol	10% (v/v)
PhosSTOP	2 x
Na_3VO_4	7 mM

4 x Upper Tris buffer

Tris-HCL	0.5 M
pH	6.8

4 x Lower Tris buffer

Tris-HCL	1.5 M
pH	8.8

Sodium dodecyl sulfate (SDS)-polyacrylamide gels

	Separating gels			Stacking gel
	6%	10%	15%	4%
40% Acrylamide/Bis-acrylamide (37.5% : 1.0% w/v)	1.5 ml	2.5 ml	3.75 ml	300 µl
Lower tris buffer (4 x)	2.5 ml	2.5 ml	2.5 ml	
Upper tris buffer (4 x)				750 µl
H_2O distilled	5.9 ml	4.9 ml	3.65 ml	1.92 ml
10% SDS (w/v)	100 µl	100 µl	100 µl	30 µl
TEMED	10 µl	10 µl	10 µl	5 µl
10% (w/v) ammonium persulfate	100 µl	100 µl	100 µl	50 µl

Buffers and solutions for ELISA

ELISA blocking buffer	
BSA	2% (w/v)
in PBS	

ELISA dilution buffer	
BSA	0.5% (w/v)
Tween-20	0.01% (v/v)
in PBS	

ELISA coating buffer	
Na_2CO_3	50 mM
$NaHCO_3$	50 mM
pH	9.6

ELISA washing buffer	
Tween-20	0.01% (v/v)
in PBS	

Buffers and solutions for Immunofluorescence

IF binding buffer	
FCS	2% (w/v)
in PBS	

IF permeabilization buffer	
Triton X-100	2% (v/v)
in PBS	

IF blocking buffer	
FCS	30% (w/v)
Triton X-100	0.01% (v/v)

IF washing buffer	
Triton X-100	0.01% (v/v)
in PBS	

Buffers and solutions for molecular biology and microbiology

Annexin-V binding buffer	
HEPES	10 mM
NaCl	140 mM
$CaCl_2$	2.5 mM
pH	7.5

SOC medium	
Tryptone	20 g/l
Yeast extract	5 g/l
NaCl	0.5 g/l
$MgCl_2$	10 mM
$MgSO_4$	10 mM
Glucose	2 mM

DEPC-water

1 ml Diethylpyrocarbonate (DEPC) in
1 l distilled H2O
→ stirred over night and autoclaved

9 Publications

Ley S, Weigert A, Weichand B, Henke N, Mille-Baker B, Janssen R A J, Brüne B. The role of TRKA signaling in IL-10 production by apoptotic tumor cell-activated macrophages. Oncogene, 2012. DOI: 10.1038/onc.2012.77.

Ley S, Weigert A, Heriche J K, Mille-Baker B, Janssen R A J, and Brüne B. RNAi screen in apoptotic cancer cell-stimulated human macrophages reveals co-regulation of IL-6/IL-10 expression. Immunobiology, 2012. DOI: 10.1016/j.imbio.2012.01.019.

Kaminski B M, Weigert A, **Ley S**, Brecht K, Brüne B, Steinhilber D, Stein J, and Ulrich S. Resveratrol-induced potentiation of the antitumor effects of oxaliplatin is accompanied by an altered cytokine profile of human-derived macrophages. Mol Nutr Food Res. *In revision.*

Ley S, Weigert A, and Brune B. Neuromediators in inflammation--a macrophage/nerve connection. Immunobiology, 2010. 215(9-10): 674-684.

Weigert A, Schiffmann S, Sekar D, **Ley S**, Menrad H, Werno C, Grosch S, Geisslinger G, et al. Sphingosine kinase 2 deficient tumor xenografts show impaired growth and fail to polarize macrophages towards an anti-inflammatory phenotype. Int J Cancer, 2009. 125(9): 2114-2121.

Cabello C M, Bair W B, 3rd, Lamore S D, **Ley S**, Bause A S, Azimian S, and Wondrak G T. The cinnamon-derived Michael acceptor cinnamic aldehyde impairs melanoma cell proliferation, invasiveness, and tumor growth. Free Radic Biol Med, 2009. 46(2): 220-231.

Cabello C M, Bair W B, 3rd, **Ley S**, Lamore S D, Azimian S, and Wondrak G T. The experimental chemotherapeutic N6-furfuryladenosine (kinetin-riboside) induces rapid ATP depletion, genotoxic stress, and CDKN1A(p21) upregulation in human cancer cell lines. Biochem Pharmacol, 2009. 77(7): 1125-1138.

Wondrak G T, Cabello C M, Villeneuve N F, Zhang S, **Ley S**, Li Y, Sun Z, and Zhang D D. Cinnamoyl-based Nrf2-activators targeting human skin cell photo-oxidative stress. Free Radic Biol Med, 2008. 45(4): 385-395.

Talks and poster presentations:

Poster presentation at the Lipid Signaling Symposium 2012 in Frankfurt: "IL-10 production by apopotic tumor cell-activated macrophages requires S1P/TRKA signaling".

Poster presentation at the British Society of Immunology Annual Congress 2011 in Liverpool, GB: "IL-10 production by apoptotic tumor cell-activated macrophages requires signaling through TrkA – validation of an adenoviral RNAi screen".

Poster presentation at the Keystone Symposia, Molecular and Cellular Biology of Immune Escape in Cancer 2010 in Keystone, USA: "High-throughput RNAi screen for molecular determinants of IL-10 production in macrophages".

Poster presentation at the EACR Special Conference, Inflammation and Cancer 2009 in Berlin: "High-throughput RNAi screen for inducers of IL-10 production in macrophages".

Talk at the Internal PhD Symposium: Research in Molecular and Cell Biological Sciences 2011 in Frankfurt: "Apoptotic cell supernatant induces interleukin 10 in macrophages – the story of a high-throughput screen validation".

10 Acknowledgement

Ich möchte mich hiermit bei all denjenigen bedanken, die mir auf verschiedenste Weise bei der Anfertigung dieser Arbeit geholfen haben. Besonderer Dank gilt:

Prof. Bernhard Brüne für die Vergabe des Themas, die Möglichkeit meine Arbeit in seinem Labor durchzuführen und für die Diskussionsbereitschaft und Kritik.

Dr. Andreas Weigert für die intensive Betreuung in den letzten Jahren, die Hilfsbereitschaft, die fruchtbaren Diskussionen und die nette Arbeitsatmosphäre.

Dem **Graduiertenkolleg GRK757/FIRST** für die finanzielle Unterstützung, die Seminarangebote und den regen wissenschaftlichen Austausch.

Dr. Blandine Mille-Baker, Dr. Richard Janssen, Anton De Groot, Brigitta Witte and all of the BioFocus/Galapagos team for giving me the opportunity to run the high-throughput screen, to ask questions, and to feel at home in the Netherlands.

Dr. Jean-Karim Hériché for helping me with the analysis of the screening data and for answering all my questions fast and precisely. Merci beaucoup!

Prof. Dr. Georg Thomas Wondrak für die beste Einführung in die Forschung die man sich als Pharmaziepraktikant vorstellen kann.

den Mitarbeitern der AG Brüne, ohne die eine erfolgreiche Durchführung nicht möglich gewesen wäre. Danke für das gute Arbeitsklima und die Zusammenarbeit.
Spezieller Dank geht an:
Nico, der immer gutgelaunt Antworten auf alle Fragen hatte.
Die lieben morgendlichen Kaffeetrinker Anne-Marie, Jojo und Daniela.
Heidi, Teckel und Carla für die gemeinsamen Kletterstunden.
Euch, sowie Christina, Barbara, Vera und Kathrin, danke ich für Eure Freundschaft.

meiner Familie, meinen Freunden und Armin dafür, dass Ihr immer für mich da seid und meine Vorhaben - auf welche Art auch immer - unterstützt.

11 Erklärung

Ich erkläre ehrenwörtlich, dass ich die dem Fachbereich Medizin der Johann Wolfgang Goethe-Universität Frankfurt am Main zur Promotionsprüfung eingereichte Dissertation mit dem Titel

Macrophage polarization by apoptotic cancer cells – a RNAi high-throughput screen and validation of interleukin 10 regulation

am Institut der Biochemie 1 / Pathobiochemie unter Betreuung und Anleitung von Professor Dr. Bernhard Brüne mit Unterstützung durch Dr. Andreas Weigert ohne sonstige Hilfe selbst durchgeführt und bei der Abfassung der Arbeit keine anderen als die in der Dissertation angeführten Hilfsmittel benutzt habe. Darüber hinaus versichere ich, nicht die Hilfe einer kommerziellen Promotionsvermittlung in Anspruch genommen zu haben.

Ich habe bisher an keiner in- oder ausländischen Universität ein Gesuch um Zulassung zur Promotion eingereicht. Die vorliegende Arbeit wurde bisher nicht als Dissertation eingereicht.

Vorliegende Ergebnisse der Arbeit wurden in den folgenden Publikationsorganen veröffentlicht:

Ley S, Weigert A, Weichand B, Henke N, Mille-Baker B, Janssen R A J, Brüne B.
The role of TRKA signaling in IL-10 production by apoptotic tumor cell-activated macrophages.
Oncogene, 2012. DOI: 10.1038/onc.2012.77.

Ley S, Weigert A, Heriche J K, Mille-Baker B, Janssen R A J, and Brüne B.
RNAi screen in apoptotic cancer cell-stimulated human macrophages reveals co-regulation of IL-6/IL-10 expression.
Immunobiology, 2012. DOI: 10.1016/j.imbio.2012.01.019.

Frankfurt, den 06.03.2012 Stephanie Ley